UNDERSTANDING THE PHYSIOLOGY IN CONTINUUM:

INTEGRATION OF INFORMATION FROM MULTIPLE "-OMICS" LEVELS

by

KUBRA KAMISOGLU

A Dissertation submitted to the

Graduate School-New Brunswick

Rutgers, The State University of New Jersey

in partial fulfillment of the requirements

for the degree of

Doctor of Philosophy

Graduate Program in Chemical and Biochemical Engineering

written under the direction of

Ioannis P. Androulakis

and approved by

_____

_____

_____

_____

_____

New Brunswick, New Jersey

October, 2015

ABSTRACT OF THE DISSERTATION

Understanding the Physiology in Continuum:

Integration of Information from Multiple "-omics" Levels

By KUBRA KAMISOGLU

Dissertation Director:

Ioannis P. Androulakis

One of the most fascinating aspects of biomedical sciences is searching for the links between the observed phenotypic changes with the underlying causes linked to known biological functions at the molecular level. These functions, however, are observed at different physiologic levels interacting physically, spatially, and/or temporally. Systems biology fundamentally studies the interactions taking place at genomic, proteomic and metabolomic levels under homeostatic conditions or in response to pathologic or pharmacologic stimuli. Each of these data-rich "-omics" fields have instrumental contributions to describe biological phenomena at their complementary levels. Integration of the knowledge from one or more such levels gives us opportunity to determine causal links more thoroughly and rationalize the focused question from initiating source to the observed end point. This dissertation is centered on extracting information from the data provided by the -omics analyses, as well as interconnecting the information gained at different levels through bioinformatics and modeling approaches. We applied these approaches to understand the impact of systemic inflammation and anti-inflammatory therapy on the metabolism in two distinct studies.

Our first focus was on the major changes arising in plasma metabolome during the response to systemic inflammation, and how these changes affect the transcriptome

of immune cells, in turn. We defined the dominant metabolic dynamics in the plasma of humans administered with bacterial endotoxin, as a surrogate for reproducing the pathophysiology of systemic inflammation. Subsequently, we integrated this analysis with transcriptional response of leukocytes to understand how their gene expression might have been affected from the metabolic landscape of the fluid environment in which they circulate. We hypothesized that the drastic changes in the immediate environment of the leukocytes might have an adaptive effect on shaping their transcriptional response in conjunction with the initial inflammatory stimuli.

Secondly, we explored the interplay between transcriptional and translational dynamics in liver in response to an anti-inflammatory drug administration. This involved the integration of temporal gene and protein expression patterns extracted from the livers of rats injected with a synthetic corticosteroid (methylprednisolone, MPL); long term use of which is associated with many metabolism related side effects. Our approach involved both combining and contrasting the same gene products in two different expression levels, in essence, pursuing the best integration approach yielding most useful mechanistic information. The significant disparity between the proteome and corresponding transcriptome in this study suggested that additional translational or post-translational implications of CSs are very plausible in addition to their direct effects on transcription; while also cautioning against the use of transcriptional data for deciphering the regulation of the functional pathways which they represent.

ACKNOWLEDGEMENTS

It is my great pleasure to thank the people helped me in one way or another throughout my studies at Rutgers and made this thesis possible.

First, I would like to thank my mentor, Dr. Ioannis P. Androulakis from the bottom of my heart. I have been amazingly fortunate to have met him at a very critical phase of my life. Since that day it has been a privilege to learn from him, to work with him and to be inspired by him. His unwavering encouragement and support have been the primary fuels that carried me through this work. He has been and always going to be a role model for me with his bright mind, his positive attitude and his fun spirit. I am truly grateful to him and I hope to have more opportunities to learn from him in the future.

My sincere thanks also go to the members of my thesis committee: Drs. Marianthi Ierapetritou, Francois Berthiaume, Siobhan A. Corbett and Beatrice Haimovich, who helped me with their valuable advices and comments in various stages of the work presented here.

I have been very fortunate to collaborate with a number of great people in various interdisciplinary research projects which eventually sculpted this thesis. I thank Drs. Steve E. Calvano, Susette M. Coyle, Beatrice Haimovich and Siobhan A. Corbett from the Department of Surgery at Rutgers-Robert Wood Johnson Medical School for allowing me to take part in the endotoxemia research which has a long and glorious history in this department. Drs. Raymond J. Langley from Lovelace Respiratory Research Institute and Stephen F. Kingsmore from Kansas City Children's Mercy Hospital generously provided us with the clinical data. I greatly appreciate their contribution and valuable comments during our joint study on evaluating the concordance between the metabolic response to endotoxemia and sepsis. It has been

a great pleasure to work with Dr. William Jusko and his group from the School of Pharmacy and Pharmaceutical Sciences, University at Buffalo on the integration of pharmacologic responses to corticosteroids. Especially I would like to thank Dr. Siddharth Sukumaran for his contributions during the transformation of our collaborative work into a publication.

I would like to acknowledge the fellowships from Rutgers - School of Engineering and Department of Chemical and Biochemical Engineering which financially supported me during my studies.

It has been a pleasure to have met and worked together with the past and current members of the Androulakis lab: Jon Pai, Rohit Rao, Kirsten Sleight, John Mattick, Shuliang Zhang, Jeremy Scheff, Qian Yang, Mehmet Ali Orman, Tung Nguyen, Vasilis Niotis, Pegy Foteinou, Meric Ovacik, and Pantelis Mavroudis. I am thankful for all the support and friendship from these people. I am also indebted to all the good friends from NJ for helping me have a life in US and create a home away from home. Especially, I am grateful to have Alper Almaz in my life to share all my troubles as well as my happiness.

Finally, I owe my deepest gratitude to my mom, Meliha, my dad, Taner, and my sisters Nevra, Hande and Nihan. They believed in me and supported me in every possible way. They raised me up whenever I felt lonely, homesick or weary. Without their support I would not have been able to make it through.

Contents

ABSTRACT OF THE DISSERTATION ii

ACKNOWLEDGEMENTS iv

List of Tables ix

List of Figures xi

Chapter 1 Introduction 1

Chapter 2 Temporal Metabolic Profiling of Plasma in Experimental Human Endotoxemia 6

2.1 Methods 7

2.1.1 Human Plasma Samples 7

2.1.2 Biochemical Profiling of Plasma Samples 8

2.1.3 Data analysis 9

2.2 Results 9

2.3 Discussion 14

2.3.1 Limitations 20

2.4 Conclusion 21

Chapter 3 Integration of Plasma Metabolomics and Leukocyte Transcriptomics in Response to Endotoxemia 22

3.1 Methods 23

3.1.1 Data analysis 24

3.2 Results 25

3.3 Discussion 31

3.3.1 Limitations 38

3.4 Conclusion 39

Chapter 4 Relevance of Endotoxemia Model to the Clinical Cases of Sepsis and SIRS 40

4.1 Methods 42
4.1.1 Metabolic Data 42
4.1.2 Data Analysis 44
4.2 Results and Discussion 46
4.2.1 Limitations 55
4.3 Conclusion 55
Chapter 5 Integration of Liver Transcriptomics and Proteomics in Response to Anti-Inflammatory Treatment 57
5.1 Methods 61
5.1.1 Animal experiments 61
5.1.2 Computational Analysis 62
5.1.3 Biological Interpretation 63
5.2 Results 63
5.2.1 Hierarchical Clustering of Concatenated Datasets: 65
5.2.2 Two-way Sequential Clustering of Individual Proteomic and Transcriptomic Datasets: 68
5.3 Discussion 72
5.4 Conclusion 78
Chapter 6 Summary and Future Perspectives 80
6.1 Summary 80
6.2 Adding the Stress Component to Endotoxemia Model 83
6.3 Enhancing PK/PD Models of MPL with Information from Multiple Levels of "–*omics*" 91
6.3.1 Building the response network 95
6.3.2 Integrating the network with existing PK/PD model for MPL 96
Bibliography 103

Curriculum Vitae 116

Appendix..... 118

Acknowledgement of Previous Publications 128

List of Tables

Table 2.1: Distribution and classification of the differential metabolites to the clusters shown in Figure 2-3. 15

Table 3.1: Functional annotation of all differentially expressed genes in the three clusters displayed in Figure 3-2. 27

Table 3.2: Classification of metabolites in the two clusters displayed in Figure 3-3. 29

Table 3.3: Functional annotation of metabolism related subset of genes in the three clusters displayed in Figure 3-5. 35

Table 4.1: Number of significantly changed metabolites and metabolic super-pathways that they belong to; determined for LPS-challenged subjects and patient groups. Significance was determined by comparing responses of each group of patients, as well as endotoxemia by comparing responses of each group of patients, as well as endotoxemia subjects, to the healthy baseline ($t_{0,LPS}$) individually. Welch's t-test was used and with correction for multiple comparisons by Benjamini and Hochberg procedure. (α=0.05). Metabolites having a p- and a q-value less than 0.05 are called significant. (Complete list is available in Appendix, Table A. 2) .48

Table 4.2: Metabolites which are significantly different than the heathy baseline (t0,LPS) in the experimental condition and either of the two time points in the clinical conditions. A lists the metabolites common for endotoxemia and sepsis; B lists those common for endotoxemia and sepsis; B lists those common for endotoxemia and SIRS. (=: no significant difference from t0,LPS. ▲/▼: less than 2 fold difference from t0,LPS; ▲▲/▼▼: more than 2 fold difference from t0,LPS; metabolite name in bold: common to both lists A and B). 50

Table 4.3: The subset of metabolites having significantly different concentrations between SS and SNS groups at either clinical time points. (Changes from the

healthy baseline, $t_{0,LPS}$: ▲/▼: less than 2 fold change; ▲▲/▼▼: more than 2 fold change, -: there was not a significant difference between SS or SNS groups)...53
Table 5.1: Functional annotation of differentially expressed genes in both transcriptional and translational levels.....67
Table 5.2: Predicted upstream regulators and their activation states (green: activated, red: inhibited) based on the gene groups obtained by hierarchical clustering. ..68
Table 5.3: Distribution of elements after clustering and sub-clustering of data in two-way analysis. 71

List of Figures

Figure 1-1: Multiscale nature of inflammatory response. 2

Figure 1-2: Inflammatory response is a complex process which has to be tightly regulated in order to balance the defense mechanisms of the host with the severity of infection/tissue damage. Loss of this control in favor of either side may have fatal consequences (adapted from (Laroux, 2004)). 3

Figure 2-1: Study flowchart illustrating sample acquisition, biochemical profiling through MS, and data analysis steps. Diagrams below each data symbol display empirical cumulative distribution of the corresponding dataset, with the number of elements indicated below the data symbols.....10

Figure 2-2: (a) Temporal changes in averaged PC1 for LPS and placebo treated subjects. (b and c) Trajectory averages in PC1-PC2 coordinates (b) and time-PC1-PC2 space (c). (Star sign indicates significance ($p<0.01$) measured by Wilcoxon rank sum test and error bar indicate standard error of the mean). (d) Per cent of the variance captured by each principal component. 12

Figure 2-3: Heat map displaying the differential patterns of metabolic response to LPS. Two clusters of plasma metabolites reflect two distinct patterns with opposing temporal directionality. Clustered metabolites and their associations with the metabolic pathways are also listed in Table 2.1. 13

Figure 2-4: Pathway associations illustrating the conversion of methionine to one of the major anti-oxidants, glutathione. Metabolites captured in the clustering analysis are indicated with a the name of the cluster and a color bar representing up-(red) or down-regulation (green) at 6h and 24h time points.....17

Figure 3-1: Designs of the transcriptomic and metabolomic studies. 23

Figure 3-2: All differential transcripts clustered into three, displaying early up-regulated, late up-regulated and down-regulated profiles. Heat map on the left

shows the transcriptional expression of all differential transcripts in these three clusters while diagrams on the right display the average expression profiles for all transcripts in each cluster (vertically in the same order as the heat map). Horizontal yellow lines on the heat map designate the limits of each cluster. 26

Figure 3-3: Differential patterns of response to LPS in plasma metabolite levels form two clusters reflecting distinct patterns with opposing temporal directionality. Heat map on the left displays temporal changes in plasma concentrations of all differential metabolites and diagrams on the right shows the average concentration profiles for all metabolites in each of those two clusters (vertically in the same order as the heat map). Horizontal yellow lines on the heat map designate the limits of each cluster. 28

Figure 3-4: Qualitative representation of the temporal differences between observed response patterns in gene expression and metabolite concentrations. 31

Figure 3-5: Subset of differentially expressed transcripts associated with metabolic processes display very similar patterns to the original clusters shown in Figure 3-2. Heat map on the left shows these early upregulation, late upregulation and downregulation patterns while diagrams on the right display the average expression profiles for all transcripts in each cluster (vertically in the same order as the heat map). Horizontal yellow lines on the heat map designate the limits of each cluster. 32

Figure 4-1: Schematic description of the experimental and clinical sources of data. 43

Figure 4-2: Scatter plots show the direction and extent of changes in the metabolites that were significantly deviated from baseline in sepsis (A) and SIRS (B) groups in relation to corresponding trends in endotoxemia. For the clinical data, plots reflect the maximum observed change from the baseline if that particular metabolite found to be significant in both time points, $t_{0,clinical}$ and $t_{24,clinical}$. 52

Figure 5-1: Structure similarity of methylprednisolon (MPL) and endogenous glucocorticoid hormone cortisol. 58
Figure 5-2: Mechanism of action of corticosteroids, adapted from (Jin et al., 2003). 59
Figure 5-3: Workflow for hierarchical clustering of the concatenated transcriptomic-proteomic dataset. 64
Figure 5-4: Heat map of clustered concatenated dataset. Red color indicates increase in expression while green indicates decrease. 66
Figure 5-5: Workflow for sequential clustering analysis carried out in both forward and reverse directions between proteomic and transcriptomic datasets. 70
Figure 5-6: Five clusters of proteins obtained by consensus clustering (a-e, left side), and heat maps of corresponding hierarchically clustered probesets (a-e, right side). Canonical pathways enriched by the proteins in these clusters are given Table A. 4. 73
Figure 5-7: Five clusters of transcripts obtained by consensus clustering (a-e, left side), and heat maps of corresponding hierarchically clustered protein datasets (a-e, right side). 75
Figure 6-1: Study design for studying the effects of hypercortisolemia coupled with infectious stimuli, mimmicking the high stress experienced by sepsis patients. Nine healthy subjects received continuous cortisol (or saline) infusion starting 24h before the bolus LPS injection and continuing until 6h after the injection. Blood samples were collected and leukocytes were isolated at multiple time points over 24h both before and after LPS administration. 84
Figure 6-2: Change in the level of plasma cortisol (a) and total number of white blood cells (WBCs) (b) and percentage of WBC subpopulations (c-e) in response to

continuous cortisol infusion and LPS administration (dashed line: saline + LPS; solid line: cortisol + LPS). 85
Figure 6-3: Transcriptional responses of leukocytes to cortisol prior to endotoxin administration in time period between -24h and 0h. 86
Figure 6-4: Overall differential response to LPS between cortisol+LPS and saline+LPS groups. 5 clusters obtained by consensus clustering were grouped into 3 based on response to cortisol between -24h and 0h as: (a) LPS dominated (17 probesets), (b) cortisol enhanced (74 probesets), and (c) cortisol suppressed (66 probesets). 89
Figure 6-5: Mechanism of receptor downregulation in liver in response to MPL administration. Starting from the kinetics of drug concentration in the plasma (D), the differential equations below the schematic define and interrelate the rates of changes in the individual elements such as the receptor mRNA (R_m), receptor protein (R), drug-receptor complex in the cytoplasm (DR) and in the nucleus (DR(N)). 92
Figure 6-6: Diverse pharmacogenomic models and accompanying differential equations to describe various mechanisms of MPL's effects on hepatic gene expression (adapted from (Jin et al., 2003)). 93
Figure 6-7: Schematic representation of the network-based indirect response model to MPL (D). Glucocorticoid receptor (R) downregulation part of the model (on the left) has already been modeled. Once the drug-receptor complex translocates into the nucleus (DR(N)), drug induces its effects on the transcription of its target genes ($mRNA_1$, $mRNA_2$) either by stimulating it (white rectangle) or by inhibiting it (black rectangle). When transcribed messages are translated to the active proteins ($Protein_1$, $Protein_2$), they can also have effects (either stimulatory (green) or inhibitory (red)) on the transcription of target genes affected by MPL. All these

effects are considered as indirect as there might be additional biological processes in between. 94
Figure 6-8: Network of MPL responsive genes determined through functional enrichment analysis of transcriptional and proteomic data, and interaction database curated from literature. 95
Figure 6-9: Gene and protein expression network (bottom) integrated into the receptor downregulation part (top) of the MPL PK/PD model. Black rectangle indicates an inhibition whereas white rectangles indicate stimulation by DR(N). The edges of the network are color-coded to indicate activating (green) and inhibiting (red) interactions of the nodes. 98
Figure 6-10: Dynamics of the response to MPL in the first part of the model that defines the regulatory effect of MPL on the glucocorticoid receptor that it binds. 99
Figure 6-11: Simulation results for all mRNA and proteins taking part in the network of the MPL response model. Blue dashed lines indicate the experimental data and black solid lines show the simulation results. 100

Chapter 1 Introduction

The life is complex, at all scales. From a single cell to the whole body, there are thousands of intricate mechanisms that control every aspect of this complexity. The ultimate aim of biomedical sciences is to establish a thorough understanding of how these control mechanisms function when we're healthy, and how the control is lost (or shifted to a new mode) when we display symptoms of a disease, in order to explain the observed phenotypic changes with the known paradigms at the molecular level. Our ability to collect information on the molecular events taking place in our bodies have been tremendously increased with the great advancements in technology, however we still have a long way to go for finding the best ways to fully utilize this information.

Today we have tens of "–omics" tools available, each of which makes it possible to observe the physiologic responses at their complementary level. They enable the examination of a broad array of cellular or systemic elements and functions through the use of vast amounts of quantitative or semi-quantitative data from various levels of biological organizations (Richards et al., 2010). Systems biology rises on these new technologies and currently its biggest challenge is to devise methods to integrate the produced vast amount of information into a conceptual framework that is holistic, quantitative and predictive (Kritikou et al., 2006). The prospect is to reach a thorough understanding of the biological mechanisms driving different processes in our bodies and get insights into how we could manipulate these processes for our benefits.

Inflammation is one of those core processes through which we produce responses against various stressors, such as pathogens or trauma. It is a complex and multiscale biological phenomenon that needs to be orchestrated under tight regulation (Laroux, 2004). Factors inducing physiological stress are sensed and translated into biological

cues that transmit signals throughout the organs and down to the cellular level. These incoming signals are then recognized and processed to produce a response in a dynamic and highly regulated manner. Collective responses of the cells are reflected at the individual organ level, and ultimately in the whole body, by changing dynamics of biological metrics (Figure 1-1).

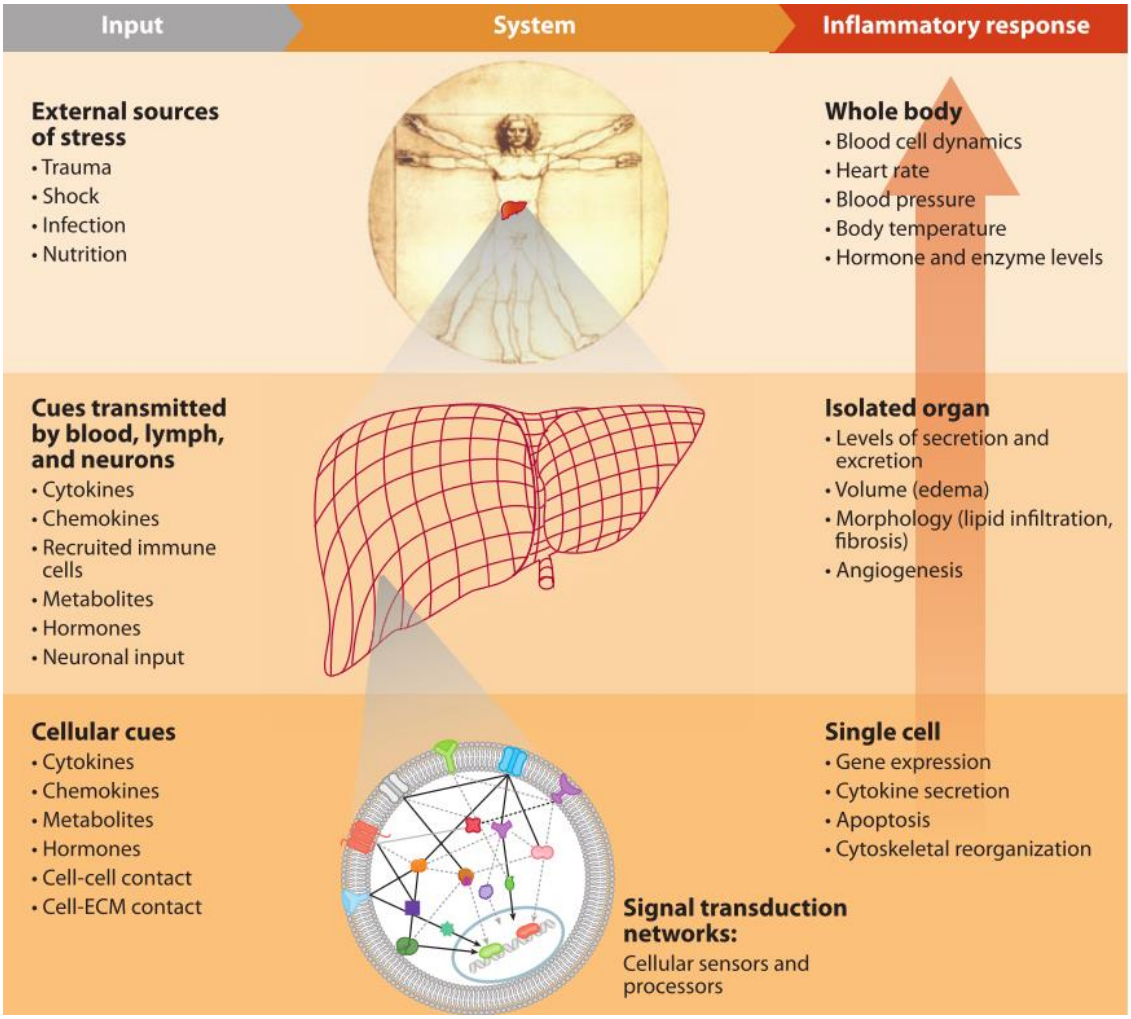

Figure 1-1: Multiscale nature of inflammatory response.

Under normal conditions, the outcome of inflammation is the mounting of required immune response for pathogens or regeneration after injury; however, in any instance

of dysregulation of this complex process, it is very likely to become a prolonged course that can damage the body further or lead to an uncontrolled systemic disease state and eventual multiple organ failure (Figure 1-2) (Bone, 1996).

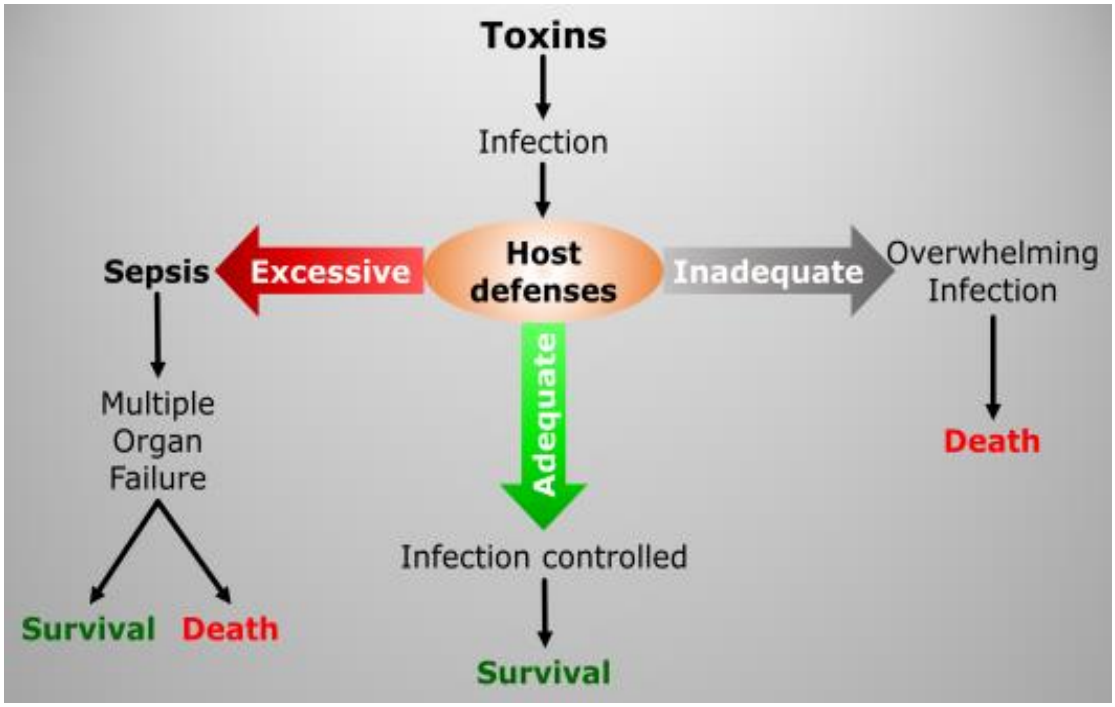

Figure 1-2: Inflammatory response is a complex process which has to be tightly regulated in order to balance the defense mechanisms of the host with the severity of infection/tissue damage. Loss of this control in favor of either side may have fatal consequences (adapted from (Laroux, 2004)).

Considering its critical role in our survival, inherent complexity and intricate relationships with other essential physiologic processes; inflammation and inflammatory diseases are among the top research fields that can benefit from adapting the systems approach. In this respect, the emerging -omics tools are very promising, since they offer the advantage of observing the inflammatory response at a much broader level together with the ability to analyze multiple variables

simultaneously which empowers the application of systems analysis for rationalizing and modeling the course of physiologic events.

Comprehending the continuum of physiologic responses to pathologic stimuli is essential for making sense of how molecular level changes develop to induce observable symptoms of a particular disease. Drugs, i.e. pharmacologic stimuli, are intended to reverse this disease progression and reduce the symptoms. For most cases the physiologic effects of drugs are also complex, involving re-directing the physiologic responses to alleviate the symptoms of a particular pathologic condition as well as inducing adverse-effects associated with off-target reactions. Analyses of the physiologic effects of drugs by monitoring a handful of markers for the targeted effects has been used for building models for drug's action for many years. Extensive –omic analyses done at multiple physiologic levels, however, also impacted this research area tremendously and initiated a shift from classic pharmacokinetic/pharmacodynamic modeling (PK/PD) towards a systems approach, named as quantitative systems pharmacology (QSP) (Jusko, 2013, Androulakis, 2015, Iyengar et al., 2012). The ultimate directions for this field are the realization of personalized and precision medicine by building progressively more accurate drug action models. However, the first steps towards these goals involve devising methods to fully utilize the wealth of information produced by the extensive analyses of pharmacologic responses.

This dissertation is centered on integrating information from multiple relevant physiologic levels in order to investigate the relationship between the inflammation and metabolism. We focused on how this critical relationship is shaped over time during the development of response to a systemic inflammatory stimuli in the human endotoxemia model as well as in response to a corticosteroid treatment in an animal model. The systems approach allowed us to track the continuum of physiologic responses; through their evolution over time and in relation to multiple dynamics

running in harmony. We extracted the coherent dynamic responses represented in the -omics analyses at multiple physiologic levels and integrated them through multiple approaches.

Chapter 2 and Chapter 3 are concerned with understanding the ways in which systemic inflammation shifts the metabolic balances and how these shifts feedback to shape inflammatory response, in turn. The analyses described in these chapters include metabolic and transcriptional responses to endotoxemia, which is an experimental model in humans that recapitulates the dynamics of systemic inflammatory response in a reproducible and safe manner in healthy subjects. In Chapter 4, we discuss the relevance of this experimental model to clinical cases of systemic inflammation and sepsis. We compare and contrast the metabolic changes observed in the subjects participated in endotoxemia study with those observed in patients battling with sepsis and systemic inflammatory response syndrome (SIRS). In Chapter 5, we switch from progression of inflammatory response to the anti-inflammatory therapy side and focus on the effects of a commonly-used corticosteroid in liver and consequently, the whole body metabolism. This analysis represents a more direct integration approach, in which we evaluate the concordance of the hepatic response to the drug treatment at gene and protein expression levels. Finally in Chapter 6, we discuss perspectives and approaches by which these studies can be advanced in the future. These include adding a stress component to endotoxemia model by continuous infusion of cortisol to make it even more relevant to clinical cases, and a network-based approach that integrates our insights from the bi-level hepatic response the corticosteroids with the existing pharmacokinetic/pharmacodynamic models.

Chapter 2 Temporal Metabolic Profiling of Plasma in Experimental Human Endotoxemia

Elective administration of bacterial endotoxin (lipopolysaccharide; LPS) to healthy human subjects has been used as a reproducible experimental procedure providing mechanistic insights into how cells, tissues and organs respond to systemic inflammation. Low doses of LPS transiently alter many physiologic and metabolic processes in a qualitatively similar manner to those observed after acute injury and systemic inflammation (Lowry, 2005, Calvano and Coyle, 2012); thus allowing the analysis of the responses to infectious stress at multiple physiological levels. This model has been extensively employed for the development and assessment of rational clinical therapies to prevent or attenuate systemic inflammatory response syndrome (SIRS) (Calvano and Coyle, 2012).

Response to endotoxemia is closely associated with alterations in metabolism. Inflammatory processes change the direction of the substrate flow from the periphery towards splanchnic organs while also triggering the release of catabolic signals in order to meet increased energy and substrate demands (Fong et al., 1990, Khovidhunkit et al., 2004); and hence, considerably altering the levels of plasma metabolites. Individual changes in the major metabolites, such as some lipids, amino acids and glucose, has been previously documented for the case of human endotoxemia (Fong et al., 1990). However, an untargeted, bioinformatics empowered approach to elucidate the effects of endotoxemia on the plasma metabolite levels is lacking.

Analysis of the complete metabolic response to systemic inflammation is of special interest since metabolic composition of a tissue is uniquely altered in response to stimuli due to collective effects of the regulations at various levels of cellular processes including transcription, translation and signal transduction. Concentrations of

metabolites in a sample at a given time, i.e. the "metabolome" (Nicholson and Lindon, 2008), can be thought of as the metabolic fingerprint representative of the state of body at that time and provide information on the dominant regulatory mechanisms. The emerging field of metabonomics, combines this unique metabolic information with bioinformatics approaches to provide an integrated temporal picture of the interactions in the system (Nicholson, 2006, Holmes et al., 2008). Since the ultimate phenotype is determined by eventual production of metabolites through the complex cellular processes trickling down from transcription, translation and signal transduction, this field offers promise in advancing the knowledge in many clinical conditions. For endotoxemia, understanding the alterations in plasma metabolome is critical; since, metabolite levels impacts the regulation of anti-inflammatory defenses, in turn, through steering critical cellular processes in immune cells (Pearce and Pearce, 2013).

This study constitutes the first attempt of a complete metabonomic analysis describing the alterations in plasma metabolite composition following exposure to LPS.

2.1 Methods

2.1.1 Human Plasma Samples

Archived blood plasma samples which had been flash frozen were used in this proof-of-principle study. These samples had been collected from 19 healthy subjects, between ages 18-40, who provided written, informed consent under guidelines approved by the Institutional Review Board (IRB) of Robert Wood Johnson Medical School. 15 of the subjects (11 males and 4 females; mean age of 22.7) had been administered National Institutes of Health (NIH) Clinical Center Reference Endotoxin, at a bolus dose of 2 ng/kg body weight as previously described (Alvarez et al., 2007, Jan et al., 2009, Jan et al., 2010). 4 control subjects (3 males and 1 female; mean age of 22.2) had been administered placebo (saline). During the protocol, subjects had received a solution of 5% dextrose and 0.45% saline crystalloid. Blood draws had

been conducted sequentially at t=1, 2, 6, and 24 hr from both groups, samples had been inventoried and stored at -80°C until the analysis.

2.1.2 Biochemical Profiling of Plasma Samples

Metabolomic analysis was performed by Metabolon (Durham, NC, USA) according to previously published methods (Evans et al., 2009). Briefly, samples were prepared by using a proprietary series of organic and aqueous extractions to attain the maximum recovery of small molecules while eliminating the protein fractions in plasma. The resulting extracts were subjected to either liquid chromatography (LC) or gas chromatography (GC) followed by mass spectroscopy (MS) analysis.

The data extraction of the raw MS data files yielded information that were loaded into a relational database in which the information was examined and appropriate QC limits were imposed. Peaks were identified using Metabolon's proprietary peak integration software, and component parts were stored in a complex data structure. Compounds were identified by comparison to library entries of purified standards or recurrent unknown entities. Identification of known chemical entities was based on comparison to metabolomic library entries of purified standards. The combination of chromatographic properties and mass spectra gave an indication of a match to the specific compound or an isobaric entity. For the samples which took multiple days to analyze, a data normalization step was performed to correct variation resulting from instrument inter-day tuning differences. The quality control and curation processes were used to ensure accurate and consistent identification of true chemical entities, and to remove those representing system artifacts, misassignments, and background noise.

2.1.3 Data analysis

After identification of the metabolites, the complete dataset of 366 metabolites with temporal profiles was rigorously analyzed through multiple steps. These included filtering for differential metabolites, principal component analysis (PCA) and clustering. Imputed and scaled (to set the median equal to 1) datasets were investigated to identify the metabolites which show differential temporal profiles between LPS and placebo groups by using software for the extraction and analysis of gene expression (EDGE) (Leek et al., 2006). The significance threshold for this test was set as q value <0.1 and p value <0.05. Using these differential metabolites, PCA was performed and the averages of first principal component (PC1) for each treatment group were plotted against time. One way ANOVA was performed to evaluate the significance of PC1 variance over time for each treatment group. Then, to compare PC1 values at each time point, Wilcoxon rank sum test is used (with 1% significance level). Finally, the datasets containing differential metabolites were concatenated to form one single matrix, which was then clustered through consensus clustering (Nguyen et al., 2009) (with p-value = 0.05) with the goal to identify the subsets of metabolites with coherent temporal profile in LPS and placebo groups. Interpretation of the biological significance these profiles demonstrate were based on the individual metabolite identities and curated metabolic pathways obtained from publicly available Kyoto Encyclopedia of Genes and Genomes (KEGG) (Lissauer et al., 2009) and Human Metabolome Database (Wishart et al., 2013) as well as Ingenuity Knowledge Base (Calvano et al., 2005).

2.2 Results

This study aimed to identify the major coherent patterns in human plasma metabolome within the 24 hours after systemic LPS exposure. The study design, a flowchart of which is shown in Figure 2-1, involved two groups of healthy subjects treated either with a bolus dose of 2 ng/kg body weight LPS or placebo (saline) injection at t=0. The

blood samples were collected from the subjects at 4 time points throughout 24 h post-treatment and the response was determined via non-targeted biochemical profiling through MS analysis.

Global biochemical profiles obtained by GC-MS and LC-MS/MS platforms represented temporal information on 366 metabolites including amino acids, short peptides, carbohydrates, lipids, nucleotides, cofactors and vitamins, xenobiotics and intermediate products of major energy production pathways. We first filtered the data through an algorithm originally designed for gene microarray experiments, Extraction

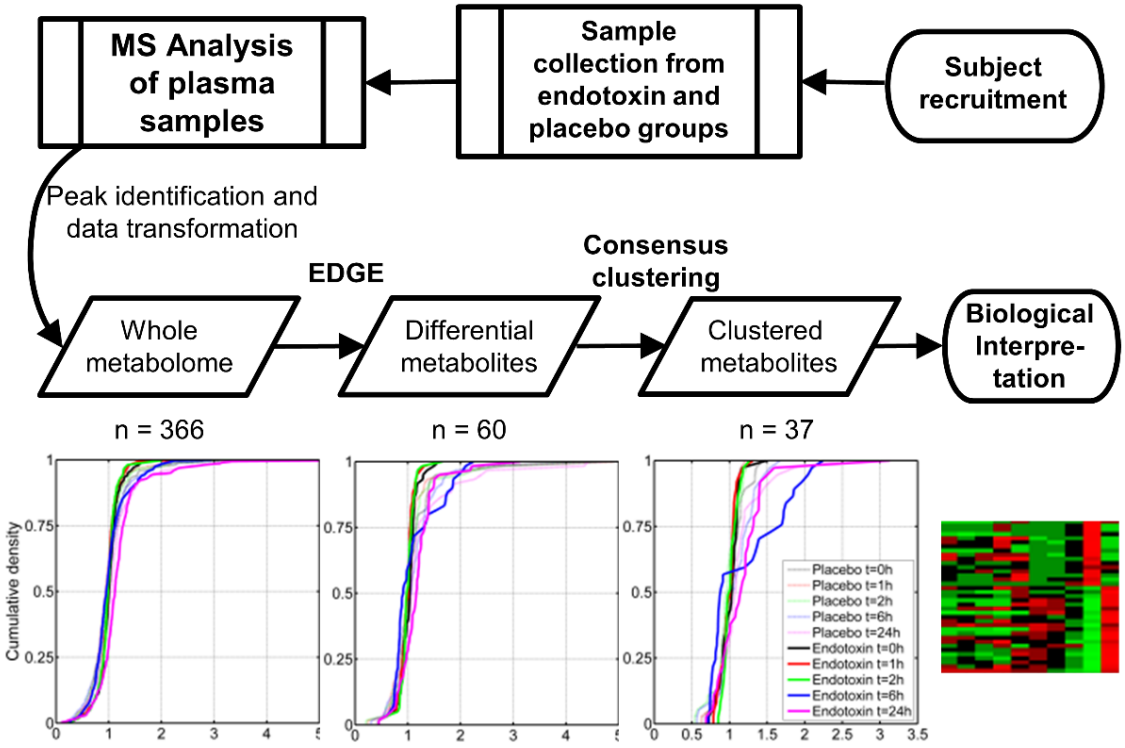

Figure 2-1: Study flowchart illustrating sample acquisition, biochemical profiling through MS, and data analysis steps. Diagrams below each data symbol display empirical cumulative distribution of the corresponding dataset, with the number of elements indicated below the data symbols.

of Differential Gene Expression (EDGE). EDGE procedure utilizes an optimal discovery procedure that uses relevant information from all the elements in the dataset in order to test each for differential expression (Leek et al., 2006). By applying this algorithm to metabolome dataset we first identified metabolites with differential temporal profiles between LPS and placebo groups. 60 out of the 366 metabolites showed differential profiles which met p-value < 0.05 and q-value < 0.1 cut-offs of EDGE software. The utility of this filtering step was also evident from the change in cumulative distributions of data before and after EDGE as shown in Figure 2-1. While both treatment groups have almost uniform distributions when the complete metabolome dataset is used, LPS treatment group became distinguishable from placebo at certain time points when only the differential metabolites were included in the analysis.

To identify the dominant patterns among the temporal profiles of these differential metabolites, PCA was performed. The averages of the first two principal components (PC1 and PC2) for the two treatment groups were plotted against time and against each other in Figure 2-2 a-c. As shown in the bar chart in Figure 2-2 d, although much of the variance (63%) was captured by the PC1, PC2 had also contributed in explaining the variability between the subjects in two experimental groups. In average, subjects treated with LPS were clearly separated in both PC1 and PC2; while saline treated subjects showed less variation in PC2, but even lesser in PC1.

Average PC1 was analyzed as a function of time in a one way between subjects analysis of variance (ANOVA) and results indicated that variation of PC1 over time for LPS groups is significant (p-value = 1.38×10^{-37}) whereas for saline group it is not ($p > 0.01$). Significance analysis of the PC1 at each time point by Wilcoxon rank sum test identified the most significant difference between the two groups at 6h (p-value = 0.00065), which separated the development and recovery phases of the LPS induced

metabolic changes. As shown in Figure 2-2 a, at 24h, average PC1 was still significantly different for the two groups, indicating that the recovery is still in progress.

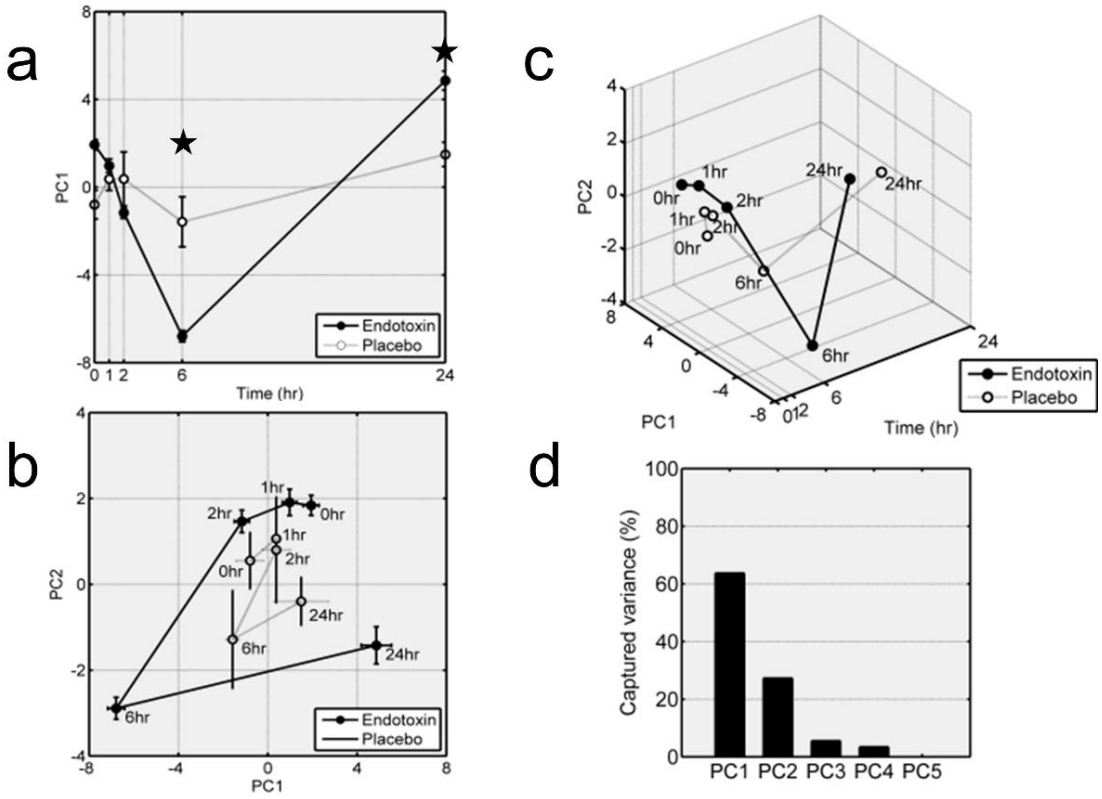

Figure 2-2: (a) Temporal changes in averaged PC1 for LPS and placebo treated subjects. (b and c) Trajectory averages in PC1-PC2 coordinates (b) and time-PC1-PC2 space (c). (Star sign indicates significance ($p<0.01$) measured by Wilcoxon rank sum test and error bar indicate standard error of the mean). (d) Per cent of the variance captured by each principal component.

To identify the subsets of metabolites with common coherent profiles, we applied consensus clustering (Nguyen et al., 2009) to the metabolites having differential temporal profiles in between LPS and placebo groups. Clustering is an essential tool for the analysis of high-content data based on organization of the signals with similar behavior. Identification of the coherent patterns which intensify and weaken over time

allows us to focus on closely associated interactions within the elements of the data. It also facilitates the recognition of temporal relationships between the sub-clusters of elements, which might imply regulatory hierarchy (Nguyen et al., 2009). It is worthwhile to note the refinement in the content of the data by comparing the difference between the empirical cumulative distributions of the clustered dataset from distributions in the previous datasets (Figure 2-1). In the clustered data, the distributions of LPS group became distinctly separated from the placebo group at each time point. Furthermore, in agreement with the PCA, distribution of the 6h data for LPS group displays an easily recognized divergence from the rest of the data.

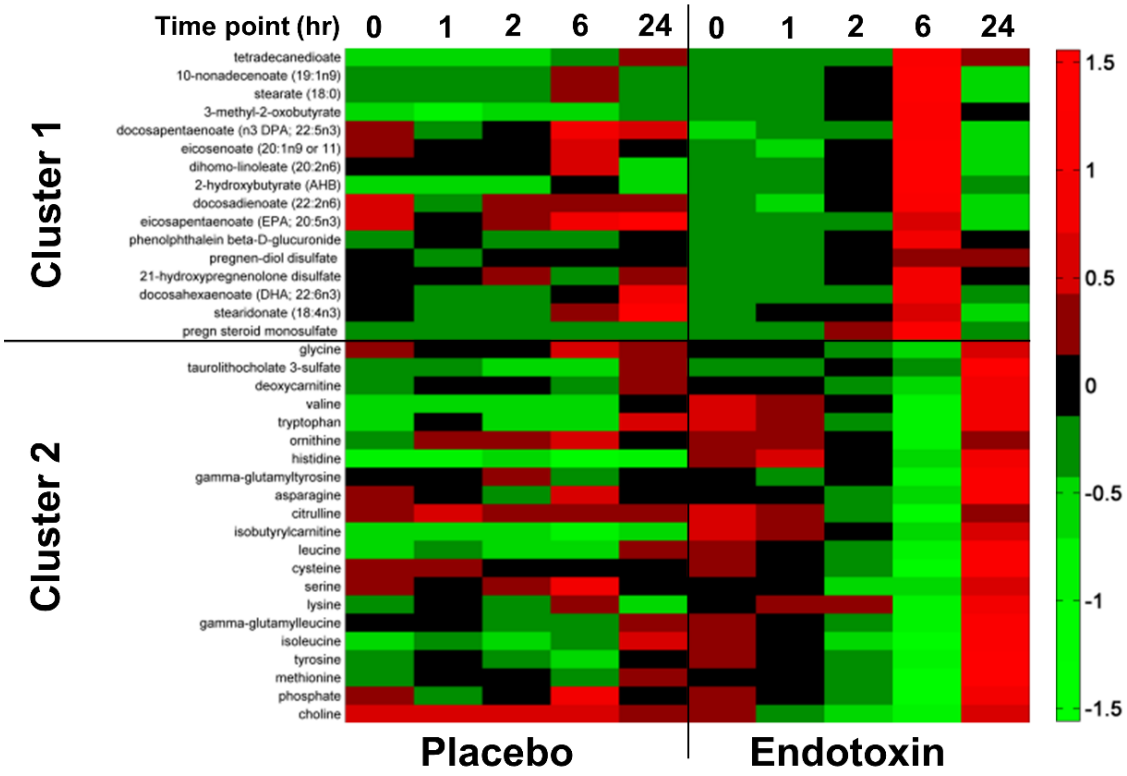

Figure 2-3: Heat map displaying the differential patterns of metabolic response to LPS. Two clusters of plasma metabolites reflect two distinct patterns with opposing temporal directionality. Clustered metabolites and their associations with the metabolic pathways are also listed in Table 2.1.

Consensus clustering of the differential metabolites further refined the data and returned 37 of the total of 60 differential metabolites, classified into one of the two clusters with opposing temporal directionality as shown in Figure 2-3. Metabolites in each cluster and their associations with the metabolic pathways are listed in Table 2.1.

The first cluster (16 metabolites) was up-regulated within the first 6h; down-regulated by the end of 24h and was mostly composed of metabolites from pathways related to lipid metabolism. The second cluster (21 metabolites), in contrast, was down-regulated within the first 6h post-LPS; then up-regulated by the 24h. Strikingly 14 out of 21 metabolites in this cluster were amino acids or their derivatives and an additional 2 were dipeptides indicating a significant regulatory shift in the protein metabolism.

2.3 Discussion

This study identified the coherent changes in temporal patterns of plasma metabolite levels in response to low dose LPS exposure by using untargeted analytical methodology and unsupervised data analysis techniques. Most striking differences between treatment and control groups were observed in amino acid and lipid levels which displayed self-resolving patterns with different directionality forming two distinct clusters. While amino acids and amino acid derivatives were steadily cleared out from plasma; lipids, mostly mono- and poly-unsaturated fatty acids, accumulated within the first 6h following LPS administration, after which the direction of the response was reversed for these two distinct patterns indicating recovery.

Table 2.1: Distribution and classification of the differential metabolites to the clusters shown in Figure 2-3.

	Biochemical	Sub-pathway	Super pathway
Cluster 1	2-hydroxybutyrate (AHB)	Cysteine, methionine, SAM, taurine metabolism	Amino acid
	3-methyl-2-oxobutyrate	Valine, leucine and isoleucine metabolism	
	Docosahexaenoate (DHA; 22:6n3)	Essential fatty acid	Lipid
	Docosapentaenoate (DPA; 22:5n3)		
	Eicosapentaenoate (EPA; 20:5n3)		
	Tetradecanedioate	Fatty acid, dicarboxylate	
	Stearidonate (18:4n3)	Long chain fatty acid	
	Dihomo-linoleate (20:2n6)		
	Docosadienoate (22:2n6)		
	10-nonadecenoate (19:1n9)		
	Eicosenoate (20:1n9 or 11)		
	Stearate (18:0)		
	21-hydroxypregnenolone disulfate	Sterol/Steroid	
	Pregn steroid monosulfate		
	Pregnen-diol disulfate		
	Phenolphthalein beta-D-glucuronide	Detoxification metabolism	Xenobiotics
Cluster 2	Asparagine	Alanine and aspartate metabolism	Amino acid
	Cysteine	Cysteine, methionine, SAM, taurine metabolism	
	Methionine		
	Glycine	Glycine, serine and threonine metabolism	
	Serine		
	Histidine	Histidine metabolism	
	Lysine	Lysine metabolism	
	Tyrosine	Phenylalanine & tyrosine metabolism	
	Tryptophan	Tryptophan metabolism	
	Citrulline	Urea cycle; arginine, proline metabolism	
	Ornithine		
	Isobutyrylcarnitine	Valine, leucine and isoleucine metabolism	
	Isoleucine		
	Leucine		
	Valine		
	Phosphate	Oxidative phosphorylation	Energy
	Taurolithocholate 3-sulfate	Bile acid metabolism	Lipid
	Deoxycarnitine	Carnitine metabolism	
	Choline	Glycerolipid metabolism	
	Gamma-glutamylleucine	Gamma-glutamyl	Peptide
	Gamma-glutamyltyrosine		

Among the **first cluster** of metabolites; 13 out of total 16 were lipids, more specifically, essential and non-essential long chain fatty acids (FAs) including 4 omega-3 FAs, *docosahexaenoate (DHA), docosapentaenoate (DPA), eicosapentaenoate (EPA)*, *stearidonate*; and 2 omega-6 FAs, *dihomo-linoleate (eicosatrienoate)* and *docosadienoate;* and a major saturated FA, *stearate,* in addition to 3 pregnenolone

derivatives taking part in steroid hormone biosynthesis. Coherent up-regulation pattern observed in these plasma FAs at 6h is consistent with the lipolysis, a well-known adaptive response to inflammation (Fong et al., 1990). The peripheral mobilization of lipid stores in the form of free FAs was initially considered as a result of catecholamine release in response to infection or injury; however increased biosynthesis and decreased oxidation in liver together with increased whole-body lipolysis are results of complex signaling interactions initiated by stress hormones such as catecholamines, as well as produced cytokines and LPS itself, collectively giving rise to accumulation of FAs in plasma. Since toll-like receptor 4 (TLR4) signaling initiated with recognition of LPS on the cell surface is responsible for expression of many cytokines, all of which have major downstream effects on metabolism, teasing apart individual direct and indirect effects of each on lipid homeostasis requires further research (Glass and Olefsky, 2012).

More pronounced increase in omega-3 FAs compared to omega-6 FAs may be related to their differential roles in the inflammatory response. These two fatty acid groups have opposing physiological functions: While omega-6 FAs give rise to pro-inflammatory prostaglandin and leukotriene synthesis, omega-3 FAs compete with omega-6 FAs to modulate this response by inducing the production of less inflammatory derivatives (De Caterina and Basta, 2001). Although, speculative at this level of global metabonomic analysis, selective concentration of omega-3 FAs in plasma in the initial 6h of response might have contributed to the resolution and recovery in the following hours. Since dietary supplementation of omega-3 FAs are shown to be associated with a moderate quenching effect on inflammation, this speculation based on the observed selective increase of omega-3 FAs might not be far from truth and might have served as an endogenous adaptive mechanism to suppress inflammation (Simopoulos, 2002). Interestingly, although increasing levels of free FAs

in plasma has been associated with insulin resistance (Agwunobi et al., 2000), glucose levels or associated metabolites in clustering analysis did not reflect a significant perturbation in any of the time points. This might have been related to the relatively fast and subtle kinetics of those metabolites.

Elevated *2-hydroxybutyrate* (or α-hydroxybutyrate; AHB) levels usually point towards increased oxidative stress because AHB is a by-product in the pathway leading to glutathione synthesis from methionine. The activity of this pathway (from methionine

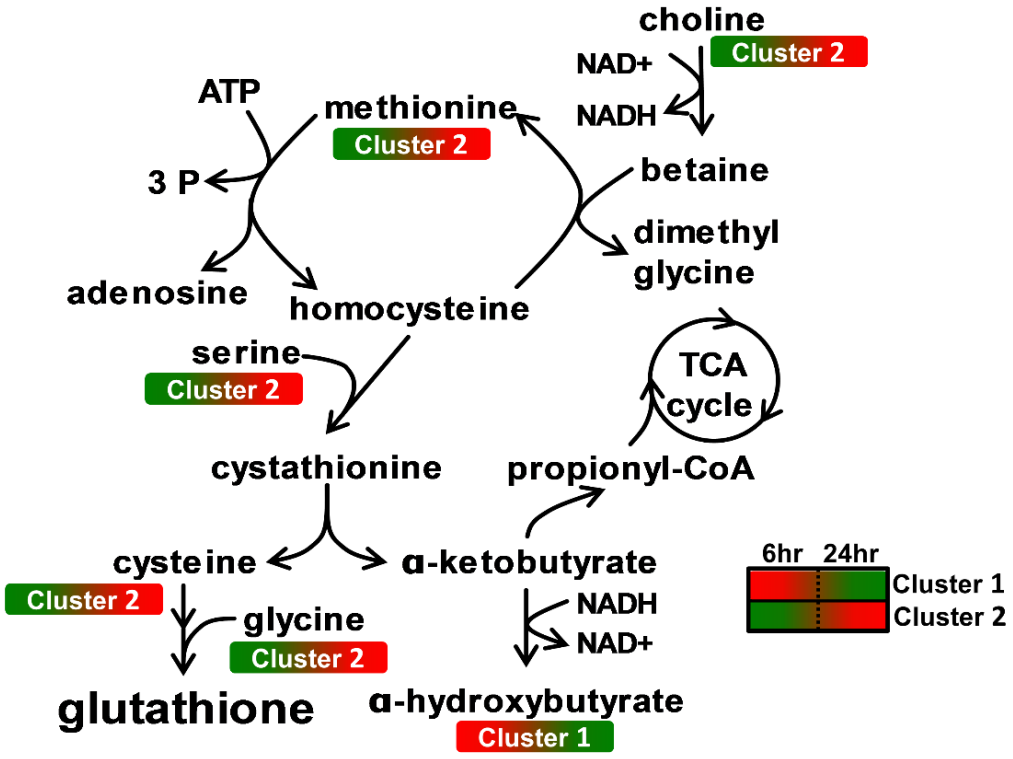

Figure 2-4: Pathway associations illustrating the conversion of methionine to one of the major anti-oxidants, glutathione. Metabolites captured in the clustering analysis are indicated with a the name of the cluster and a color bar representing up-(red) or down-regulation (green) at 6h and 24h time points.

→ cystathionine → cysteine → glutathione as shown in part of Figure 2-4) varies in response to the demands against elevated cellular oxidative stress (Lord and Bralley, 2008, Gall et al., 2010).

Increased oxidative stress shifts the flow of homocysteine away from transmethylation to methionine toward transulfuration to cystathionine, increasing the flow towards glutathione synthesis. Glutathione is one of the most important antioxidant proteins and plays a crucial role in mitigating the oxidative damage of reactive oxygen species, formation of which in liver is potently triggered by inflammation (Jaeschke, 2011). Therefore, increased AHB levels at 6h post-LPS coinciding with plummeting levels of *methionine*, *serine, cysteine* and *glycine* at the same time point can be interpreted as an indication of increased activity of hepatic oxidative defense mechanisms to effectively regulate the inflammatory response induced by LPS. Reverse of the first conversion in this pathway (homocysteine→methionine) is possible with incorporation of methyl groups to methionine. One source of the methyl groups for this reaction is betaine, which is derived from *choline* (Niculescu and Zeisel, 2002). Choline is in the second cluster which shows similar kinetics with the opposite direction of the first cluster, consistent with the opposing directionality in the reactions in this pathway.

3-methyl-2-oxobutyrate (or α-ketoisovaleric acid, KIV) is a branched chain keto-acid (BCKA) and a degradation product of valine which is formed in the initial step of branched chain amino acid (BCAA) catabolism. This conversion exclusively takes place in skeletal muscle due to relatively high activity of BCAA aminotransferase and it is an essential part of the BCAA-BCKA cycling between liver and muscle (Mattick et al., 2013, Holeček, 2002). Increase in KIV levels following LPS exposure occurs at the same time where *valine* concentrations are decreased in plasma, indicating an increase in BCAA catabolism to meet the increased metabolic demands of liver, which can utilize

KIV for transamination to other BCAAs for incorporation into acute phase proteins, or complete their degradation for energy production.

The accumulation of intermediates in the steroid hormone biosynthesis pathways such as *21-hydroxypregnenolone*, *pregnenolone sulfate*, *pregnanediol* in LPS treated subjects may suggest an increased capacity for steroid biogenesis which is required for the production of hormones to regulate glucose homeostasis and suppress inflammation. Increase in various derivatives of corticosteroid hormones were anticipated considering the primary roles of these hormones in regulation of inflammatory response and metabolism, and also were consistent with earlier studies (Fong et al., 1990, Agwunobi et al., 2000).

The **second cluster** displayed a response pattern almost exactly in the opposite direction of the first cluster. Concentrations of the metabolites in this cluster gradually decreased until 6h after LPS administration, preceding a recovery period in the following 18h. 14 out of 21 metabolites within this cluster were amino acids, strongly indicating their primary role in the immediate response to inflammatory insult. These 14 amino acids include 12 proteinogenic amino acids (*asparagine, cysteine, methionine, glycine, serine, histidine, lysine, tyrosine, tryptophan, isoleucine, leucine* and *valine*) and 2 core members of urea cycle (*citrulline* and *ornithine*). Presence of members of the urea cycle together with amino acid degradation pathway intermediates (*isobutyryl carnitine* and *deoxycarnitine*) indicates that amino acids are not only used as the building blocks for the acute phase proteins in liver, but also utilized as the substrates for energy production. Compensation for this rapid clearance of amino acids from plasma starts after 6h and is achieved possibly by the breakdown of protein reserves in skeletal muscle. Presence of proteolytic breakdown products (*gamma-glutamylleucine*, *gamma-glutamyltyrosine*) in this cluster might be associated with this process being incomplete.

Taurolithocholic acid 3-sulfate is a product of bile acid sulfation, which is a minor pathway under normal conditions. In the presence of intrahepatic cholestasis, associated with inflammation (Khovidhunkit et al., 2004), this reaction escalates, increasing the aqueous solubility and, consecutively, renal clearance of these compounds (St-Pierre et al., 2001). Therefore, an increase in the plasma concentration of these sulfated bile acids might indicate a decline in the renal function in response to LPS-induced inflammation. Furthermore, increased *phosphate* levels have also been suggested as a potential risk factor linked to renal failure (Voormolen et al., 2007). These two independent markers of declined renal function also being associated with the same temporal pattern, therefore, might be suggestive of an impairment of normal renal function in the LPS treated subjects.

2.3.1 Limitations

It should be emphasized that, although experimental model of human endotoxemia simulates systemic inflammation fairly well, it can be best described as a TLR4 agonist induced systemic inflammation (Calvano and Coyle, 2012). In this experimental model, the subjects are pre-screened medically to confirm normal general health; therefore care should be taken when extrapolating the implications of the results to clinically more complex conditions, such as sepsis. Another limitation of the study is related to the utilized data filtering and clustering procedures. Although these techniques ensure that subsets of metabolites with coherent temporal profiles are captured; at the same time, they might have masked some subtle changes which might be significant but not necessarily correspond to the observed dominant patterns. Metabolites which have a quickly resolving perturbation early in the time course, such as lactate (Michaeli et al., 2012), can be an example to this limitation. Furthermore, there is limited number of time points in the study and that the last two time points are considerably far from each other. We observe significant changes in the

metabolites starting at 6h which mostly resolve by 24h; however it is likely that some metabolites with different kinetics and show perturbations between these two time points might have been overlooked.

2.4 Conclusion

LPS administration in healthy humans significantly alters the homeostasis of lipid and protein metabolism in humans in the first 6h. Within 24h post-treatment, metabolite balances are mostly restored. Perturbation observed in the levels of plasma lipids may well be associated with the established lipolytic effect of inflammation, whereas amino acid deficiency observed early in response is likely due to increased hepatic uptake to meet the higher substrate demand for the synthesis of acute phase proteins and anti-oxidant defenses. Increase in some of the markers associated with renal failure later in the time course suggested that kidney function may have been deteriorated in subjects treated with LPS.

Chapter 3 Integration of Plasma Metabolomics and Leukocyte Transcriptomics in Response to Endotoxemia

Global transcriptomic studies of circulating leukocytes in experimental human endotoxemia previously elucidated the intricate regulatory schemes governing the inflammatory response (Calvano et al., 2005, Nguyen et al., 2011). However, inflammatory response is also closely associated with alterations in metabolism. In Chapter 2, we discussed the drastic effect of a mild inflammatory stimulus on the homeostasis of the whole-body metabolism (Kamisoglu et al., 2013b). This single level analysis uncovered the temporal patterns in the host metabolism reflecting collective impacts of regulations at various organs and at multiple levels of cellular processes including transcription, translation and signal transduction. For endotoxemia, understanding the alterations in plasma metabolome is critical, since metabolite levels impact the regulation of anti-inflammatory defenses, in turn, through directing critical cellular processes in immune cells (Pearce and Pearce, 2013).

Building on this knowledge; we integrated the transcriptional response of leukocytes with systemic metabolic response to understand how inflammation-induced changes in the composition of plasma, in turn, affects the transcriptional processes in the leukocytes. We hypothesized that the drastic changes in the immediate environment of the leukocytes might have an adaptive effect on shaping their transcriptional response in the regulation of metabolism in conjunction with the initial inflammatory stimuli.

3.1 Methods

This is a meta-study aiming to integrate biological insights gained from two levels of -*omics* analyses on the response to systemic inflammation induced by LPS in humans. The designs of both transcriptomic and metabonomic studies are shown in Figure 3-1.

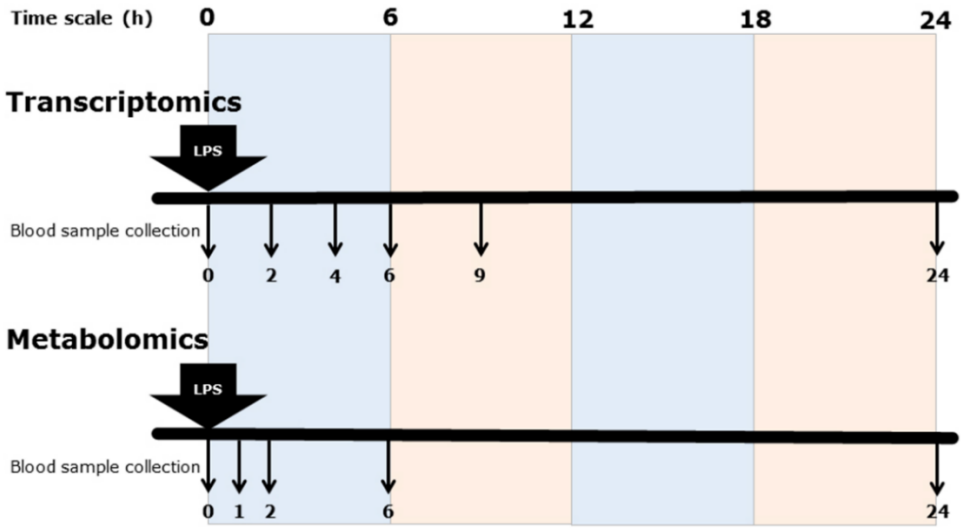

Figure 3-1: Designs of the transcriptomic and metabolomic studies.

For the transcriptomic study, 4 subjects (1 female and 3 male) had received LPS at a bolus dose of 2 ng/kg body weight and 4 subjects (1 female and 3 male) had received saline. Blood samples were collected before (t=0h) and 2, 4, 6, 9 and 24h after LPS administration. Leukocytes were recovered by centrifugation; total cellular RNA was isolated from the leukocyte pellets and hybridized onto Hu133A and Hu133B oligonucleotide arrays (Affymetrix). Further details about the experimental design are presented in the original analysis (Calvano et al., 2005). The transcriptional analysis generated expression measurement data of over 44000 probesets in total, which is also publicly available through the GEO Omnibus Database (http://www.ncbi.nlm.nih.gov/geo/) under the Accession No: GSE3284. Complete

details of the profiling of plasma metabolome has previously been described in Chapter 2.

3.1.1 Data analysis

Data analysis for both transcriptomic and metabolomic datasets started first by filtering for differential expression over time. Transcripts and metabolites with differential temporal profiles were determined by using EDGE software (Leek et al., 2006). The significance cut-off for the transcriptomic dataset were $p<0.05$ at 0.10 false discovery rate. To determine the potential co-regulatory relationships, differentially expressed transcripts and metabolites with differential temporal profiles were hierarchically clustered using `clustergram` function in the Bioinformatics toolbox of MATLAB (Mathworks, Natick MA). The two clusters were obtained by using `correlation` as the distance metric.

Pathway enrichment analysis of genes in the clusters were done in Enrichr (Chen et al., 2013) using the gene-set libraries of Kyoto Encyclopedia of Genes and Genomes (KEGG) (Kanehisa and Goto, 2000). Three types of enrichment scores are calculated by Enrichr to assess the significance of overlap between the input list and the gene sets in each gene-set library for ranking a term's relevance to the input list. These are Fisher exact test, z-score of the deviation from the expected rank by the Fisher exact test, and a combined score that multiplies the log of the p-value computed with the Fisher exact test by the z-score. The pathways which have a combined score higher than 1.0 were called significant. The combined score had been devised since Fisher exact test had a slight bias that affects the ranking of terms solely based on the length of the gene sets in each gene-set library (Chen et al., 2013).

The goal in the current analysis was to reveal transcriptional regulation of leukocyte metabolic processes, specifically, then to assess if these regulatory patterns might

have been affected by concurrent fluctuations of metabolite levels in the surrounding plasma along with the initial stimuli. For this purpose, we opted to focus the transcriptional analysis to the genes that are associated with metabolic processes *only*. Therefore, any differential transcripts which code for genes that are not associated with any of the metabolic pathways were filtered out. Gene set libraries and pathway classifications in KEGG database were used as reference at this filtering process. Then, clustering analysis was repeated for the remaining transcripts. Clustered metabolism associated genes were functionally annotated through Enrichr similar to the complete transcriptome described above.

3.2 Results

This study aimed to integrate the biological insights gained from two levels of *-omics* analyses on the response to systemic inflammation induced by LPS in humans. We integrated the analyses of transcriptional data obtained from circulating leukocytes and metabolomic data from plasma considering that the inflammatory processes considerably affect levels of plasma metabolites through collective impacts of regulations at various organs and at multiple levels of cellular processes including transcription, translation and signal transduction; and the responses of inflammatory cells might have been affected from the metabolic landscape of the fluid environment in which they circulate.

3330 of the transcripts, coding for 2562 unique genes, were differentially expressed based on $p<0.05$ and $q<0.1$ cut-offs applied on EDGE. Hierarchical clustering of these differentially expressed transcripts forms three characteristic patterns of response as discussed in the complete transcriptional analysis previously. These three patterns reflect early up-regulation, late up-regulation, and down-regulation of genes in response to LPS stimulus (Foteinou et al., 2009). Profiles of these three clusters are

shown in Figure 3-2 (on the right) together with the heat map of corresponding transcripts (on the left).

Simultaneously with these changes in leukocyte transcription, metabolite concentrations in the plasma also drastically change due to the effects of inflammatory signaling in the whole body. The metabolomic dataset included temporal concentration data of 366 plasma metabolites, and 60 out of these 366 had differential temporal

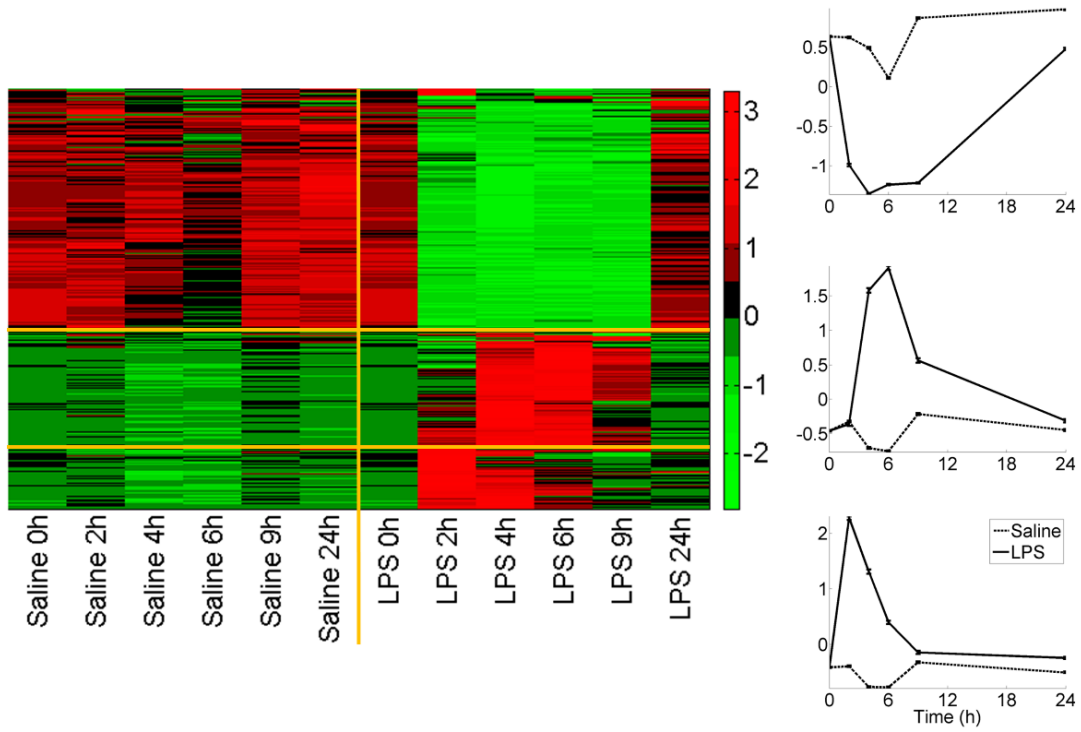

Figure 3-2: All differential transcripts clustered into three, displaying early up-regulated, late up-regulated and down-regulated profiles. Heat map on the left shows the transcriptional expression of all differential transcripts in these three clusters while diagrams on the right display the average expression profiles for all transcripts in each cluster (vertically in the same order as the heat map). Horizontal yellow lines on the heat map designate the limits of each cluster.

Table 3.1: Functional annotation of all differentially expressed genes in the three clusters displayed in Figure 3-2.

	Pathway	Genes
Early Up	Toll-like Receptor Signaling Pathway	IL1B, MAP2K6, MAPK3, CCL3, NFKBIA, CCL4, MAP2K3, NFKB2, TICAM1, TNF, IL8
	Hematopoietic Cell Lineage	IL1B, IL1A, CSF2, IL1R2, TNF, MME, GP1BB, CD24, ITGA1, CD55
	Adipocytokine Signaling Pathway	NFKB2, CAMKK2, IRS2, IRS1, TNF, NFKBIE, NFKBIB, NFKBIA
	Cytokine-Cytokine Receptor Interaction	IL1R2, BMP2, CXCL1, CSF2, CXCL3, CXCL2, CCL20, IL8, IL17RA, IL1B, IL1A, CCL3, CCL4, ACVR1B, IFNGR2, TNF
	MAPK Signaling Pathway	MAP2K6, MAPK3, IL1R2, MAP2K3, NFKB2, CACNG5, GADD45B, DUSP2, PDGFA, IL1B, IL1A, MAP4K4, MAPKAPK2, CACNA1S, ACVR1B, TNF
	Apoptosis	NFKB2, IL1B, IL1A, BID, TNF, NFKBIA, CFLAR
	FCε RI Signaling Pathway	MAP2K6, PRKCD, MAPK3, CSF2, TNF, MAP2K3
	Arachidonic Acid Metabolism	PTGS2, GGT1, GPX3, CYP4F3, CYP4F2
Late Up	Toll-like Receptor Signaling Pathway	TLR1, TLR2, TLR4, TLR5, CXCL11, TLR8, PIK3CG, RELA, MAPK8, SPP1, TOLLIP, NFKB1, NFKB2, IFNAR1, STAT1, MAPK14, IRF7, CD14
	Jak-STAT Signaling Pathway	IL6ST, STAT5B, CSF3R, PIK3CG, SOCS3, PIM1, GRB2, IL4R, CSF2RB, IL13RA1, IFNAR1, OSM, IL10RB, SOS2, IL2RG, STAT1, STAT3, CISH, STAT2, IRF9, JAK3
	Apoptosis	NFKB1, NFKB2, IL1RAP, CSF2RB, FAS, PIK3CG, IRAK2, RELA, TNFRSF10C, IL1R1, TNFRSF1A, IRAK3, CFLAR, TNFSF10
	Adipocytokine Signaling Pathway	NFKB1, NFKB2, SOCS3, RELA, MAPK8, NFKBIB, TNFRSF1A, ACSL1, ACSL4, ACSL3, STAT3, JAK3
	Cytokine-Cytokine Receptor Interaction	IL6ST, FAS, IL1R1, HGF, IL4R, IL1RAP, IL13RA1, TNFRSF10C, CCR1, IL10RB, IL18R1, IL18, CXCL11, IL17RA, CSF3R, TNFSF10, CSF2RB, IL18RAP, IFNAR1, OSM, TNFSF13B, TNFRSF1A, IL2RG
	Hematopoietic Cell Lineage	CD44, IL4R, CSF3R, IL1R1, ITGAM, FCGR1A, CD24, CR1, CD55, CD59, CD14
	FCε RI Signaling Pathway	PIK3CG, LYN, MAPK8, LCP2, GRB2, SOS2, FCER1G, VAV1, MAPK14
	MAPK Signaling Pathway	FAS, MAPK8, IL1R1, NFKB1, NFKB2, CACNG3, MAP3K13, MKNK1, SOS2, DUSP5, DUSP3, RPS6KA2, MAPK14, CD14, STK3, ARRB2, GRB2, CACNA1A, TNFRSF1A
	B Cell Receptor Signaling Pathway	NFKB1, NFKB2, PIK3CG, LYN, LILRB3, NFKBIB, VAV1
	T Cell Receptor Signaling Pathway	NFKB1, NFKB2, PIK3CG, LCP2, GRB2, NFKBIB, SOS2, PTPRC, VAV1
Down	Ribosome	RPL36A, RPL19, RPL14, RPL13, RPL11, RPL12, RPL35A, RPS16, RPS12, RPS13, RPS10, RPS11, RPS25, RPS29, RPL7, RPL6, RPL9, RPL8, RPS20, RPL10A, RPS21, RPS23, RPS24, RPL23A, RPS6, RPS5, RPS8, RPS7, RPL18A, RPL37A, RPS2, RPS3, RPS3A, RPL35, RPS15A, RPL37, RPL38, RPL30, RPL32, RPL31, RPL27, RPL24, RPL28, RPL29, RPL13A, RPL21
	Hematopoietic cell lineage	FLT3LG, CD3G, CD3D, CD3E, CD36, CD33, HLA-DRA, HLA-DRB1, IL7R, CD4, CD5, CD7, CSF1R, CD1C, ITGA4, ITGA6, IL5RA
	T Cell receptor signaling pathway	AKT3, CD3G, CD3D, CD3E, CD40LG, LCK, RASGRP1, ZAP70, PPP3CC, CD4, NFATC2, NFATC3, PIK3R1, NFATC1, ITK, VAV2, FYN
	Cell Cycle	CDC16, CUL1, ANAPC1, ANAPC5, RBL1, WEE1, ANAPC10, CHEK2, ATR, CDKN1C, PCNA, MAD1L1, TP53, CDK6, MCM6, CCND2, BUB3, YWHAQ
	N Glycan Biosynthesis	GANAB, FUT8, ALG1, STT3B, RPN2, MGAT4A, ST6GAL1, MAN2A1, MGAT2

profiles from control (at $p<0.05$ and $q<0.05$). These profiles displayed two distinct patterns of metabolomic changes, as shown in Figure 3-3 (right).

The two clusters of metabolites showed either strong up- or down-regulation within the first 6 hour post-LPS, and changed direction to move toward resolution then on. The metabolite groups which showed the highest deviation were peaking lipids (essential and long chain fatty acids, lysolipids, sterols/steroids) and plunging amino

acids. All metabolites with differential temporal profiles grouped in two clusters are listed in Table 3.2 together with their molecular classifications.

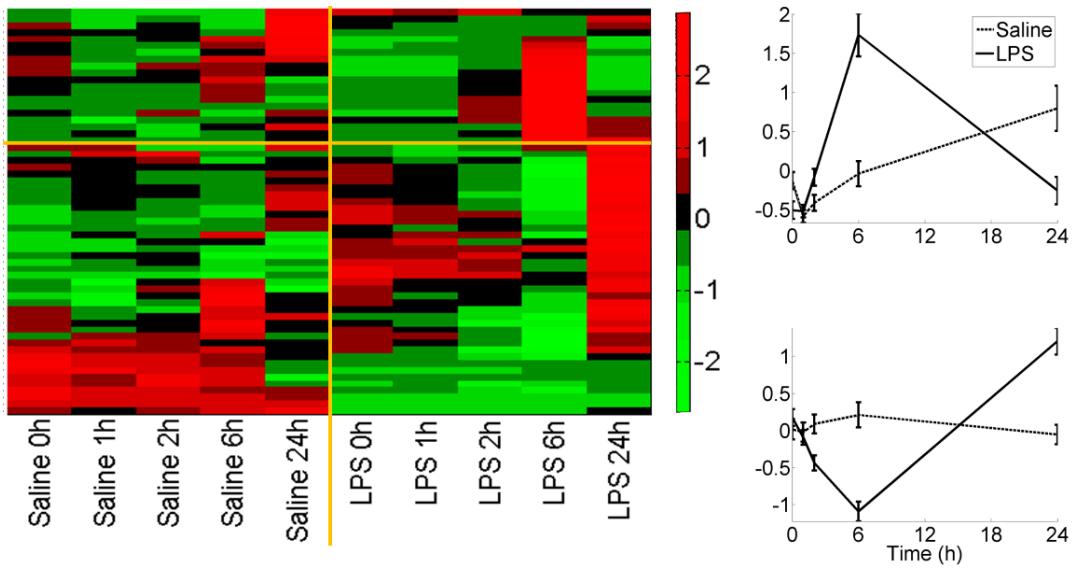

Figure 3-3: Differential patterns of response to LPS in plasma metabolite levels form two clusters reflecting distinct patterns with opposing temporal directionality. Heat map on the left displays temporal changes in plasma concentrations of all differential metabolites and diagrams on the right shows the average concentration profiles for all metabolites in each of those two clusters (vertically in the same order as the heat map). Horizontal yellow lines on the heat map designate the limits of each cluster.

It is worth noting that metabolomic alterations require more time to display distinct separation from the normal levels compared to transcriptional changes. In the heat map of metabolites shown in Figure 3-3 (left) we did not observe strong metabolic response until 6h post-LPS while the transcriptional profiles of treatment and control groups (Figure 3-2) display a clear distinction starting from the first data point. This is also highlighted in Figure 3-4, which qualitatively displays the temporal associations between the transcriptomic and metabolomic clusters. The profile of early up-regulated

Table 3.2: Classification of metabolites in the two clusters displayed in Figure 3-3.

	Biochemical	Sub-pathway	Super pathway
Cluster 1	2-hydroxybutyrate (AHB)	Cysteine, methionine, SAM, taurine metabolism	Amino acid
	3-methyl-2-oxobutyrate	Valine, leucine and isoleucine metabolism	
	xylose	Nucleotide sugars, pentose metabolism	Carbohydrate
	docosapentaenoate (n3 DPA; 22:5n3)	Essential fatty acid	Lipid
	docosahexaenoate (DHA; 22:6n3)		
	eicosapentaenoate (EPA; 20:5n3)		
	tetradecanedioate	Fatty acid, dicarboxylate	
	2-hydroxydecanoic acid	Fatty acid, monohydroxy	
	stearate (18:0)	Long chain fatty acid	
	10-nonadecenoate (19:1n9)		
	dihomo-linoleate (20:2n6)		
	eicosenoate (20:1n9 or 11)		
	docosadienoate (22:2n6)		
	stearidonate (18:4n3)		
	1-oleoylglycerophosphoethanolamine	Lysolipid	
	pregnen-diol disulfate	Sterol/Steroid	
	21-hydroxypregnenolone disulfate		
	pregn steroid monosulfate		
	phenolphthalein beta-D-glucuronide	Detoxification metabolism	Xenobiotics
	quinate	Food component/Plant	
Cluster 2	asparagine	Alanine and aspartate metabolism	Amino acid
	2-aminobutyrate	Butanoate metabolism	
	methionine	Cysteine, methionine, SAM, taurine metabolism	
	cysteine		
	betaine	Glycine, serine and threonine metabolism	
	serine		
	glycine		
	histidine	Histidine metabolism	
	pipecolate	Lysine metabolism	
	lysine		
	tyrosine	Phenylalanine & tyrosine metabolism	
	phenyllactate (PLA)		
	tryptophan betaine	Tryptophan metabolism	
	tryptophan		
	citrulline	Urea cycle; arginine-, proline-, metabolism	
	ornithine		
	isobutyrylcarnitine	Valine, leucine and isoleucine metabolism	
	leucine		
	valine		
	isoleucine		
	methyl-beta-glucopyranoside	Fructose, mannose, galactose, starch, and sucrose metabolism	Carbohydrate
	heme	Hemoglobin and porphyrin metabolism	Cofactors and vitamins
	pantothenate	Pantothenate and CoA metabolism	
	beta-tocopherol	Tocopherol metabolism	
	phosphate	Oxidative phosphorylation	Energy
	taurolithocholate 3-sulfate	Bile acid metabolism	Lipid
	3-dehydrocarnitine	Carnitine metabolism	
	deoxycarnitine		
	choline	Glycerolipid metabolism	
	1-eicosadienoylglycerophosphocholine	Lysolipid	
	1-heptadecanoylglycerophosphocholine		
	1-arachidonoylglycerophosphocholine		
	7-alpha-hydroxy-3-oxo-4-cholestenoate (7-Hoca)	Sterol/Steroid	
	5alpha-pregnan-3beta,20alpha-diol disulfate		
	gamma-glutamylleucine	Gamma-glutamyl	Peptide
	gamma-glutamyltyrosine		
	4-ethylphenylsulfate	Benzoate metabolism	Xenobiotics
	desmethylnaproxen sulfate	Drug	
	homostachydrine	Food component/Plant	
	ergothioneine		

cluster (shown in yellow color) in the transcriptomic dataset indicates the immediate effects of LPS administration in the gene expression of leukocytes, whereas the earliest changes in the metabolomic data becomes significant after first couple of hours, and coincides with the late-upregulated transcriptomic cluster (shown in red color).

Immediately following LPS administration, the transcriptional landscape became overcrowded with the elements of signaling cascades required for the healthy onset and resolution of the inflammatory response. In accordance with our main objective of assessing the transcriptional regulation of metabolic processes specifically, we followed a method that functionally narrows down the focus so as to uncover metabolism associated transcripts that might have been otherwise masked by the overwhelming majority of inflammatory genes dominating transcriptional landscape.

General classification information of the KEGG Pathway database was used as the reference for this purpose, and any of the differentially expressed transcripts which were not associated with any metabolic processes in the database were removed, then clustering analysis was repeated for the remaining transcripts. After this functional change in the focus of analysis, 264 differential metabolite-associated transcripts remained which code for 214 unique proteins. Three dominant transcriptional patterns shown in Figure 3-2 previously were retained in this subset of metabolism associated genes as shown in Figure 3-5**.** Significantly enriched metabolism-associated pathways obtained from functional annotation of these three clusters are listed in Table 3.3.

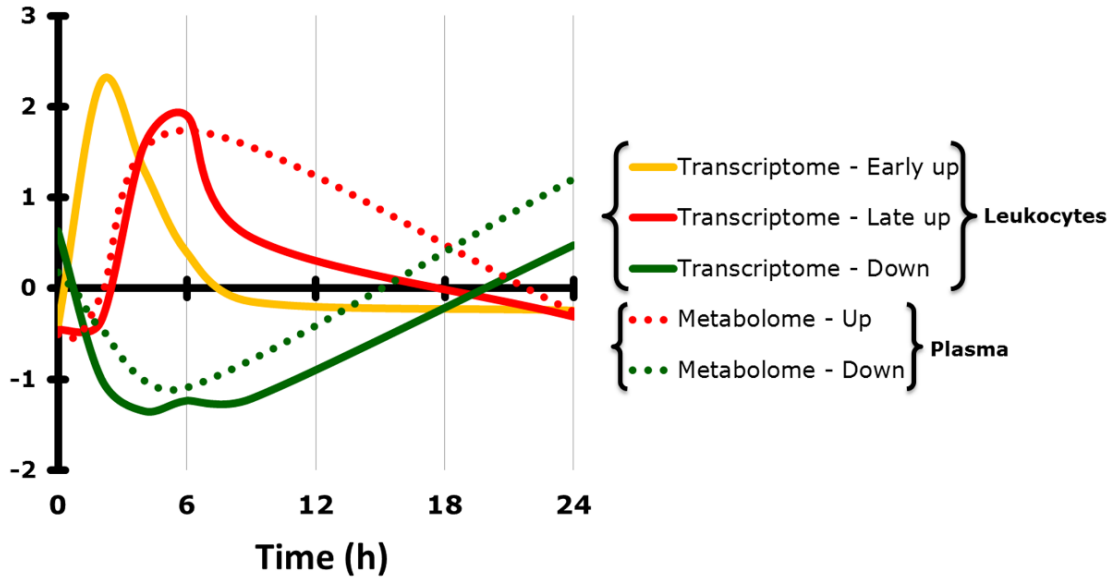

Figure 3-4: Qualitative representation of the temporal differences between observed response patterns in gene expression and metabolite concentrations.

3.3 Discussion

We observed the most drastic changes in metabolism occuring later in the time course compared to transcriptomic alterations in response to LPS. The reason for this is that the alterations in the metabolome reflect the collective response of peripheral organs which may be distal to the initial inflammatory stimulus. This lag in the responsiveness at metabolic level relative to gene expression also becomes obvious when the temporal profiles of clusters from both analyses are overlaid as shown in Figure 3-4.

Functional annotation of the early up-regulated genes in leukocytes (Table 3.1) gives us information about immediate inflammatory actions of the leukocytes, which are also accompanied by the alterations of intracellular metabolic processes which are subject to transcriptional regulation. We do not expect a significant effect of plasma metabolites at this very early stage of leukocytes' response since the deviation of metabolite concentrations from normal is relatively moderate then. A good example

for this is arachidonic acid metabolism pathway, the key link between fatty acids and eicosanoid family of inflammatory mediators. These mediators, most importantly, include prostaglandins, thromboxanes, leukotrienes and lipoxins which are not only essential for initial phases of the inflammation but also participate in the programming of the termination of it at the local sites of inflammation (Serhan and Savill, 2005). This immediate up-regulation is followed by another group of genes up-regulated around 4-6h post-LPS (shown in Figure 3-2 and listed in Table 3.1 as Late Up). This

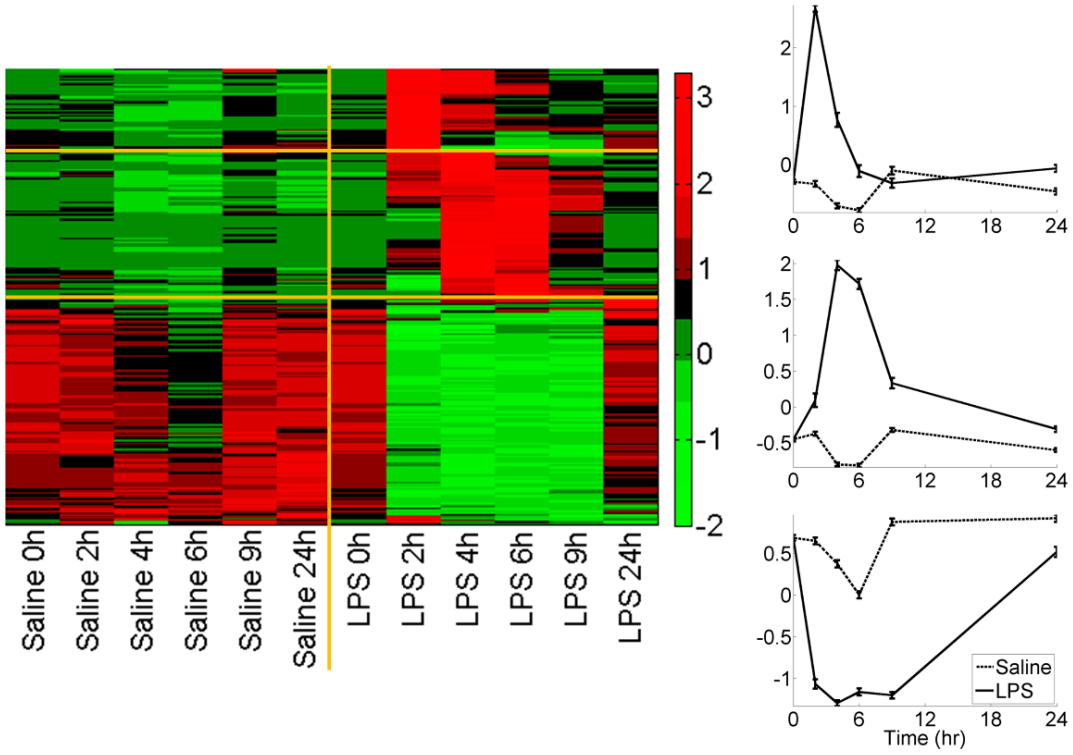

Figure 3-5: Subset of differentially expressed transcripts associated with metabolic processes display very similar patterns to the original clusters shown in Figure 3-2. Heat map on the left shows these early upregulation, late upregulation and downregulation patterns while diagrams on the right display the average expression profiles for all transcripts in each cluster (vertically in the same order as the heat map). Horizontal yellow lines on the heat map designate the limits of each cluster.

later response also coincides with the time period at which plasma metabolites show the highest deviation from their normal levels (shown in Figure 3-3 with metabolites listed in Table 3.2). Temporally, we observed the most significant divergence between the treatment and control groups at 6h post-LPS, when lipids (essential and long chain fatty acids, lysolipids, sterols/steroids) reached their peak concentration and amino acids plummeted. In other words, at this time period, leukocytes were circulating within lipid-rich and amino acid-depleted environment. We hypothesized that; this altered environment can have an effect on the gene expression of leukocytes, in conjunction with the inflammatory signaling initiated by LPS.

Adipocytokine signaling pathway is an important cross-road where inflammatory signaling and metabolic effects intersect. The late-up cluster of genes (Table 3.1) include many elements playing role in this pathway such as ACSL (Acyl-CoA Synthetase Long-Chain) family of enzymes (ACSL1, ACSL3, ACSL4) in addition to many inflammatory elements (NFKB1, NFKB2, SOCS3, RELA, TNFRSF1A, STAT3, JAK3). ACSL enzymes esterify long chain fatty acids and convert them to intracellular free fatty-acids. This is a pre-requisite step for any down-stream metabolic reactions of fatty acids. Increase in the gene expression of these enzymes may reflect an adaptation response of the leukocytes to the high lipid concentration of plasma. Furthermore, ceramide produced down-stream of these enzymes have been shown to mediate synergistic effects with LPS, stimulating the cytokine production (Rubinow et al., 2013).

The final groups of differential transcripts are distinguished by strong-down regulation starting early after LPS delivery and recovering steadily after around 9h post-LPS (Figure 3-2, upper right diagram). As the expression of these transcripts was lowered, the plasma concentrations of amino acids were also moving in parallel and reaching their trough around 6h post-LPS. Perhaps the most striking transcriptional response

to altered plasma composition is observed in this cluster, as numerous ribosomal proteins, translation initiation factors and signaling elements are included here. As listed in Table 3.1 (Down), ribosome appears at the top of the list with the highest enrichment score. Although translational control is recognized as a well-known beneficial mechanism to shut-off inflammatory processes before they become detrimental (Mazumder et al., 2010), the role of plasma composition as an environmental factor on this is not clear.

It is worth emphasizing that the proteins which regulate inflammatory processes dominate the transcriptome after LPS stimulus, which is fundamental for the development and resolution of the inflammatory response naturally. However, co-current shifts in metabolism are also essential to accommodate the material and energy demands of these inflammatory processes (Khovidhunkit et al., 2004). Presumably, these metabolic shifts are also happening in response to the environmental changes imposed on the circulating leukocytes. Therefore, to facilitate the extraction of the transcriptional information related to metabolic changes in leukocytes and draw meaningful associations with their environment described by the metabolomic data, we opted to filter the entire transcriptome after this global characterization to focus exclusively on metabolite-associated regulations for the rest of the analysis. Table 3.3 lists the pathways which differential subsets of metabolite-associated genes in the three clusters shown in Figure 3-5 are enriched in. This "supervised" enrichment analysis allowed us to uncover and inter-relate the most important regulatory changes in leukocyte metabolic processes happening at the transcriptional level.

Table 3.3: Functional annotation of metabolism related subset of genes in the three clusters displayed in Figure 3-5.

	Pathway	Genes
Early Up	Arachidonic Acid Metabolism	PTGS2, GGT1, GPX3, CYP2C9, CYP4F3, CYP4F2
	Glutathione Metabolism	GGT1, GSR, OPLAH, GPX3, G6PD
	Pentose Phosphate Pathway	TKT, G6PD, PGM1
	Phosphatidylinositol Signaling System	ITPKA, DGKD, DGKG, PLCD1
	Starch and Sucrose Metabolism	PGM1, GBA, GBE1, PYGL
	Cyanoamino Acid Metabolism	GGT1, GBA
	Glycan Structures Degradation	GALNS, GBA
	Sphingolipid Metabolism	GBA, DEGS1
	Glycan Structures Biosynthesis 1	B4GALT4, NDST1, GALNT13
	Androgen and Estrogen Metabolism	HSD17B3, CYP19A1
	Inositol Phosphate Metabolism	ITPKA, PLCD1
Late Up	Glycan Structures Biosynthesis 1	ST3GAL2, ST3GAL4, C1GALT1C1, EXT1, B4GALT5, NDST2, CHSY1, GALNT1, GALNT14
	O Glycan Biosynthesis	GALNT1, ST3GAL2, GALNT14, B4GALT5, C1GALT1C1
	Sphingolipid Metabolism	SGPP2, GALC, SPTLC2, UGCG
	Galactose Metabolism	HK3, MGAM, UGP2
	Glycan Structures Biosynthesis 2	ST3GAL2, ST3GAL4, UGCG, PIGV
	Ppar Signaling Pathway	ACSL1, ACSL4, ACSL3, GK
	Fructose and Mannose Metabolism	PFKFB3, PFKFB2, HK3
	Fatty Acid Metabolism	ACSL1, ACSL4, ACSL3
	Pyrimidine Metabolism	CANT1, PNPT1, UPP1, UPB1
	Inositol Phosphate Metabolism	PTEN, PIK3CG, INPP5A
	Tryptophan Metabolism	AFMID, TDO2, CYP1B1
Down	N Glycan Biosynthesis	GANAB, FUT8, ALG1, STT3B, RPN2, MGAT4A, ST6GAL1, MAN2A1, MGAT2
	Glycan Structures Biosynthesis 1	HS2ST1, RPN2, MGAT2, MGAT4A, ST6GAL1, ALG1, XYLT1, CHST12, MAN2A1, GANAB, FUT8, GALNT6, STT3B, GALNT12
	Oxidative Phosphorylation	NDUFAB1, COX5A, COX6C, ATP5C1, COX7C, NDUFV1, ATP5D, UQCRH, ATP5G2, ATP5G3, ATP6V0A1, ATP6V0A2
	Propanoate Metabolism	LDHB, ALDH3A2, ACSS1, MCEE, ALDH6A1, SUCLG2
	Purine Metabolism	NUDT5, NME7, ADSL, ZNRD1, PDE7A, POLD2, PDE8A, POLR1D, POLR2K, ATIC, PAPSS2
	Glycerolipid Metabolism	AGPAT3, ALDH3A2, DGKA, DGKE, PPAP2A, LIPA, AKR1B1
	Pyruvate Metabolism	LDHB, ALDH3A2, ACSS1, GLO1, AKR1B1, MDH1
	Lysine Degradation	ALDH3A2, AASDHPPT, HADH, SHMT2, EHMT2, RDH11
	Pyrimidine Metabolism	POLR1D, NME7, POLR2K, ZNRD1, DCTD, AK3, POLD2
	Valine Leucine and Isoleucine Degradation	BCAT1, ALDH3A2, MCEE, HADH, ALDH6A1
	Glycerophospholipid Metabolism	PHOSPHO1, AGPAT3, DGKA, GPD1L, DGKE, PPAP2A
	Phosphatidylinositol Signaling System	PIK3C2A, INPP4B, INPP4A, DGKA, DGKE, INPP5B
	One Carbon Pool By Folate	SHMT2, MTHFR, ATIC, MTR
	Glycan Structures Biosynthesis 2	PIGL, B3GALNT1, PIGB, PIGX, PIGT
	Glycolysis and Gluconeogenesis	LDHB, ACSS1, FBP1, ALDH3A2, GPI
	Glycosylphosphatidylinositol Anchor Biosynthesis	PIGX, PIGT, PIGL, PIGB

As in the case of global transcriptome analysis, after filtering for the association with metabolic pathways, arachidonic acid metabolism again appeared as the immediate responder to LPS stimuli. Immune cells including monocytes, macrophages, and neutrophils utilize arachidonic acid as the precursor for the production of inflammatory mediators which substantially contribute to the clinical presentation of systemic

inflammation. PTGS2 (prostaglandin endoperoxide 2, also known as inducible form of cyclooxygenase) is the key enzyme in the synthesis of prostaglandins and thromboxanes, some downstream effects of which include analgesia, hyperalgesia, osmoregulation, febrile response, and antithrombosis depending on the synthesized and secreted final form and the cell type receiving this signal (Andreasen et al., 2008).

Arachidonic acid metabolism is also closely related to the free radical generation and oxidative stress in the immune cells. It is known to directly stimulate NADPH oxidase, an enzyme complex in leukocytes, (notably in neutrophils) that leads too free radical production for microbicidal activity (Pompeia et al., 2000). Moreover, arachidonic acid pathway is coupled with glutathione (GSH) metabolism through two shared enzymes: gamma-glutamyltransferase 1 (GGT1) and glutathione peroxidase 3 (GPX3). GSH metabolism is a critical pathway for the inflammatory response since GSH is the master regulator of the intracellular redox state in close association with inflammatory processes (Gaté et al., 1999). GGT1 is the enzyme that initiates the catabolism of GSH, therefore increasing levels of GGT1 leads to reduced GSH concentrations and higher oxidative stress (Motley et al., 2004). On the other hand, GPX3 utilize GSH to detoxify hydrogen peroxide, therefore act as an antioxidant (Urbanska et al., 2014).

During the detoxification of hydrogen peroxide, glutathione disulfide (GSSG) is produced. Replenishment of GSH resources from GSSG requires NADPH and glucose-6-phosphate dehydrogenase (G6PD) which is a key component for the antioxidant defenses while also being the rate limiting enzyme of pentose phosphate pathway (Chandra et al., 2008). Essentially, glutathione metabolism appears to be activated in conjunction with arachidonic acid pathway and a number of other pathways associated with carbohydrate metabolism.

Genes associated with carbohydrate metabolism appear in all three clusters indicating active modulation of energy strategies throughout the response. Enzymes favoring the

energy production from glycolysis (PGM1, HK3) are upregulated while those channeling the reactions away from pentose phosphate pathway and citric acid cycle (GPI, LDHB) are downregulated. Along with these regulations, downregulation of quite high number of mitochondrial elements (NDUFAB1, COX5A, COX6C, COX7C, NDUFV1, ATP5D, UQCRH, ATP5C1, ATP5G2, ATP5G3, ATP6V0A1, ATP6V0A2) point towards a shift of energy production from oxidative phosphorylation to glycolysis. This phenomenon is named as Warburg effect that is first observed in tumor cells (Warburg, 1956). For the inflammatory cells, a high energy demand exists, similar to that of tumor cells, due to increased biosynthetic activity. To meet this demand cells incline towards glycolysis rather than oxidative phosphorylation although it is not as efficient in terms of ATP production yield. This is likely because glycolysis can be strongly up-regulated and it can generate biosynthetic intermediates from the pentose phosphate pathway required for the generation of inflammatory products (Liu et al., 2012a, Maciver et al., 2008). This early initiation phase of inflammation therefore has been termed as anabolic which progressively transforms into adaptation phase associated with catabolism requiring fatty acid oxidation until the restoration of homeostasis (Liu et al., 2012b, Liu et al., 2012a). This phenomenon is also clearly observed in the current model of systemic inflammation. Within 6 hours of LPS administration there is a strong upregulation of the genes associated with lipid metabolism, primarily ACSL-1, -3 and -4, as previously pointed out. In parallel, there is a surge of plasma lipid concentrations. These observations nicely confirm previous studies defining the changes in bioenergetics during initiation and adaptation phases within the inflammatory cells as well as throughout the body. However, a chicken and egg question still remains pertaining to initiating factor of these homeostasis recovery mechanisms.

Amino acid metabolism also displays an adaptation response to the changing plasma conditions. Genes functioning in the degradation pathways of amino acids (ALDH3A2, AASDHPPT, HADH, SHMT2, EHMT2, RDH11, BCAT1, MCEE, ALDH6A1) are found in the cluster which is downregulated. Since this response coincides with the strong depletion of circulating amino acids in the plasma, it might be speculated as precautious response to prevent exhaustion of intracellular amino acid resources during this so-called adaptation phase.

A group of pathways related to the degradation and biosynthesis of glycans is enriched in all clusters. Glycan biosynthesis is an essential process for the immune system since the newly produced protein messengers as well as cell-surface receptors require glycosylation as a post-translational modulation mechanism for functioning properly. From the enrichment analysis of the metabolism related genes, we observed that, in general, biosynthesis of O-glycans were upregulated while that of N-glycans were downregulated. Since both types of biosynthesis would likely be involved in the numerous elements that immune cells need to produce during inflammatory response (Haslam et al., 2008), answering why these genes would display disparate dynamics is out of the scope of this article and possibly be answered in the near future through studies focusing in human immune system in the newly emerging fields of glycomics and glycoproteomics.

3.3.1 Limitations

One limitation of our study was the fact that transcriptomic and metabolomic data were derived from different subject populations. This was related to the inherent nature of a meta-analysis and we believe that while a comparison performed on the plasma and leukocyte samples collected from same subjects would be stronger, this does not invalidate the work presented. The results obtained from the original transcriptomic analyses performed on whole blood have been supported by others who

have examined the transcriptome of leukocyte subsets, also utilizing the human endotoxemia model (Talwar et al., 2006). This indicates that the global transcriptome changes observed in this model are reproducible and represent a valid data set with which to perform the comparison with the metabolomic data discussed in this work.

3.4 Conclusion

This study was focused on the metabolic processes which were controlled at the transcriptional level to develop an understanding on the associations with the altered conditions in the immediate environment of leukocytes. At the global transcriptome level, we observed that lipid associated metabolic pathways were being activated while protein translation machinery was being slowed down in parallel with the peaking lipid and plunging amino acid levels in plasma. We hypothesized that drastic changes in the immediate environment of the leukocytes might have an adaptive effect in this response in conjunction with the initial stimuli. Furthermore, focusing exclusively only on metabolism associated transcripts uncovered alterations in bioenergetics and defenses against oxidative stress that can shed light into the mechanisms underlying mitochondrial dysfunction and shifts in energy production observed during inflammatory processes.

Besides describing the metabolic response of human body to a basic inflammatory cue at the systemic level together with affected immune mechanisms, this study can inspire future translational studies as the *-omics* analyses becomes routine in clinical practice. Because blood is the biological sample fastest and the least invasive to collect from patients while yielding most useful information about the state of the body. Therefore, benchmarking the metabolic state of the system and transcriptional state of the immune cells by single biological sample may expedite clinical decision making and help reduce mortality in critical cases.

Chapter 4 Relevance of Endotoxemia Model to the Clinical Cases of Sepsis and SIRS

Sepsis is defined as the combination of an infection with multiple features of "systemic inflammatory response syndrome" (SIRS) (Levy et al., 2003) and is one of the oldest and most enigmatic conditions in medicine. There are more than a million cases of sepsis per year in United States (Hall et al., 2011) and it is estimated to be 19 million cases per year worldwide (Angus and van der Poll, 2013, Lagu et al., 2012). According to the Center for Disease Control, the cost of hospitalization is in the order of $15 billion, with an anticipated further increase in the future (Reinhart et al., 2012). Despite several decades of intensive research and efforts to bring new therapies to the bedside, the number of cases and sepsis-associated deaths are still soaring (Angus and van der Poll, 2013, Rittirsch et al., 2007). Current treatment guidelines include cardiorespiratory resuscitation and non-specific protocols aimed to mitigate immediate threats of uncontrolled infection (Angus and van der Poll, 2013). A significant barrier to progress is the perceived inadequacy of experimental models that can reproduce the pathophysiology of the disease in humans.

The high degree of variability among patients and multiple aspects of the disease, including patient gender, age and comorbidities complicate the design of relevant experimental models and clinical studies. Moreover, the initiating cause of infection and the physiologic responses that follow are also highly variable (Deitch, 1998). All these factors explain, at least in part, the difficulty in translating experimental results to the clinic and consequently, the lack of success in development of effective therapies (Rittirsch et al., 2007).

Endotoxemia model has served as a valuable experimental venue for more than six decades (Wolff, 1973, Andreasen et al., 2008, Lin and Lowry, 1998). It is a model of

systemic inflammation, rather than a true mimic of sepsis. Nonetheless, early transient physiochemical changes and biochemical pathway activation in this model are strikingly similar to those observed during early hyperdynamic phase of resuscitated injury and infection (Lowry, 2005). The LPS challenge triggers chills, myalgias, nausea, increase in core body temperature and heart rate, most of which begin to abate within 6-8 h (Lowry, 2005, Calvano and Coyle, 2012, Andreasen et al., 2008). Genome-wide analyses of circulating leukocytes revealed transcriptional signatures indicative of changes in protein translation and glycolysis (Haimovich et al., 2010), which shared similar characteristics with those observed in trauma patients (Calvano et al., 2005). These studies helped elucidate the intricate regulatory schemes governing the response to endotoxemia (Nguyen et al., 2011, Calvano et al., 2005) and provided the foundations for *in silico* models of systemic inflammation (Foteinou et al., 2009, Foteinou et al., 2011, Scheff et al., 2011, Foteinou et al., 2010, Scheff et al., 2012b, Scheff et al., 2010, Scheff et al., 2012a). In Chapter 2, we discussed the effects of LPS-induced inflammation on the whole body metabolism in humans (Kamisoglu et al., 2013b). In contrast with other methods applied to the endotoxemia model, metabolomics reflects the combined output of all tissues in the body (Kosmides et al., 2013). Unsupervised multivariate analyses identified prominent changes in lipid and protein metabolism, which peaked at 6 hours post LPS infusion. Subsequently, to better understand how the inflammatory responses at the level of cells and whole body correlate in humans, we integrated the analysis of plasma metabolome with that of leukocyte transcriptome as discussed in Chapter 3.

Recently, Community Acquired Pneumonia and Sepsis Outcome Diagnostic study (CAPSOD) (Langley et al., 2013) provided an integrated analysis of clinical features, plasma metabolome and proteome, describing the patterns of metabolic perturbations in critically ill patients presenting with symptoms of systemic inflammatory response

syndrome (SIRS) or sepsis. This study, the first of its kind, examined clinical features as well as the plasma metabolome, and proteome, of patients upon arrival at the emergency department (ED) and 24 hours later. An important and novel outcome of the study was the realization that metabolic differences could ultimately be used as markers predicting survival.

Since the endotoxemia model utilizes LPS as stimulus, rather than intact bacteria, there is an ongoing concern that the data derived from this model are of limited relevance to our understanding of sepsis-induced inflammatory mechanisms, although recent analyses of the leukocyte transcriptome seemed to argue otherwise (Haimovich et al., 2010). The availability of new metabolomic data (Kamisoglu et al., 2013b, Langley et al., 2013) offered the opportunity to compare responses detected in LPS-challenged subjects to those of critically ill patients at the level of the entire organism. In this retrospective study we aimed to objectively determine the relevance of the information content gained by parallel analyses of LPS-challenged subjects (Kamisoglu et al., 2013b) and patients with or without community-acquired sepsis (Langley et al., 2013).

4.1 Methods

4.1.1 Metabolic Data

This is a retrospective analysis utilizing metabolomes obtained from subjects who participated in experimental endotoxemia study and from patients with or without community-acquired sepsis. Experimental protocol for human endotoxemia model has been previously described in Section 2.1 and in (Kamisoglu et al., 2013b).

Metabolomic data for the clinical cases of systemic inflammation were obtained from Community Acquired Pneumonia and Sepsis Outcome and Diagnostics (CAPSOD) study (Langley et al., 2013). Approval for this study was obtained by institutional ethics

committees and details were filed at ClinicalTrials.gov (NCT00258869). Protocols and identified clinical features in the different classes of patients were previously published. The study (Langley et al., 2013) included 1152 individuals with suspected, community-acquired sepsis (acute infection and ≥2 SIRS criteria) in the emergency departments at three urban, tertiary-care hospitals in the United States between 2005 and 2009. Each patient or their legal designates provided informed consent. Medical history, physical examination, and acute illness scores (APACHE II and SOFA) were recorded at enrollment ($t_{0,clinical}$) and 24 hours later ($t_{24,clinical}$). Infection status and outcome through day 28 were independently adjudicated by board-certified clinicians. Clinical care given for the patients was not standardized and was determined by individual providers. After independent audit of infection status and outcomes, 150 patients were chosen for derivation studies. Non-targeted mass spectrometry based analyses of the

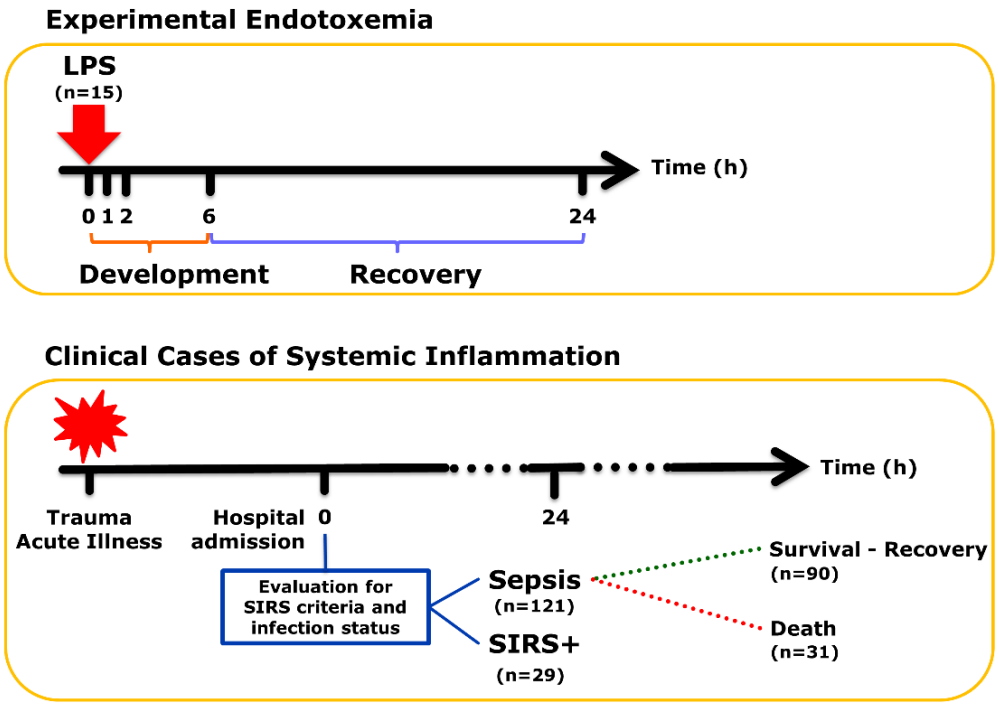

Figure 4-1: Schematic description of the experimental and clinical sources of data.

patient's blood samples were done by Metabolon similarly with endotoxemia study. Figure 4-1 represents the overall structures of the two studies.

150 patients chosen for derivation studies within CAPSOD cohort were classified to represent cases of uncomplicated sepsis (n=27), severe sepsis (n=25), septic shock (n=38), non-infected SIRS ("ill" controls, indicated as SIRS, presumed septic at enrollment but later determined to have noninfectious reasons for SIRS; n=29), or sepsis non-survival (SNS, n=31) (Figure 4-1, bottom). No significant difference among subgroups of sepsis survivors (uncomplicated sepsis, severe sepsis, septic shock) were reported for plasma metabolites (Langley et al., 2013). Therefore, the data from these patients were collapsed into a single group referred to as sepsis survivors (SS, n=90) for the purposes of this study. Furthermore, in the first part of the analysis, metabolic data from sepsis survivors (SS) and sepsis non-survivors (SNS) were pooled to assess the similarities and differences between sepsis and non-infected SIRS, and referred to as the Sepsis group (n=121). In the subsequent analysis, data from SS and SNS groups were used individually to investigate the association of metabolic changes in endotoxemia with those observed in either surviving or non-surviving sepsis patients.

4.1.2 Data Analysis

MS analysis of plasma samples from the human endotoxemia study provided temporal information on 366 metabolites at five time points. Previous results of the principal component analysis on this dataset showed that the 6h time point (t_6) was the most critical since the maximum difference between control and treatment groups was observed at this time point (Kamisoglu et al., 2013b). This agreed well with prior transcriptional studies indicating that the maximal change in leukocyte gene expression was observed 6h after the LPS administration (Calvano et al., 2005, Talwar et al., 2006). Therefore, this data point was considered to represent the peak of metabolic response to endotoxemia and used as reference for the assessment of

concordance between experimental and clinical data in this study. MS analysis of the samples from CAPSOD study, on the other hand, had identified 370 metabolites at $t_{0,clinical}$ (time of hospital admission) and 401 metabolites at $t_{24,clinical}$ (24 h after admission). In this study, both clinical and experimental datasets were individually normalized by setting the median equal to 1. Missing values were imputed with the observed minimums after normalization. The metabolite lists were consolidated. Only the metabolites commonly identified in the endotoxemia (Kamisoglu et al., 2013b) and clinical (Langley et al., 2013) studies were analyzed further. The final dataset included 177 common metabolites from both studies (Kamisoglu et al., 2013b, Langley et al., 2013). Outliers were removed using the median absolute deviation, $\mathrm{MAD} = 1.4826 \times \left|(x_i - \mathrm{Median}_j(x_j)\right|$, of each metabolite, determined in each individual group (Leys et al., 2013, Hampel, 1974). Subsequently score for each data point was calculated $z_i = \frac{\left|x_i - \mathrm{Median}_j(x_j)\right|}{\mathrm{MAD}}$ and data points with score above 3 were removed from the dataset. The number of removed outliers for each group is reported in the appendix, Table A. 1.

The baseline of the human endotoxemia study, i.e., samples collected before LPS administration ($t_{0,LPS}$), defined the "baseline" in this study. We identified the 6h time point as the peak of metabolic response in endotoxemia model in our previous metabolomics study (Kamisoglu et al., 2013b), as well as transcriptomic analysis (Foteinou et al., 2009, Nguyen et al., 2011), and hypothesized that this time point represents the point of transition from the development and recovery phases of the response. For the clinical data collection, the starting point was the time of hospital admission ($t_{0,clinical}$), whereas the second clinical time point was 24 hours later ($t_{24,clinical}$). Since the data obtained for the clinical patients lacks internal controls, for obvious reasons, the responses of each group of patients, as well as endotoxemia

subjects, were compared independently to the healthy baseline ($t_{0,LPS}$). For comparing the means of metabolites in each condition relative to the healthy baseline, Welch's t-test was used without assuming equal variances (α=0.05). The number of subjects in experimental endotoxemia group (n=15) was much smaller than the number of patients in the clinical groups to assume normal distribution required for t-test. However at both $t_{0,LPS}$ and $t_{6,LPS}$ the data passed Kolmogorov-Smirnov test for each metabolite allowing the application of t-test. Q-values were calculated according to Benjamini and Hochberg procedure (Benjamini and Hochberg, 1995) and metabolites having a p- and a q-value less than 0.05 are called significant. We also evaluated how dispersed the data for each metabolite is in clinical cases with respect to those at the baseline. Variances of the significant metabolites in each condition were also plotted relative to the variances at the baseline, and shown in Figure A. 1 in appendix.

We lastly focused on changes in metabolites within subpopulations of sepsis patients who ultimately survived, and those who did not. For this purpose, dynamics within sepsis group were examined using the data from SS and SNS groups. Metabolites that statistically differed between these groups at either time point were determined by t-test as described earlier. The magnitude of changes in plasma metabolites relative to $t_{0,LPS}$ were calculated for each group. These changes were compared between the SS and SNS groups at both time points and with the endotoxemia group at $t_{6,LPS}$.

4.2 Results and Discussion

Endotoxemia induced by elective administration of LPS to healthy subjects has served as an invaluable tool for obtaining mechanistic insight into homeostatic inflammatory responses. Previous studies compared transcript- and protein- expression patterns in immune cells obtained from LPS treated subjects and trauma patients, revealing significant overlap (Visser et al., 2012, Haimovich et al., 2010). More recently, metabolomics analyses in both LPS administered subjects (Kamisoglu et al., 2013b)

and patients with symptoms of systemic inflammation at time of presentation to emergency departments were published (Langley et al., 2013, Glickman et al., 2010). Building on these prior studies, here we aimed to objectively compare metabolic indices obtained from experimental studies and clinical sources.

The inherent dynamics of a clinical and an experimental study are obviously disparate although they focus on related physiologic phenomena. The first time point in a clinical study is generally at a point that had already deviated from what can be called a "healthy state", whereas experimental studies usually measure divergence from the "healthy state" under controlled conditions. In this study, we aimed to evaluate the significance of observed metabolic perturbations in endotoxemia and how they relate to corresponding changes observed in patients with symptoms of community-acquired sepsis at time of presentation to the emergency departments. In line with our objective, we chose to evaluate each condition and each time point based on its deviation from one common baseline that reflects a healthy state ($t_{0,LPS}$). Table 4.1 shows the number of metabolites which had significantly different concentration compared to $t_{0,LPS}$ at each time point available for each condition. The first column in Table 4.1, shows the total information content of the final consolidated dataset with total number of metabolites associated with each metabolic super-pathway. Complete list of metabolites, their pathway classification, and extent of changes from baseline are provided in Table A. 2**,** in appendix.

At the peak of the response to LPS, i.e., at $t_{6,LPS}$, there were 83 metabolites (47% of the total 177 common metabolites) which significantly deviated from baseline. In contrast, the number of metabolites that significantly differed from baseline for the clinical groups was considerably smaller (varying between 19-26 metabolites, or 11-15% of the total 177 common metabolites).

Table 4.1: Number of significantly changed metabolites and metabolic super-pathways that they belong to; determined for LPS-challenged subjects and patient groups. Significance was determined by comparing responses of each group of patients, as well as endotoxemia by comparing responses of each group of patients, as well as endotoxemia subjects, to the healthy baseline ($t_{0,LPS}$) individually. Welch's t-test was used and with correction for multiple comparisons by Benjamini and Hochberg procedure. (α=0.05). Metabolites having a p- and a q-value less than 0.05 are called significant. (Complete list is available in Appendix, Table A. 2)

		LPS (n=15)	**Sepsis** (n=121)		**SIRS** (n=29)	
Super pathway	**Total**	**t6**	**t0**	**t24**	**t0**	**t24**
Amino acid	55	28	3	5	3	4
Carbohydrate	16	4	1	2	2	2
Cofactors and Vitamins	7	3	2	1	2	1
Lipid	75	36	10	16	12	16
Energy	4	4	0	1	1	1
Nucleotide	8	3	0	0	1	0
Peptide	3	3	0	0	0	0
Xenobiotics	9	2	3	1	0	1
Total	**177**	**83**	**19**	**26**	**21**	**25**

We hypothesize that much larger number of metabolites that changed significantly in response to endotoxin as compared to the clinical cases reflects, at least in part, the fundamental difference between physiologic variability of responses elicited in subjects who participated in the controlled endotoxemia study and patients. The endotoxemia study cohort included relatively young and healthy subjects whereas the patient cohort that participated in the CAPSOD study was variable, in terms of age and comorbidities among others. In addition, the trigger itself, i.e., LPS, activates a single TLR4-dependent signaling pathway, whereas infectious agents and trauma activate multiple ones, leading to greater variability in responses. In order to evaluate the level of dispersion in the clinical data with respect to the experimental; variance of each significant metabolite at each clinical condition was calculated and plotted against the corresponding variance at the baseline. These plots are shown in Figure A. 1 in

appendix. As highlighted in these plots, variances of the metabolites measured in the patients were statistically higher than those measured in endotoxemia study participants at the baseline, $t_{0,LPS}$, reflecting the fundamental differences in variability between the two groups.

Next, we sought to determine the similarities and differences among the subsets of significant metabolites that changed significantly in sepsis and SIRS groups which were also significant in endotoxemia. Our intention was to be maximally inclusive of the clinically observed changes. Therefore, we focused on metabolites that were significantly different from the baseline at either one of the two clinical time points as well as in endotoxemia. Table 4.2 A lists the metabolites common to endotoxemia and sepsis and Table 4.2 B lists those common to endotoxemia and SIRS. Metabolites that are common to both lists A and B are typed in bold. Triangles depict the direction (apex up: increase, apex down: decrease) and magnitude (1 triangle: less than 2 fold change, 2 triangles: more than 2 fold change) of the difference relative to the baseline ($t_{0,LPS}$). Although the total number of metabolites in common with endotoxemia is close for the two clinical cases (16 in Table 4.2 A and 18 in Table 4.2 B), the agreement between the directions of change was strikingly different. Bilirubin, docosapentaenoate (DPA) and palmitolate were the only three metabolites common to LPS, sepsis and SIRS groups, which changed in the same direction. Of the 16 metabolites common to LPS and sepsis (Table 4.2 A), 15 changed in the same direction. Only one, xylose, changed in an opposite direction. In marked contrast, of the total 18 metabolites common to the endotoxemia and SIRS groups, 10 changed in the opposite direction (Table 4.2 B).

Table 4.2: Metabolites which are significantly different than the heathy baseline (t0,LPS) in the experimental condition and either of the two time points in the clinical conditions. A lists the metabolites common for endotoxemia and sepsis; B lists those common for endotoxemia and sepsis; B lists those common for endotoxemia and SIRS. (=: no significant difference from t0,LPS. ▲/▼: less than 2 fold difference from t0,LPS; ▲▲/▼▼: more than 2 fold difference from t0,LPS; metabolite name in bold: common to both lists A and B).

A		**LPS**	**Sepsis**	
metabolite name	**super pathway**	**t6**	**t0**	**t24**
2-hydroxybutyrate (AHB)	Amino acid	▲	=	▲
mannose	Carbohydrate	▲	=	▲
xylose	Carbohydrate	▲	=	▼
hexanoylcarnitine (C6)	Lipid	▲	▲	▲
bilirubin	Cofactors and vitamins	▲▲	▲	▲▲
docosapentaenoate (DPA; 22:5n3)	Lipid	▲▲	=	▲
palmitoleate (16:1n7)	Lipid	▲▲	▲	▲
pregnen-diol disulfate	Lipid	▲▲	▲	▲
citrulline	Amino acid	▼	▼	▼
histidine	Amino acid	▼	=	▼
serine	Amino acid	▼	=	▼
threonine	Amino acid	▼	▼	=
2-palmitoyl-GPC (16:0)	Lipid	▼	▼	▼
uridine	Nucleotide	▼	=	▼
gamma-glutamyltyrosine	Peptide	▼	=	▼
catechol sulfate	Xenobiotics	▼▼	▼	=
B		**LPS**	**SIRS**	
metabolite name	**super pathway**	**t6**	**t0**	**t24**
alpha-ketobutyrate	Amino acid	▲	=	▼
N-acetylglycine	Amino acid	▲	=	▼
xylose	Carbohydrate	▲	=	▼
citrate	Energy	▲	▲	▲
arachidonate (20:4n6)	Lipid	▲	▲	▲
docosahexaenoate (DHA; 22:6n3)	Lipid	▲	▲	=
eicosapentaenoate (EPA; 20:5n3)	Lipid	▲	=	▲
octadecanedioate (C18)	Lipid	▲	=	▼
bilirubin	Cofactors and vitamins	▲▲	▲	=
3-hydroxybutyrate (BHBA)	Lipid	▲▲	=	▼▼
docosapentaenoate (DPA; 22:5n3)	Lipid	▲▲	▲	=
hexadecanedioate (C16)	Lipid	▲▲	▼▼	▼
palmitoleate (16:1n7)	Lipid	▲▲	▲	▲
5-oxoproline	Amino acid	▼	▼	=
proline	Amino acid	▼	=	▲
serine	Amino acid	▼	▲	=
1-linoleoyl-GPC (18:2)	Lipid	▼	▲	▲
1-oleoyl-GPC (18:1)	Lipid	▼	=	▲

Scatter plots shown in Figure 4-2 A and B highlight this distinction in response. The axes of the scatter plots indicate the log2 fold changes in metabolite concentrations. The x-axes show the change at $t_{6,LPS}$ from baseline, $t_{0,LPS}$. The y-axes show the maximum change in the clinical data at either $t_{0,clinical}$ or $t_{24,clinical}$, relative to $t_{0,LPS}$ (if the changes at both time points were significant, the higher of the two values is shown). Positive direction shows an increase in concentration, while negative shows a decrease. Accordingly, the concentrations of metabolites in the first and third quadrants change in parallel with the observations in endotoxemia; while the ones in the second and fourth quadrants change in opposite direction. The response reflected by the direction and magnitude of change in septic patients agrees well with response to LPS within this common subset. However, for SIRS group, the directions of change are not in agreement with those in endotoxemia for more than half of the metabolites. This suggests that, at the whole body metabolome level, SIRS elicits a unique response with distinctive features. One such feature is the marked decrease in sulfated androgenic hormones (epiandrosterone sulfate, androsterone sulfate, dehydroisoandrosterone sulfate (DHEA-S), 5alpha-pregnan-3beta,20alpha-diol disulfate) (Table A. 2, in appendix).

Lower plasma concentration of one of these metabolites, DHEA-S, has previously been associated with other systemic inflammatory diseases such as systemic lupus erythematosus and inflammatory bowel disease (Straub et al., 1998). This supports the idea that the inflammatory response without apparent infectious stimuli might elicit distinctive features not shared with sepsis or endotoxemia. It has been previously suggested that acute inflammatory stresses from different etiologies result in highly similar responses in humans at the genomic level (Seok et al., 2013). The observed distinct metabolomic responses to systemic inflammation with or without confirmed infection, however, suggests that metabolome is much better at differentiating and

understanding the various pathophysiologies of the different systemic inflammatory responses. Identified unique features of the inflammatory response in different contexts may aid in improving the diagnosis or the development of more targeted therapies.

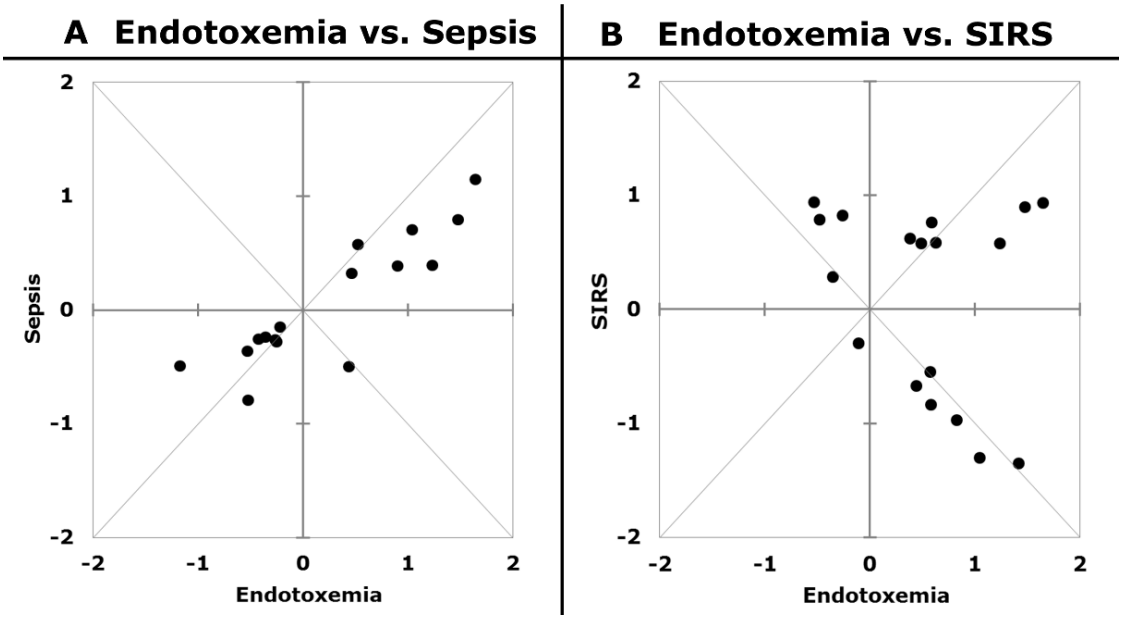

Figure 4-2: Scatter plots show the direction and extent of changes in the metabolites that were significantly deviated from baseline in sepsis (A) and SIRS (B) groups in relation to corresponding trends in endotoxemia. For the clinical data, plots reflect the maximum observed change from the baseline if that particular metabolite found to be significant in both time points, $t_{0,clinical}$ and $t_{24,clinical}$.

Next we compared the trends of changes in metabolites within subgroups of clinical patients who ultimately survived (SS) or did not survive (SNS), and how they related with those in endotoxemia. In total, there were 78 differential metabolites between SS and SNS groups at either t_0 or t_{24}. Among these, 23 were also differential for endotoxemia group at t_6. The direction and magnitude of changes in these 23 metabolites are shown in Table 4.3. When comparing the number of differential

metabolites at either t_0 and t_{24} of the SS and SNS groups, it is clear that the difference in metabolites becomes substantially more pronounced with time. Alignment of trends in SS and SNS groups at t_{24} with those in endotoxemia at t_6 revealed that the peak

Table 4.3: The subset of metabolites having significantly different concentrations between SS and SNS groups at either clinical time points. (Changes from the healthy baseline, $t_{0,LPS}$: ▲/▼: less than 2 fold change; ▲▲/▼▼: more than 2 fold change, -: there was not a significant difference between SS or SNS groups).

		Sepsis Survivors (n=90)		**Sepsis Non-Survivors** (n=31)		**LPS** (n=15)
metabolite name	**super pathway**	**t0**	**t24**	**t0**	**t24**	**t6**
2-hydroxybutyrate (AHB)	Amino acid	▲	-	▲	-	▲
N-acetylglycine	Amino acid	▼	▼	▲	▼	▲
xylose	Carbohydrate	-	▼	-	▲	▲
malate	Energy	-	▲	-	▲	▲
10-nonadecenoate (19:1n9)	Lipid	-	▲	-	▲	▲
2-hydroxypalmitate	Lipid	▲	-	▲	-	▲
hexanoylcarnitine (C6)	Lipid	▲	▲	▲▲	▲▲	▲
pregn steroid monosulfate	Lipid	▲	-	▼	-	▲
3-hydroxybutyrate (BHBA)	Lipid	-	▲	-	▲▲	▲▲
2-methylbutyroylcarnitine (C5)	Amino acid	▼	▼	▲	▲	▼
3-indoxyl sulfate	Amino acid	-	▼	-	▲	▼
5-oxoproline	Amino acid	-	▼	-	▲	▼
histidine	Amino acid	-	▼	-	▼	▼
isobutyrylcarnitine (C4)	Amino acid	-	▼	-	▲	▼
N-acetylornithine	Amino acid	-	▼	-	▼▼	▼
tryptophan	Amino acid	-	▼	-	▼	▼
threitol	Carbohydrate	-	▼	-	▲	▼
phosphate	Energy	▼	▼	▲	▲	▼
1-linoleoyl-GPC (18:2)	Lipid	-	▼	-	▼	▼
1-oleoyl-GPC (18:1)	Lipid	-	▼	-	▼	▼
2-palmitoyl-GPC (16:0)	Lipid	▼	▼	▼▼	▼▼	▼
propionylcarnitine (C3)	Lipid	▲	▼	▲	▲	▼
allantoin	Nucleotide	▼	▼	▲	▲	▼

response to LPS is in line with the sepsis survivor metabolic response, especially at the first day into their treatment. In Chapter 2, we identified the 6h time point as the peak of metabolic response in endotoxemia model, stating that this time point represents the point of transition from the development and recovery phases of the response. The

fact that the metabolic changes in the recovering patients shift towards this response pattern strengthens the notion that the metabolic, as well as transcriptional responses, characteristic to the endotoxemia model represent necessary and "healthy" responses to an infectious stimuli. This is further evidence of likely allostatic response for survivors, i.e., placing the host at the appropriate level of distress required for graceful resolution parallel to the one develop in the LPS model, versus the systemic maladaptation observed in non-survivors (Langley et al., 2013). Based on this rationale, the endotoxemia model could be classified as a model of "normal, healthy responses". It is interesting to note that Matzinger (Matzinger, 2002) more than a decade ago proposed that the Toll-like receptors, including TLR4, evolved to serve as host defense mechanisms against major injury and trauma. Matzinger also proposed that the bacteria evolved to use this receptors system to its own advantage. This idea begins to explain why, when sufficiently controlled, LPS induced responses might be protective and necessary rather than harmful.

The major goal of the CAPSOD study was to identify metabolite changes at sepsis presentation that predicted survival or death. Upon stratification of sepsis patients based on 28-day survival, the direction of change of 21 of 23 metabolites was the same in endotoxemia and sepsis survival (Table 4). The most important metabolite group that differentiated surviving and non-surviving CAPSOD patients was acyl-carnitines (Langley et al., 2013). In our analysis, we observed a similar trend with all significantly changed acyl-carnitines exclusively higher than the $t_{0,LPS}$ baseline at both time points in sepsis non-survivors (Table A. 3), whereas for the surviving patients, around half of the acyl-carnitines were below the baseline. For the endotoxemia group, the direction of change in acyl-carnitine concentrations at $t_{6,LPS}$ were the same as that of sepsis survivors (4 of total 12 acyl-carnitines were significant at $t_{6,LPS}$).

4.2.1 Limitations

Firstly, the timing of the data collection, and therefore the phase of the response that is being studied, can vary greatly depending on the lag time from the initiating event to the presentation to an emergency department. Secondly, the nutritional input, being non-controlled either before or after the hospital admission, could have affected the plasma metabolite concentrations as an independent factor. Thirdly, some of the CAPSOD patients either had prior comorbidities were likely to affect the metabolome, such as diabetes mellitus; or, were also developing conditions which further exacerbated response, including compromised renal function, a likely major contributor to the observed metabolome.

4.3 Conclusion

Therapeutic strategies that are successfully translated into the clinic are very few and mostly non-specific in the field of critical care. This is due, in part, to the complex and dynamic physiological processes involved. Heterogeneity of the patient populations and consequent challenges in performing insightful clinical studies also have contributed to the lack of progress in this realm of medicine (Angus and van der Poll, 2013, Cain et al., 2014). Emerging *-omics* tools that are capable of examining physiologic responses at the systems level are promising especially for complex conditions such as sepsis and SIRS (Maslove and Wong, 2014). The major caveat related to these tools is that; since the biological processes are analyzed at a higher level, inter-species differences become as relevant to the response as the sought-after question itself. Therefore utility of the animal models has been questioned recently in the scientific community (Osuchowski et al., 2014, Seok et al., 2013).

The human endotoxemia model has been serving as a useful experimental platform for gaining insight into the mechanisms governing systemic inflammation. It is a recognized fact that this model does not fully replicate the magnitude of physiologic

stress created by trauma or infection (Lowry, 2005, Calvano and Coyle, 2012); however it gives researchers the opportunity to study the mechanisms underlying the response to systemic inflammation and relevant therapy options without the inter-species differences obscuring the interpretation of the results.

Progression of response to systemic inflammation induced by endotoxemia in immune cells has been described at the genomic level (Talwar et al., 2006, Calvano et al., 2005). Moreover, comparison of the response to experimental stimuli and traumatic/infectious insults revealed significant overlap of common features both at the gene (Haimovich et al., 2010) and protein expression levels (Visser et al., 2012). In the light of these observations, the current study aimed at an objective evaluation of the concordance between experimental and clinical cases of systemic inflammation and benchmarked endotoxemia against sepsis of various origins at the level of metabolic response. Plasma metabolome can be thought of as the metabolic fingerprint representative of the state of body at any given time and provide information on the dominant regulatory mechanisms at various levels of cellular processes including transcription, translation, and signal transduction. For effective provision of critical care, understanding the alterations in plasma metabolome is crucial, because metabolite levels impact the regulation of anti-inflammatory defenses, in turn, through steering critical cellular processes and immune mechanisms. Therefore, we think that the assessment of the relevance of endotoxemia as an experimental model representing critical illness is important.

We believe that the observed concordance between the responses of LPS treated subjects and sepsis patients at the metabolome level despite observed variability in clinical data strengthens the relevance of endotoxemia to clinical research as an elementary tool and gives valuable insights into the metabolic changes necessary for proper response to inflammatory stress at the systemic level.

Chapter 5 Integration of Liver Transcriptomics and Proteomics in Response to Anti-Inflammatory Treatment

Our studies in systemic inflammation showed us that even a benign inflammatory stimulus such as LPS can drastically affect our metabolic homeostasis. We further showed that changing metabolite levels in response to the inflammatory processes in the body impact the regulation of anti-inflammatory defenses, in turn, through directing critical cellular processes in immune cells. This is because the metabolite levels in plasma reflect the available supplies of immune cells and drastic shifts in these levels have potential to alter the cellular processes where these supplies are utilized. Evaluating the changes in metabolic processes is also critical for assessing the overall effect of a therapy. Although the drugs are designed to provide a therapeutic benefit to the patient by specifically acting on their biological targets, in most cases the drug molecules themselves or their metabolic products have certain side effects that require thorough evaluation. Since inflammatory processes are intricately connected to many physiologic functions, this issue becomes significantly important in the design of anti-inflammatory therapies. In this chapter, we focused on understanding the effects of one of the most commonly used anti-inflammatory drug on liver. Liver is the master regulator of the metabolism, therefore evaluating the effects of a drug on hepatic processes is critically important to understand and caution against its potential undesirable effects on whole body metabolism.

The specific drug which was the focus of our analyses was methylprednisolone (MPL), which is a synthetic corticosteroid (CS) shown in Figure 5-1. CSs are widely used as anti-inflammatory and immunosuppressive agents in the treatment of a variety of inflammatory and auto-immune conditions including organ transplantation,

rheumatoid arthritis, lupus erythematosus, asthma and allergic rhinitis (Barnes, 1998, Swartz and Dluhy, 1978).

The mechanism of action of CS drugs is basically magnifying the physiological actions of the endogenous glucocorticoid hormones, which have anti-inflammatory properties depending on their secretion level and the time at which they are secreted. These hormones also have diverse effects on a variety of physiological processes including carbohydrate, lipid and protein metabolism, immune-regulation, bone homeostasis and developmental processes (Vegiopoulos and Herzig, 2007, Barnes, 1998).

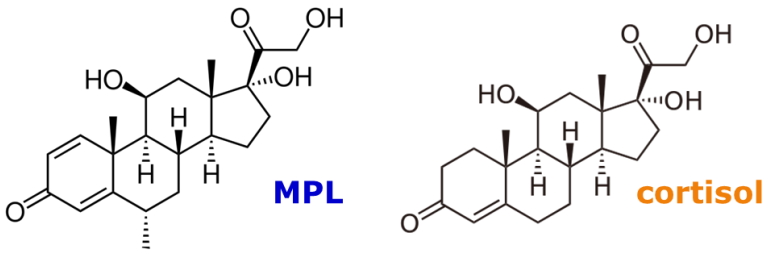

Figure 5-1: Structure similarity of methylprednisolon (MPL) and endogenous glucocorticoid hormone cortisol.

Although short-term use of CSs are beneficial for reducing the inflammation in the short-term, their long-term use is associated with serious side-efffects because of their diverse effects on other physiological functions, especially in hepatic processes (Morand and Leech, 1999, Andrews and Walker, 1999).

The well-established molecular mechanisms of action for CS (illustrated in Figure 5-2) include the passive diffusion of the highly lipophilic CS molecule through the cell membrane and binding to the cytosolic glucocorticoid receptor, which is held inactive through the association with heat shock proteins (Schaaf and Cidlowski, 2002). Binding of the drug to the receptor causes conformational changes, phosphorylation and

activation of receptor resulting in the formation of a homodimer of the drug receptor complex (Oakley and Cidlowski, 2011, Schaaf and Cidlowski, 2002). This activated complex translocates into the nucleus and binds to regulator sites, glucocorticoid regulatory elements (GREs) in the DNA, resulting in the regulation of transcription rate.

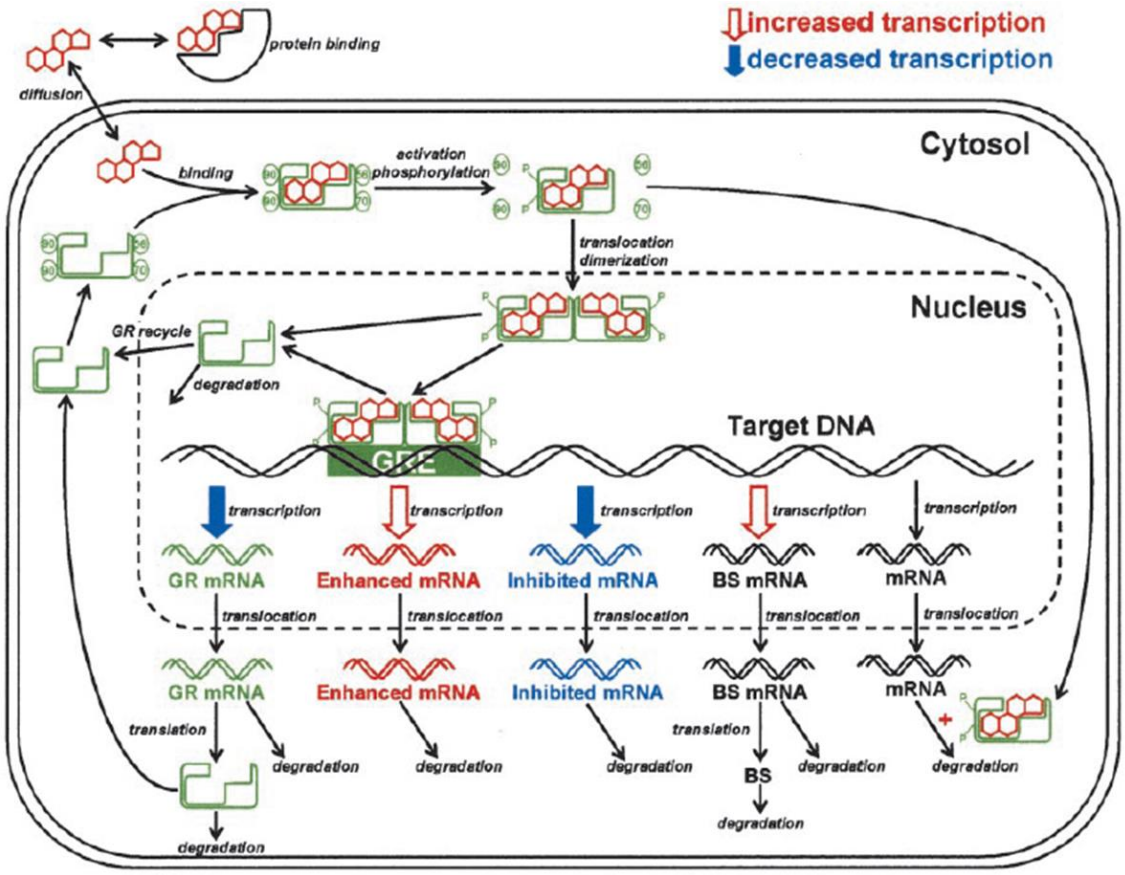

Figure 5-2: Mechanism of action of corticosteroids, adapted from (Jin et al., 2003).

However, in addition to direct binding, the activated complex can regulate gene expression by other mechanisms including tethering and composite binding to other transcription factors, activators, or repressors (Barnes, 1998, Schaaf and Cidlowski, 2002). Some of the critical transcription factors that are affected by CS include NF-κB,

AP-1 and STAT. In addition to these genomic mechanisms, studies have shown that CS can regulate pathways by signaling through its receptor in a transcription-independent manner, although the exact mechanisms for the non-genomic effects are still unclear (Schaaf and Cidlowski, 2002).

Because of the diverse effects of CS and different molecular mechanisms potentially involved in these actions, an "-omics" approach can be effective in gaining better understanding of the effects of CS on different pathways and functions (Nguyen et al., 2010). Previous studies used gene microarrays to profile temporal changes in mRNA expression in multiple tissues following CS administration in rats (Almon et al., 2007a, Almon et al., 2003, Almon et al., 2007b, Almon et al., 2005). These studies characterized global dynamics of the system that are regulated by CS at the transcriptional level. Although this information is useful and highly relevant, direct profiling of the protein expression changes and integrating the information from the genomic and proteomic response will provide deeper insights into CS actions, given their diverse and complex mechanisms. Recently, a high-throughput methodology was developed that uses an ion current-based liquid chromatography/mass spectrometry (LC/MS) strategy, allowing comprehensive and accurate profiling of the tissue proteome (Tu et al., 2012). Using this methodology the temporal changes in the expression of thousands of proteins in rat liver after MPL administration has been characterized (Nouri-Nigjeh et al., 2014a). With this new information from the protein expression level, it is possible to evaluate complementarities across transcription and translation of the target genes and get a more complete understanding about the mechanisms of action of this drugs. With this objective, this study describes the tandem analysis of rich time-series transcriptomic and proteomic data in rat liver in response to MPL.

5.1 Methods

5.1.1 Animal experiments

All animal experiments were performed at the University of Buffalo and protocols adhered to "Principles of Laboratory Animal Care" (NIH publication 85-23, revised in 1985) and were approved by the University at Buffalo IACUC committee.

Proteomics: Sixty adrenalectomized (ADX) Wistar rats were injected with 50 mg/kg methylprednisolone (MPL) intramuscularly and sacrificed at 12 different time points between 0.5 and 66 h post-dosing (5 animals / time point). Five animals, injected with saline and sacrificed at random time points in the same time window, served as controls. In order to remove the high concentrations of blood protein, it was necessary to use perfused tissue for proteomic analyses, which precluded the use of the same tissues employed for transcriptomics (below). Proteins from perfused and flash frozen livers were extracted, digested and analyzed using a nano-LC/LTQ/Orbitrap instrument. The Nano Flow Ultra-high Pressure LC system (nano-UPLC) consisted of a Spark Endurance autosampler (Emmen, Holland) and an ultra-high pressure Eksigent (Dublin, CA) Nano-2D Ultra capillary/nano-LC system, with a LTQ Orbitrap mass spectrometer (Thermo Fisher Scientific, San Jose, CA) used for detection. Protein quantification was based on the area under the curve (AUC) of the ion-current-peaks. A more extensive description of the experimental setup and the analytical methodology can be found in the previously published study (Nouri-Nigjeh et al., 2014b).

Transcriptomics: Forty-three ADX Wistar rats were given a bolus dose of 50 mg/kg MPL intravenously. Animals were sacrificed at 16 different time points between 0.25 and 72 h post-dosing. Four untreated animals sacrificed at 0 h served as controls. The mRNA expression profiles of the liver were arrayed via Affymetrix GeneChips Rat Genome U34A (Affymetrix, Inc.), which contained 8800 full-length sequences and

approximately 1000 expressed sequence tag clusters (Jin et al., 2003). This dataset was previously submitted to the GEO (GSE490).

5.1.2 Computational Analysis

Hierarchical Clustering of Concatenated Dataset

Data analysis for both proteomic and transcriptomic datasets started first by filtering for differential expression over time. Proteins and transcripts with differential temporal profiles were determined by using EDGE software. We employed within-class differential expression to extract profiles that have a differential expression over time (Storey et al., 2007, Leek et al., 2006, Storey et al., 2005). Integration of these two datasets for any further analysis required matching the object identifiers which was achieved through running a comparison between two filtered datasets in Ingenuity Pathway Analysis (IPA, Ingenuity® Systems, www.ingenuity.com). This analysis helped us identify the genes which were differentially expressed both at the transcriptional and translational levels. In order to find potential co-regulatory relationships at these two levels, hierarchical clustering was used for first-pass analysis. For this purpose, temporal transcriptomic and proteomic data for the common genes were first concatenated and then clustered using the `clustergram` function in the Bioinformatics toolbox of MATLAB (Mathworks, Natick MA). The two clusters obtained by using `correlation` as the distance metric.

Two-way Sequential Clustering of Individual Proteomic and Transcriptomic Datasets

While hierarchical clustering analysis described above identifies the potential co-regulatory schemes for the genes in the intersection of transcriptomic and proteomic datasets; it fails to capture the dynamics in the rest of the genes which may also show differences in expression over time, although they may not co-exist in both datasets.

In order to evaluate the overall dynamic patterns and extract the most useful information integrating these two dataset, a consensus clustering (Nguyen et al., 2009) method was applied to these two datasets separately. First, proteins with differential temporal profiles were clustered using p-values of 0.05 for significant clusters and an agreement level of 0.70 for the genes in each cluster. Then, probe sets corresponding to the proteins in each cluster were identified through the comparison function in IPA as before. Temporal profiles of these probe sets corresponding to the proteins were compiled and separately sub-clustered through the less stringent hierarchical clustering method, again using `clustergram` function in MATLAB.

The reverse of the same procedure was also performed - starting from transcriptional analysis and continuing with the corresponding proteomic analysis. Here, differential transcriptional profiles were first determined and then clustered using the same procedures described above. As with the previous analysis, proteins that were coded by the probesets within each of these clusters were then identified and sub-clustered.

5.1.3 Biological Interpretation

Functional annotations of proteins and transcripts at each level of analysis were conducted in IPA by running a core analysis for each cluster and evaluating the enriched canonical pathways (at p-value threshold of 0.05) and predicted upstream regulators obtained in IPA.

5.2 Results

Studies focused on understanding the relationship between global mRNA transcription and protein translation have produced mixed results, many of which concluded that the transcriptomic and proteomic data is far from being easily described as complementary (Greenbaum et al., 2003, Haider and Pal, 2013, Waters et al., 2006, Hegde et al., 2003, Nicholson et al., 2004). This study aimed to compare and contrast

the transcriptional and translational changes in liver induced by the exposure to a synthetic CS at a pharmacological dose. Although high-throughput -*omics* analyses have been obtained from samples collected from two independent studies; the strain of experimental animals, dose and type of pharmacologic agent, sampled tissue, sampling procedures, and most of the time points for sample collection were the same for these studies. These conditions allowed us to assume that the experiments are similar enough to conduct individual and integrated bioinformatics analyses. The preprocessing before performing the first-pass analysis involved identifying the significant genes whose both transcripts and proteins existed in the individual datasets. The followed procedure is schematically shown in Figure 5-3. Differential expression analysis through EDGE identified that 475 out of 959 proteins and 1624 out of around 8800 transcripts had temporal profiles that significantly varied over time (meeting p-value < 0.05 and q-value < 0.01 cut-offs). After this filtering step, both datasets were fed into IPA in order to match distinct identifiers used (Swiss-Prot IDs for proteins and Affymetrix IDs for transcripts). A comparison between two datasets indicated that 163 genes were commonly found in both transcriptomic and proteomic datasets; i.e., both mRNAs and proteins corresponding to these genes were differentially expressed over time.

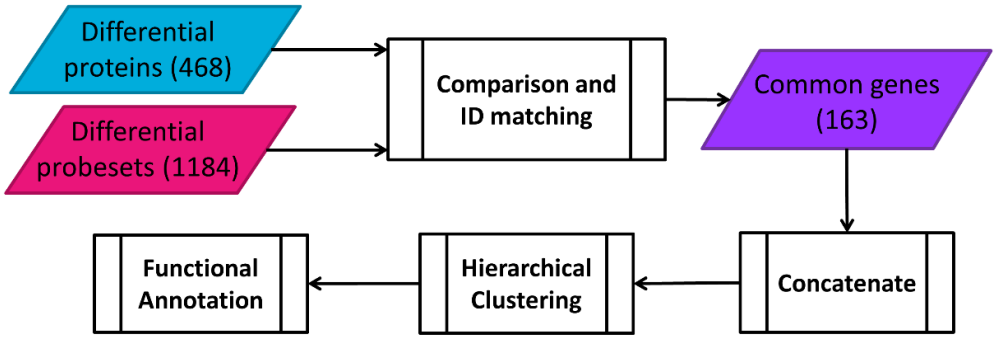

Figure 5-3: Workflow for hierarchical clustering of the concatenated transcriptomic-proteomic dataset.

5.2.1 Hierarchical Clustering of Concatenated Datasets:

Temporal transcriptional and protein expression data for 163 common genes were concatenated and clustered through hierarchical clustering by using correlation as the distance metric. Overall, this analysis identified two dominant patterns as shown in Figure 5-4. Cluster 1 was populated with 80 genes for which corresponding mRNA and protein expression profiles were essentially parallel in direction, while for 83 genes in Cluster 2 the directionality was reversed. For both clusters, the first 8 hours is seemingly the most critical time period during which mRNA and protein expression profiles change direction. Genes in Cluster 1 display up-regulation for both mRNA and protein expression profiles in the first 8 hours, after which down-regulation predominates, markedly in the transcriptional profiles. In the second cluster, early down-regulation predominates for transcriptional profiles; however corresponding protein expression profiles are not complementary. While down-regulation is observed in these transcripts most notably in the first 8 hours; expression of the same proteins seems to be up-regulated in the same time frame. After the 8th hour; both transcriptional and protein expression profiles approach basal levels, though from opposite directions; elevated mRNA levels start to be down-regulated and reduced protein levels start to be up-regulated.

Functional annotation of the genes in these two clusters, obtained through enrichment analysis in IPA, is shown in Cluster 1 (where direction of regulation is similar) included a number of genes coding for heat shock proteins, which take part in the negative regulation of CS signaling through direct protein-protein interaction with glucocorticoid receptor to prevent its translocation to nucleus (Chrousos and Kino, 2005). Complementary transcriptional and proteomic profiles of these genes indicated that this is a negative feed-back control induced by MPL which is regulated at the transcriptional level. Proteins functioning in the regulation of protein degradation and

translation machinery were also among the genes in Cluster 1 (including PSMCs, HSPs, EIFs, RPLs and RPSs), implying that these processes are also controlled at the transcriptional level after CS exposure. In contrast, functions enriched by the genes in Cluster 2 appear to be regulated at post-transcriptional levels, likely through control of mRNA processing, initiation of protein translation or protein stability, since the transcriptional profiles are not emulated by protein expression (Waters et al., 2006). Among these functions most notable are the modulation of oxidative stress, lipid metabolism and bile acid biosynthesis.

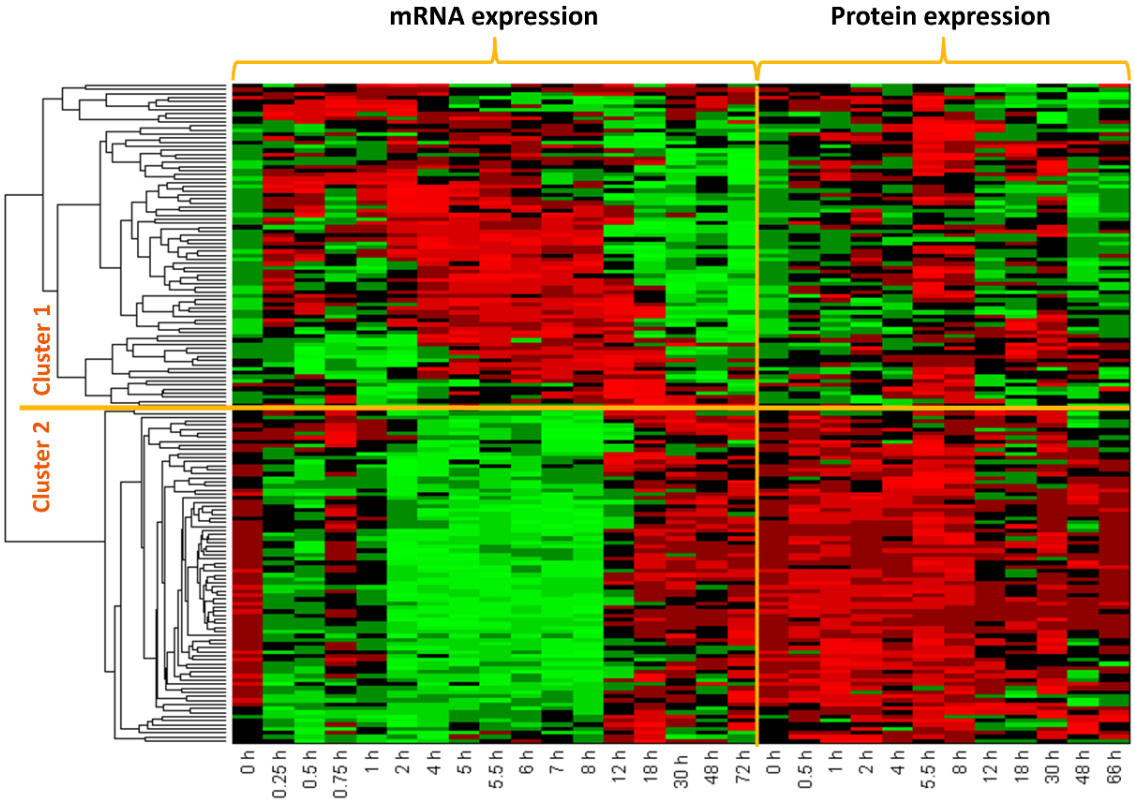

Figure 5-4: Heat map of clustered concatenated dataset. Red color indicates increase in expression while green indicates decrease.

Table 5.1: Functional annotation of differentially expressed genes in both transcriptional and translational levels.

<table>
<tr><th>Cluster 1</th><th>Cluster 2</th></tr>
<tr><td>mRNA expression is essentially parallel with protein expression</td><td>mRNA expression and protein expression moves in opposite directions</td></tr>
<tr><td colspan="2">Functional Annotation</td></tr>
<tr><td>CS signaling</td><td rowspan="3">Xenobiotic metabolism, Oxidative stress modulation, Hormone degradation
Cytochrome p450 family
Sulfo-transferases
Glutathione S-transferases
Aldehyde dehydrogenases
Catalase</td></tr>
<tr><td>Protein ubiquitination
Proteasome
Heat shock proteins</td></tr>
<tr><td>Protein translation
Eukaryotic translation factors and ribosomal proteins</td></tr>
<tr><td>Urea cycle enzymes</td><td>Fatty acid oxidation, Valine-tryptophan degradation, Ketolysis</td></tr>
<tr><td>Hormone degradation
Sulfo- and glucuronyl-transferases</td><td>Bile acid biosynthesis</td></tr>
</table>

Possible upstream regulators that can explain the observed changes in gene/protein expression are also identified through IPA core analysis based on the prior knowledge of expected effects between the upstream regulators and target genes/proteins in the dataset. Definition of upstream regulator, however, is used rather loosely here, as almost any type of molecule that affects the expression of other molecules can be upstream regulators whether they are transcription factors, kinases or hormones. The analysis first examines how many known target genes of each candidate upstream regulator are present in the dataset. It then compares the direction of change in those targets with what is expected from the literature in order to predict relevant upstream regulators. If the observed direction of change is consistent with a particular activation state (i.e., activated or inhibited) of that candidate regulator then a prediction is made about the activation state. Using the genes coexisting in both transcriptomic and proteomic datasets, a number of upstream regulators were identified for each time point and predicted results are shown in Table 5.2. Two clusters obtained through hierarchical clustering were examined separately; however there are common

Table 5.2: Predicted upstream regulators and their activation states (green: activated, red: inhibited) based on the gene groups obtained by hierarchical clustering.

	0.5 h	1 h	2 h	4 h	5.5 h	8 h
Cluster 1			NFE2L2 SLC13A1	SLC13A1	NFE2L2 SLC13A1 LEP	NR1I3 LEP
Cluster 2	ZBTB20	NFE2L2		NR1I3	ZBTB20	ACOX1 NR1I3 NR1I2 NFE2L2
	12 h	**18 h**	**30 h**	**48 h**	**66 h**	
Cluster 1	NR1I3	SLC13A1	NFE2L2 LEP SLC13A1		LEP	
Cluster 2				ZBTB20	ZBTB20 NFE2L2	

predicted regulators of the elements in different clusters. Reliability of a predicted element increases as the number of times it is identified from consecutive datasets and also if there is a coherent pattern in its predicted state (i.e., whether it is activated or inhibited). Based on this, Nuclear Factor Erythroid-Derived 2-Like 2 (NFE2L2) seems to reliably contribute to the observed gene/protein expression patterns by inducing early up-regulation and late down-regulation.

Two other important genes are solute carrier family 13 (sodium/sulfate symporter), member 1 (SLC13A1) and leptin (LEP), both of which seem to have an inhibitory effect on gene/protein expression throughout the time course of the study.

5.2.2 Two-way Sequential Clustering of Individual Proteomic and Transcriptomic Datasets:

The approach followed for the first part of the analysis described above imposes the stringency that a gene has to be differentially expressed both in the transcriptional

and translational levels to be included in the final hierarchically clustered dataset. To fully characterize the temporary patterns of protein translation induced by MPL and to get additional insights into how that process is connected with the transcriptional events during the corresponding time frame, we also followed a sequential approach as schematically shown in Figure 5-5. What is distinct about the sequential approach is that it allows focusing on each dataset independently of the other, i.e., regardless of the complementary dataset being also differentially expressed. This increases the number of elements in clustering analysis. Consensus clustering, on the other hand, is an inherently more stringent approach compared to hierarchical clustering, eliciting the most coherent expression patterns in the dataset. Therefore this second approach, with stringency in coherent expression at one level rather than commonality at both levels, aims to identify the dominant patterns in one level of regulation (transcription or translation) and to check how closely it is associated with the patterns in the other level.

First, an in-depth analysis of the proteomic dataset was done in order to capture the dynamics of protein expression in liver following MPL dosing. EDGE identified 475 out of 959 proteins to be differentially expressed over time. Consensus clustering revealed 5 coherent temporal profiles containing 217 of the 475 regulated proteins. The detailed distribution of these 5 clusters is given in Table 5.3. The first two clusters (Figure 5-6 a-b) show early up-regulation within the first 5.5 hours after MPL, followed by a recovery period. Proteins in Clusters 3 through 5 (Figure 5-6 c-e) display later increase in expression, peaking at 5.5, 8 and 18 hours following the MPL dose.

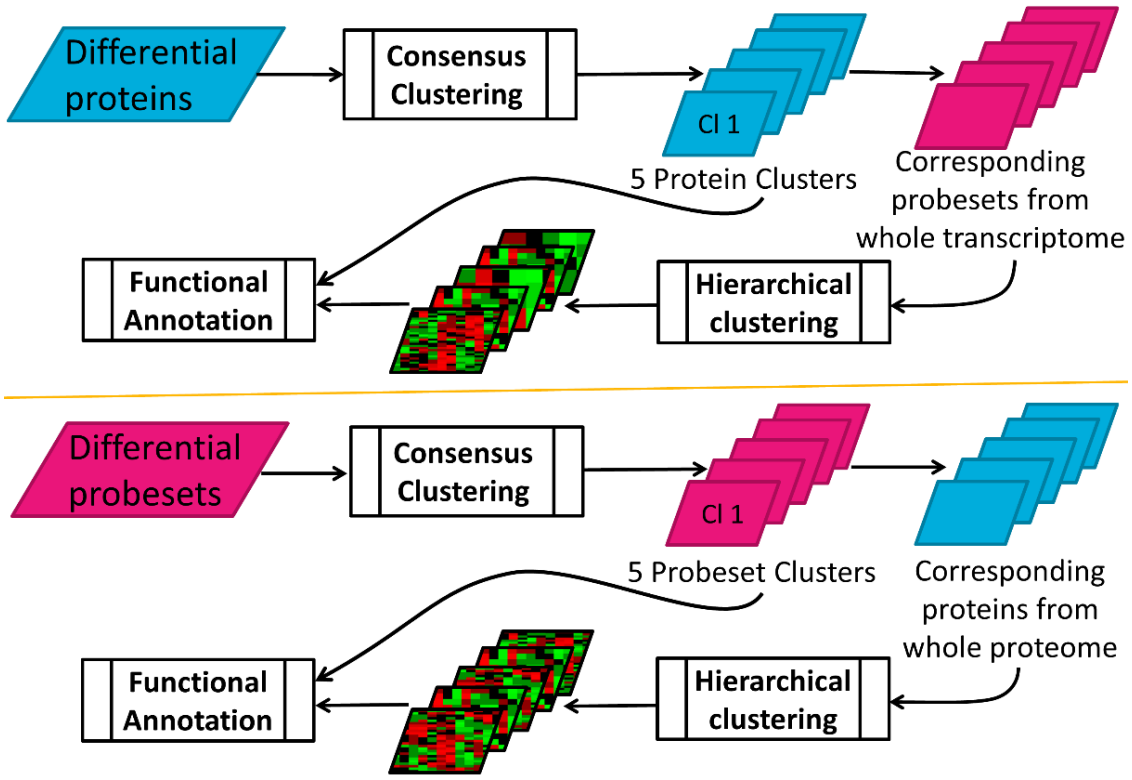

Figure 5-5: Workflow for sequential clustering analysis carried out in both forward and reverse directions between proteomic and transcriptomic datasets.

Hierarchical clustering of the corresponding probesets for each protein cluster was used to investigate the dependency of protein translation (or lack of it) on transcription. Of the 217 clustered proteins, 158 showed regulation of its mRNA as well. Interestingly, this analysis showed that, while a small number of the transcripts roughly correlate with expression of corresponding proteins, in most of the clusters a greater number of transcripts displayed the opposite pattern. This is consistent with the observations in hierarchical clustering of the concatenated dataset and emphasizes the prominent role of post-transcriptional regulation in establishing the pharmacologic effects of MPL in liver.

Table 5.3: Distribution of elements after clustering and sub-clustering of data in two-way analysis.

Proteomics → Transcriptomics		
	# of proteins	Corresponding # of probesets in the transcriptomic dataset
Cluster 1	44	34
Cluster 2	30	27
Cluster 3	72	45
Cluster 4	42	29
Cluster 5	29	23
Transcriptomics → Proteomics		
	# of probesets	Corresponding # of proteins in the proteomic dataset
Cluster 1	413	66
Cluster 2	155	30
Cluster 3	92	25
Cluster 4	334	85
Cluster 5	138	11

In addition, this analysis was repeated in the reverse direction; i.e., starting from the transcriptomic dataset and progressing to the proteomic dataset. 1624 of the probe sets were differentially expressed, 1132 of those were in 5 clusters obtained by consensus clustering. Only 217 of these 1132 probe sets had corresponding proteins in the proteomic dataset. Distribution of these 217 proteins to their correspondent transcript clusters is shown in Table 5.3. Two of the clusters were considerably more densely populated than the others. The transcriptional profiles of these clusters are shown in Figure 5-7 a and d (left side), and they can be considered as the most dominant early-up/late-down-regulation and early-down/late-up-regulation patterns. Heat maps on the right display the expression patterns of corresponding proteins for each cluster. Compared to the first part of sequential clustering analysis, considerably fewer proteins actually correlate with the transcriptional profile of their respective clusters. Especially for the most densely populated cluster, Figure 5-7 d, only a couple of proteins show early-down/late-up-regulation pattern in parallel with the corresponding temporal pattern of the first cluster. The only cluster in which

expression of the majority of proteins go more or less in parallel with the temporal profile of the corresponding transcriptional cluster is the first cluster (Figure 5-7 a).

Considering that protein expression is a more reliable predictor of function, the annotation analysis was based on the proteomic data in this part of the analysis. The proteins included in the clusters shown in Figure 5-6 were functionally annotated through core analysis in IPA, pathways with an enrichment score higher than 0.05 were considered significant and obtained results are shown in Table A. 4. The protein clusters were numbered according to the time at which the peak activity was observed. Four clusters displayed increasing activity sequentially within the first 8h and one showed a relatively delayed activity, around 18h after MPL dosing.

5.3 Discussion

Characterization and analysis of global gene expression changes has become an integral part in studying mechanisms of actions of various pharmacological agents (Butte, 2002). Developments in high-throughput methodologies such as microarrays allowed relatively affordable and faster characterization of gene expression. These genomic approaches offer a powerful tool in understanding drug effects at the molecular level and aid in target and biomarker discoveries and in gaining insights into modulation of relevant pathways. Previous studies with microarrays (Almon et al., 2007a, Almon et al., 2003, Almon et al., 2005) helped in understanding of various pathways modulated by CS at the transcriptional level that are either common across tissues or unique to certain tissue types (Yang et al., 2009, Nguyen et al., 2010). Through clustering and other bioinformatic analyses of time series; genes sharing similar expression patterns across different dosing regimens and gene clusters showing distinct temporal profiles were identified and related to drug effects/side-effects (Nguyen et al., 2010).

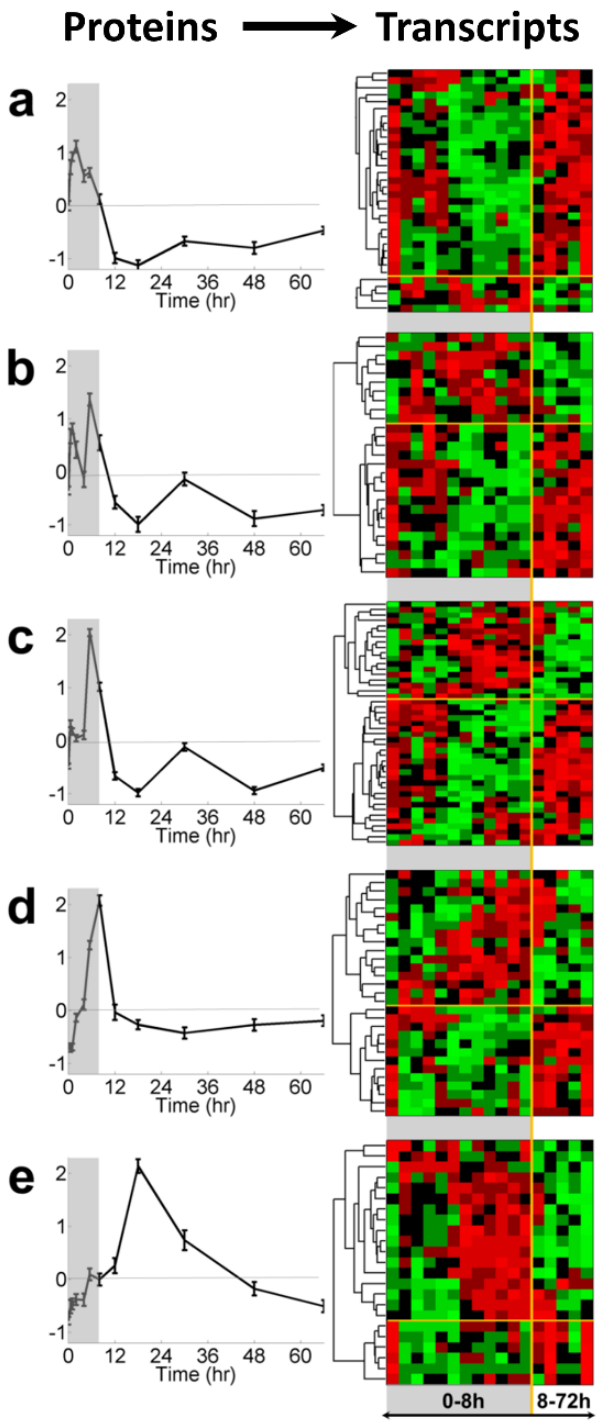

Figure 5-6: Five clusters of proteins obtained by consensus clustering (a-e, left side), and heat maps of corresponding hierarchically clustered probesets (a-e, right side). Canonical pathways enriched by the proteins in these clusters are given Table A. 4.

Although information on mRNA expression changes helps in understanding mechanisms of drug action, some studies show that message expression changes may not correlate well with protein changes and hence might not accurately reflect drug effects (as the majority of pathway modulators and drug targets are proteins) (Nishizuka et al., 2003, Shankavaram et al., 2007). Hence characterization of changes in protein expression at the proteome level (along with gene expression profiling) will not only reveal the dynamic and temporal features of drug-induced protein changes, but will also provide rich biological information which may lead to improved understanding of diverse drug effects at both transcriptional and translational levels.

Comprehensive, accurate, and reliable profiling of protein expression remains highly challenging because of the extreme diversity of the chemical and physical properties of proteins, the large dynamic ranges in concentrations in most proteomes, and the fact that drug-responsive proteins are often low-abundance. Recently developed robust and highly sensitive label-free quantification strategy allowed accurate expression profiling of complex tissue proteomes, with the capacity for analyzing large numbers of biological samples (Tu et al., 2012). This strategy was utilized to characterize the temporal changes in expression of thousands of proteins after a single dose of MPL.

Availability of rich time-series datasets for changes in both mRNA and protein expression after single-dose administration of MPL allowed us to integrate both transcriptional and translational states and enabled us to perform a unique analysis to compare and contrast the two. With this analysis we developed an algorithm to compare temporal changes in both gene and protein expression. This allowed us to examine the relationship between the two and to differentiate the transcriptional and translational effects of CS dosing. These drugs affect a wide range of pathways that are involved in metabolism (carbohydrates, lipids and proteins), immune-regulation

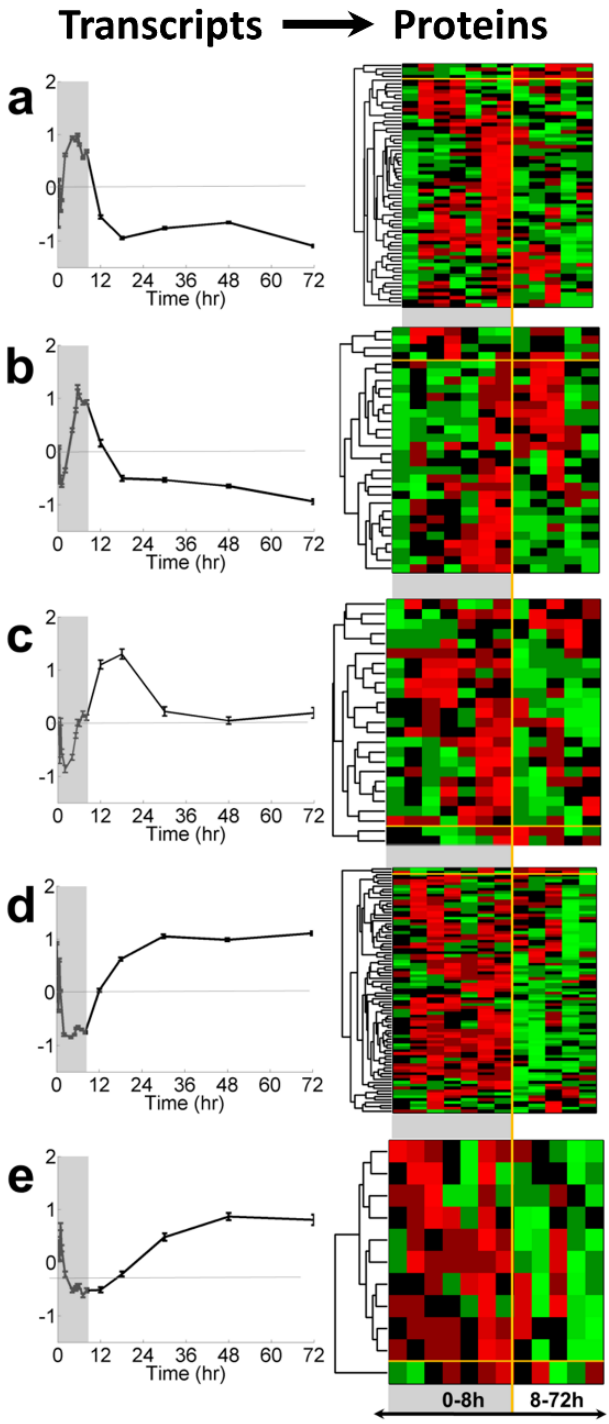

Figure 5-7: Five clusters of transcripts obtained by consensus clustering (a-e, left side), and heat maps of corresponding hierarchically clustered protein datasets (a-e, right side).

and other critical cellular functions (Swartz and Dluhy, 1978, Bialas and Routledge, 1998). Because CS regulate diverse sets of genes and proteins, the dynamic effects of these drugs provide a relevant system to compare, contrast, and integrate both the genomic and proteomic data. Although the data were obtained from different but very similar animal studies, it is reasonable to integrate the two for the following reasons: both studies were performed in the same strain of rats (Wistar) that were adrenalectomized and maintained under similar conditions; MPL was given in both studies and identical doses of 50 mg/kg were used. The only major difference between the two studies is that the gene expression analysis were performed in animals that were given an intravenous dose of the drug and the proteomic measurements were performed in rats given an intramuscular injection of MPL. However, our previous studies comparing the two routes of MPL dosing indicated that though there are some early differences in the pharmacokinetic profiles of MPL, the pharmacodynamics of an important biomarker tyrosine aminotransferase (TAT) expressed in liver were comparable (Hazra et al., 2007).

With the hierarchical clustering of the concatenated genomic and proteomic data we identified two dominant patterns, one of which showed up-regulation of expression at both mRNA and protein levels (Cluster 1, Figure 5-4). Most of the genes and proteins in this cluster show similar temporal patterns (with peak expression occurring at similar times) or with a slight delay in the peak expression time of the protein compared to the gene profiles. Some of the classic pharmacodynamics markers for CS actions, including tyrosine aminotransferase (TAT) and aspartate aminotransferase (GOT1), fall into this category with up-regulation of both the mRNA and protein expression after MPL dosing. Similarly, this group includes genes/proteins involved in

glucocorticoid signaling confirming the direct pharmacological action of MPL at both the genomic and proteomic levels (Hazra et al., 2008).

One of the primary effects of CS in liver is to stimulate gluconeogenesis (production of glucose) from amino acids released by protein breakdown in muscle (because of CS action) through deamination and utilization of the carbon backbone for glucose production in the liver. As a result, the excess amines are removed through the urea cycle to maintain proper homeostasis (Hazra et al., 2008, Bialas and Routledge, 1998). As shown in Table 5.1, Cluster 1 includes genes and proteins involved in the urea cycle that are up-regulated after MPL dosing and both gene and protein expression share similar temporal profiles.

The other functions that are enriched in Cluster 1 include those involved in protein translation and processing (Table 5.1). Ribosomal proteins and translational factors that play critical roles in protein translation and heat shock proteins that help in proper chaperoning of newly formed proteins show up-regulation at both gene and protein levels (Warner and McIntosh, 2009). All genes/proteins in Cluster 1 represent direct transcriptional effects of CS, resulting in temporal expression changes in mRNA that translate to concurrent or slightly delayed protein expression changes. Since mRNA profiling is more straightforward, well established, and cheaper than the protein counterpart, an important point to note here is that mRNA expression markers can be representative of their corresponding proteins in assessing the effects of CS actions for genes/proteins populated in Cluster 1.

Genes and protein expression profiles in Cluster 2 are more intriguing and we have very limited understanding of the biology and mechanisms behind this observation. Although previous studies have been conducted in identifying differences in the changes at the transcriptional and translational levels for one or selected few proteins,

global assessment through high throughput methodologies have never tried to address this issue (Nouri-Nigjeh et al., 2014b, Sukumaran et al., 2011, Qu et al., 2006).

Studies that have characterized and compared genomic and proteomic data have almost always been single time-point studies that do not provide the relevant temporal information necessary to identify and characterize transcriptional and translational differences (Gry et al., 2009, de Godoy et al., 2008). These single time-point high throughput studies showed poor correlation between mRNA and protein expression data (Gry et al., 2009). Analysis from our study shows that some of the functional pathways involved in lipid, protein and xenobiotic metabolism that are important pharmacological targets of CS showed different temporal expression patterns for mRNA and proteins. This suggests that in addition to the direct transcriptional effects of CS, there could be additional translational or post-translational effects that result in different protein expression temporal patterns compared to the mRNA profiles. Factors including regulation of microRNAs (which can alter protein translation) and direct or indirect translational controls could produce the different mRNA and protein profiles (He and Hannon, 2004). Whatever the mechanisms that control the difference between gene and protein expression are, mRNA profiles in Cluster 2 cannot be directly used for deciphering the regulation of the functional pathways they represent.

5.4 Conclusion

The results of present study elicited both expected and unexpected relationships between mRNA transcription and protein translation in liver after single CS dose. Roughly half of the genes commonly found in both transcriptomic and proteomic datasets had complementary temporal profiles indicating regulation at the transcriptional level. Some of the functions that these genes are associated with were regulation of corticosteroid signaling, protein degradation and translation machinery. The lack of complementarity between message and protein expression profiles in the

other half of genes was intriguing. Although our understanding of the involved mechanisms is limited at this point, this result suggested additional translational or post-translational impacts of CS in addition to their direct transcriptional effects.

Independent from the corresponding profiles, we also examined the rich time-series data through stringent two-way clustering and sub-clustering approach. We used proteomic data, to portray the cellular landscape after CS dose due to its higher priority in representing the actual phenotype. This allowed us to define the prominent temporal shifts in protein expression and to determine associated cellular functions.

Chapter 6 Summary and Future Perspectives

6.1 Summary

This dissertation is centered on extracting physiologic information from time-course data provided by the -omics analyses and integrating multiple levels of analyses in relevant biological context. Underlying theme in the included work is pathogenesis and treatment of inflammation, though examined at two different host species due to the very nature of available in vivo models. Specifically, our work involved the assessment of self-limited systemic response to inflammation in an experimental endotoxemia model in healthy humans; and hepatic response to corticosteroid therapy in a murine model.

Elective administration of bacterial endotoxin to healthy human subjects has long been used as a reproducible experimental procedure providing mechanistic insights into how cells, tissues and organs respond to systemic inflammation. This response is closely associated with alterations in metabolism, since inflammatory processes considerably affect the levels of plasma metabolites. We performed the first complete metabonomic analysis in human endotoxemia model by describing the temporal alterations of plasma metabolites within the first day of LPS treatment. Dominant temporal patterns of metabolite concentrations extracted by principal component analysis pointed out to the critical time point which separated the development and recovery phases of LPS induced metabolic changes. Clustering approach identified the metabolite subsets with common coherent profiles exhibiting closely associated interactions while also facilitating the recognition of temporal relationships between the clusters of elements. Prominent roles of lipid and protein metabolism in regulating the response to systemic inflammation and their dynamics displaying opposing directionality were highlighted. Overall, this single level analysis uncovered the temporal patterns in the host

metabolism reflecting collective impacts of regulations at various organs and at multiple levels of cellular processes including transcription, translation and signal transduction.

Building on this knowledge; we integrated the transcriptional response of leukocytes with plasma metabonomics to understand how their gene expression might have been affected from the metabolic landscape of the fluid environment in which they circulate. We hypothesized that the drastic changes in the immediate environment of the leukocytes might have an adaptive effect on shaping their transcriptional response in conjunction with the initial inflammatory stimuli. In line with this hypothesis, we observed that the regulation of oxidative stress and selection of bioenergetic routes displayed parallel changes with associated metabolite levels in plasma. Besides describing the metabolic response of human body to an inflammatory cue at the systemic level together with affected immune mechanisms; this study can inspire future translational studies as the -omics analyses becomes routine in clinical practice. Because blood is the biological sample fastest and the least invasive to collect from patients while yielding most useful information about the state of the body. Therefore, benchmarking the metabolic state of the system and transcriptional state of the immune cells by single biological sample may expedite clinical decision making and help reduce mortality in critical cases.

In the context of human endotoxemia model, we have previously published on the effects of altered glucocorticoid levels and rhythms on immune function reflected by the human leukocyte transcriptome. This study was concerned with hypercortisolemia frequently observed after severe traumas and highlighted the prominent role of glucocorticoids in priming the circulating leukocytes against an impending infectious threat closely associated with their role as endogenous stress hormones. This single-level –omics study is described in the following future perspectives section to serve as

a primer for a prospective metabolomic study with the objective of identifying the impact of stress component to the systemic inflammatory response at the whole body level.

Having studied the human endotoxemia model extensively, we were interested in objectively assessing the relevance of this model to what is actually observed in clinical cases of systemic inflammation, most importantly in sepsis patients. For this purpose, we evaluated the relevance of changes observed in plasma metabolites of subjects who participated in the endotoxemia study with those of sepsis and SIRS patients. Response to endotoxemia at the metabolome level elicited changes that agree well in direction and magnitude with those observed in sepsis patients, and gave insight into metabolic changes that constitute a homeostatic response. Observed concordance strengthened the relevance of endotoxemia to clinical research as a physiological model of sepsis.

On the therapy side, we focused on the effects of synthetic corticosteroids (CS) which are extensively used for their anti-inflammatory and immunosuppressive agents in the treatment of a variety of conditions. Long term use of these drugs are associated with many side-effects including metabolic syndrome, dyslipidemia and muscle atrophy because of their strong effects on the metabolism. Liver is one of the primary targets of CS action and almost all its functions, critical for the maintenance of metabolic homeostasis, are strongly influenced by CSs. To investigate the changes in hepatic processes, we analyzed the temporal proteomic expression of livers from CS administered adrenalectomized rats. Taking advantage of the complementary transcriptional analysis in the same animal model, we pursued an integrated approach for expression analysis at both transcriptional and translational levels. Our approach involved both combining and contrasting the same gene products in two different datasets, in essence, pursuing the best integration approach yielding most useful

mechanistic information. The significant disparity between the actual proteome and corresponding transcriptome in this study suggested that additional translational or post-translational implications of CSs are very plausible in addition to their direct effects on transcription; while also cautioning against the use of transcriptional data for deciphering the regulation of the functional pathways which they represent. This study also provided the foundation for new generation pharmacokinetic/pharmacodynamics (PK/PD) models of these drugs. Current models of CS actions reflect the dynamics at the gene expression level. We have built a preliminary network-based model, described in the following future perspectives section, to augment these models with the new insights gained from functional analyses at the proteomic level. The ultimate objective of this modeling effort in the future is to devise a mathematical framework that can reflect the identified drug-responsive gene and protein expression patterns and accurately represent the physiological actions of CSs.

6.2 Adding the Stress Component to Endotoxemia Model

Our metabolomic study on human endotoxemia described in Chapter 2 points out significant changes in the whole body metabolism in response to LPS, which was later integrated with the transcriptional response as described in Chapter 3 and implied that these metabolic changes affect the transcriptional programming of leukocytes, in turn. As we further discussed in Chapter 4, this model is a valuable experimental platform reflecting the necessary and healthy physiological response to systemic inflammation, the core component of sepsis. However, in addition to the presence of this core response to pathogens; major physical and psychological traumas, such as those experienced by sepsis patients, are also associated with hypercortisolemia, which emerges due to the disruption of the cortisol secretion rhythm and the increase in total cortisol concentration (Deuschle et al., 1997, Vaughan et al., 1982, Frayn, 1986,

Boonen et al., 2013). Understanding how this alteration challenges the immune system and its function is of great clinical interest, and is particularly relevant to the management of critically ill or injured patients, in order to prevent complications.

In the experimental human endotoxemia model, we analyzed the effects of hypercortisolemia, concentrating exclusively on leukocyte transcriptional response (Kamisoglu et al., 2013a). In this study, natural circadian rhythm of cortisol was blunted in healthy volunteers by continuous cortisol infusion for 30h at a concentration that mimics hypercortisolemia induced by a major physiologic stressor. At the 24th hour of this infusion period, LPS is administered as a bolus injection and transcriptional responses of leukocytes within 24h periods both before and after the LPS challenge were investigated by gene expression analysis. Figure 6-1 illustrates the details of the design of this study.

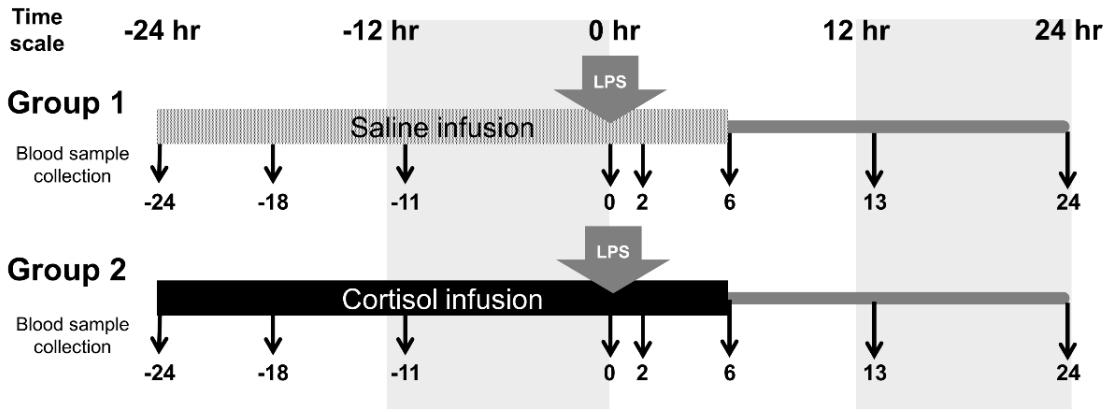

Figure 6-1: Study design for studying the effects of hypercortisolemia coupled with infectious stimuli, mimmicking the high stress experienced by sepsis patients. Nine healthy subjects received continuous cortisol (or saline) infusion starting 24h before the bolus LPS injection and continuing until 6h after the injection. Blood samples were collected and leukocytes were isolated at multiple time points over 24h both before and after LPS administration.

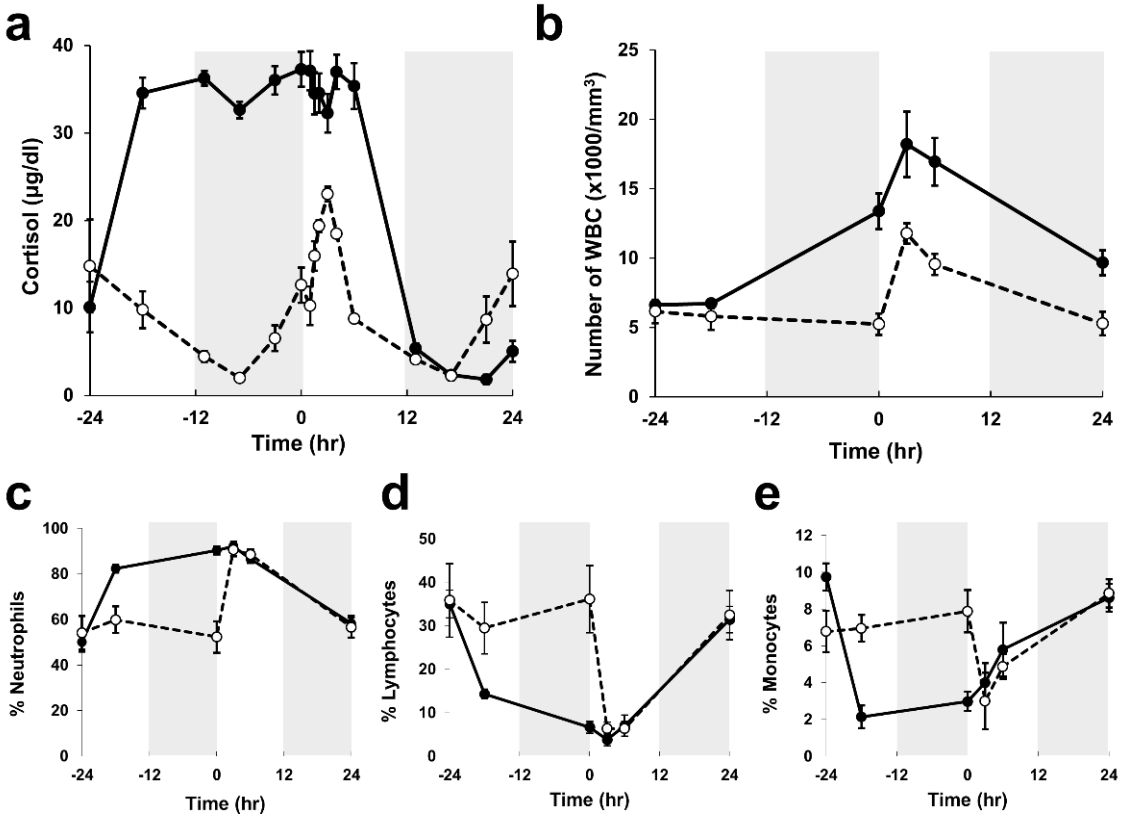

Figure 6-2: Change in the level of plasma cortisol (a) and total number of white blood cells (WBCs) (b) and percentage of WBC subpopulations (c-e) in response to continuous cortisol infusion and LPS administration (dashed line: saline + LPS; solid line: cortisol + LPS).

We observed that in the control subjects, plasma cortisol levels showed the expected circadian pattern (Yeager et al., 2011) and rapidly increased following LPS administration. In cortisol infused subjects, cortisol levels were steady throughout the 30h infusion period around twice the normal daily peak level of control subjects (~35 µg/dL) and did not show any further increase upon LPS administration (Figure 6-2 a). Cortisol concentration returned to normal levels within 12h in both groups. This pattern showed us that the followed dosing strategy successfully blunted the natural rhythm of cortisol and clamped the concentration at a level associated with stress-induced physiologic conditions.

As a result of this change in the natural cortisol rhythm and exerted hypercortisolemia, there were significant alterations in both the total number of leukocytes (white blood cells, or WBCs), and the WBC differentials. The total number of cells at 0h (before LPS administration) was at a level comparable to that observed after LPS administration for the saline infused control group with a relative increase in the percentage of neutrophils, and a significant decrease in the percentage of lymphoctyes and monocytes (Figure 6-2 c-e). Following LPS administration, both groups demonstrated an increase in the number of WBCs at a similar rate (Figure 6-2 b). Interestingly, the

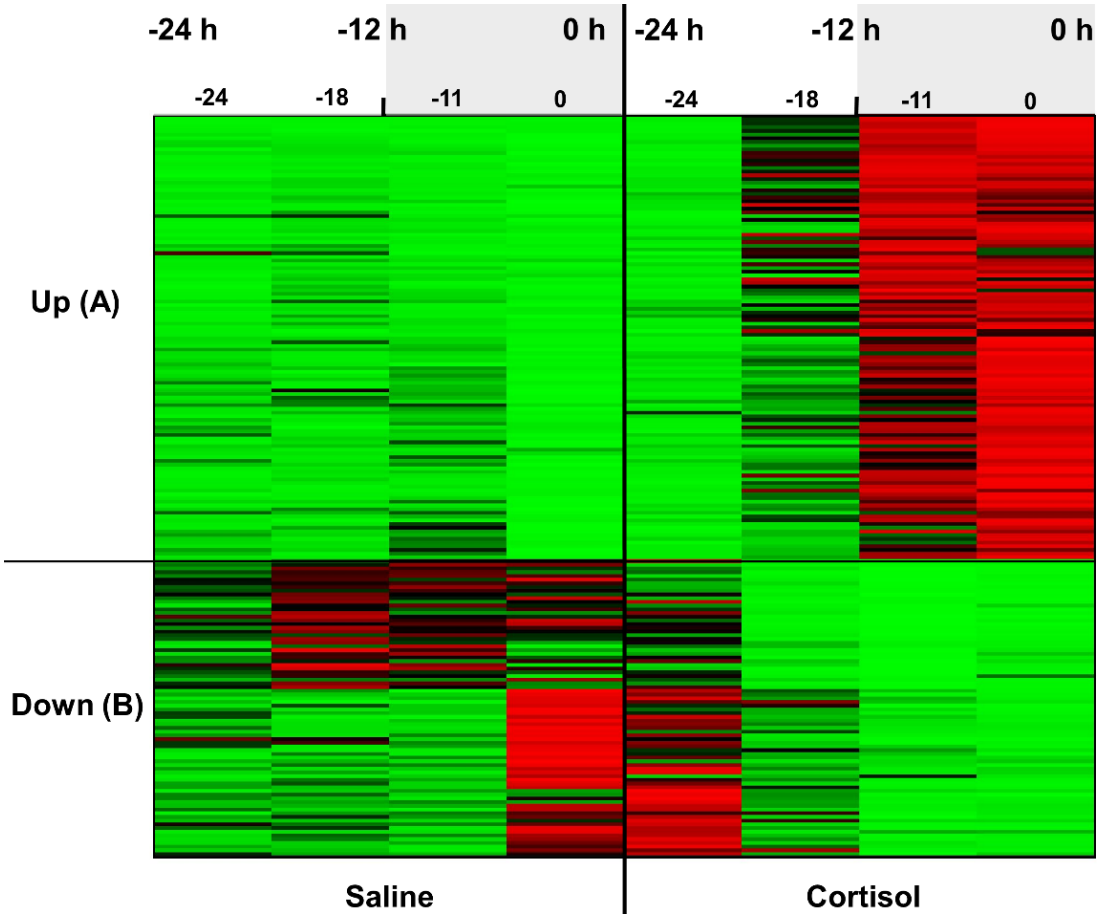

Figure 6-3: Transcriptional responses of leukocytes to cortisol prior to endotoxin administration in time period between -24h and 0h.

leukocyte subpopulations as a percentage of the total leukocyte count were not significantly different by 3h post LPS administration.

Besides the total number of leukocytes and differential counts, their transcriptional programming were also significantly affected from the hypercortisolemia. In cortisol treated group, 120 transcripts were up-regulated and 80 probesets were down-regulated compared to control group as shown Figure 6-3. Table A. 5 lists

representative genes from the up- and down-regulated groups of clusters together with the functional groups that they are associated with, in the context of this study. As a consequence of the continuous cortisol infusion, we observed enhanced expression of genes encoding for a number of pattern recognition and cytokine receptors, receptor regulatory elements and signal transduction elements; as well as, reduced expression of the genes encoding for elements of protein translation process, and mitochondrial proteins.

Increased receptor and signal transduction protein expression were indicative of a priming effect of the cortisol on the immune function, where cells were sensitized to recognize potential infectious threats or endogenous danger signals. These observations agree well with the previous studies investigating the effects of stress or direct cortisol delivery on the immune function and response to LPS challenge which demonstrated amplified pro-inflammatory receptor expression and function on immune cells (Shieh et al., 1993, Hawrylowicz et al., 1994, Zhang and Daynes, 2007) and subsequently enhanced inflammatory response to LPS (Yeager et al., 2009, Lim et al., 2007, Frank et al., 2010, Johnson et al., 2002, Gundersen et al., 2006, Galon et al., 2002).

Up-regulation of cytoskeletal proteins and extracellular matrix degradation enzymes also imply an increased mobility and enhanced ability for extravasation to penetrate

the tissues or engulf pathogens. These are key events for the inflammatory function of leukocytes and the enhancing effect of cortisol on these functions supports its permissive role on inflammatory response as supported by earlier studies (Galon et al., 2002, van der Goes et al., 2000)

Tuning down the protein translation process can also be regarded as part of the priming effect since it points toward re-prioritization of cellular resources and energy which would presumably allow better energy management when the anticipated threat is encountered. Decreased protein synthesis together with the increased expression of protein degradation enzymes indicates a catabolic state which is characteristic of cortisol action and in line with its role as a stress hormone (Sapolsky et al., 2000, Shah et al., 2000, Shah et al., 2002).

Despite the significant transcriptional program changes in leukocytes prior to 0h the overall response to LPS did not significantly differ between cortisol and saline treated groups for the majority of the genes involved, as reflected in the clusters obtained from differentially expressed genes throughout the full study period. Both cortisol and saline treated groups displayed similar up- and down-regulation responses as reflected in the 0– 24h periods of the heat map shown in Figure 6-4 b and c. These groups of clusters correspond well to the first part of the study, and are therefore named according to the observed response to cortisol as: Cortisol enhanced and cortisol suppressed. However, the magnitude of the up-regulation response observed after LPS administration was higher in the cortisol-pretreated group compared to control. The cluster shown in Figure 6-4 a displays a unique pattern where the overall response seems to be driven predominantly by LPS, which was reflected as strong up-regulation within the first 2h of LPS administration; and had a higher intensity for the cortisol treated group. The fact that LPS response was much higher for this cluster in the cortisol group when compared to control suggests that while cortisol might not have

directly affected transcription of the genes in this cluster, it may have had an indirect affect, perhaps through the modulation of up-stream signaling cascades. The net result is that the response to the subsequent inflammatory challenge (i.e. LPS) was intensified.

Table A. 6 lists the functional classifications of the genes included in the clusters shown in Figure 6-4. The probesets associated with the LPS dominant cluster include the major players known to regulate the inflammatory response such as: Cytokines and chemokines (Il1B, CCl20, CCL3, and IL1RN), signal transduction elements that

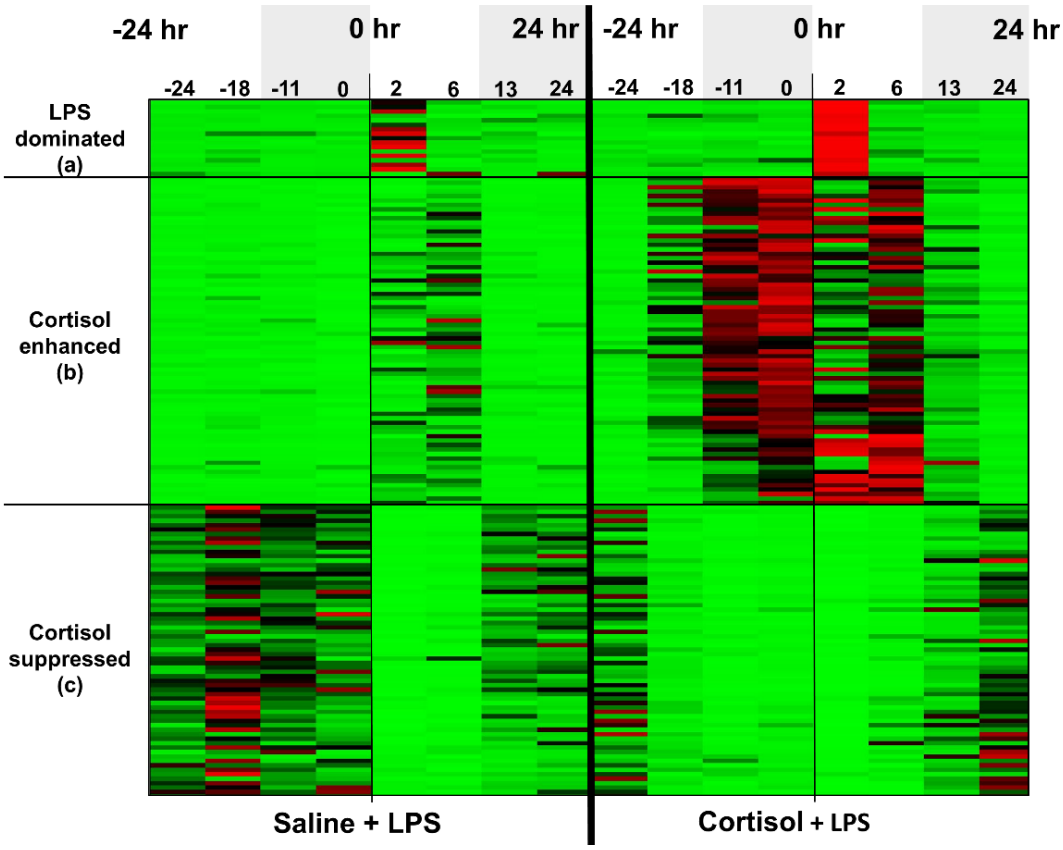

Figure 6-4: Overall differential response to LPS between cortisol+LPS and saline+LPS groups. 5 clusters obtained by consensus clustering were grouped into 3 based on response to cortisol between -24h and 0h as: (a) LPS dominated (17 probesets), (b) cortisol enhanced (74 probesets), and (c) cortisol suppressed (66 probesets).

negatively regulate pro-inflammatory signaling (NFKBIA and TNFAIP3) and receptors mediating recruitment of leukocytes to sites of inflammation (ICAM, THBS1).

Results of this study showed us that hypercortisolemia associated with major physiologic stress significantly affected the response of leukocytes to an impending infectious stimuli. Coupled dose and rhythm manipulation of plasma cortisol levels promoted the priming of circulating leukocytes associated with sensitization of their surveillance function and tuning down of energy-intensive processes which may be linked to increasing their efficiency in responding to subsequent infectious threats. Specifically related to cellular metabolism, we observed significant downregulation of ribosomal and mitochondrial proteins, as well as the defenses against oxidative stress.

The insights gained from this study regarding the permissive effect of cortisol on subsequent inflammatory response, together with earlier studies focused on cortisol delivery prior to acute inflammatory challenge (Yeager et al., 2011, Yeager et al., 2008, Yeager et al., 2009, Smyth et al., 2004, Barber et al., 1993, Frank et al., 2010), has also been used in building a mathematical model of acute inflammatory response that reflects the time of day dependence related to the secreted cortisol levels (Mavroudis et al., 2015).

In the future, it would be of great interest to integrate the information from metabolic alterations in the extended version of experimental human endotoxemia model since hypercortisolemia is also closely associated with hypermetabolic response observed in traumatic conditions (Brillon et al., 1995). Establishing the detailed definitions of hormonal and metabolic controls on the inflammatory response through the use of –omic tools in a model highly relevant to clinical cases of systemic inflammation is not only important for deciphering the regulatory mechanisms in control during acute inflammation but may also provide insights about more subtle connections between stress, metabolic and inflammatory diseases.

6.3 Enhancing PK/PD Models of MPL with Information from Multiple Levels of "–*omics*"

Modeling the responses of the body to a drug is a fundamental process in the drug development and it helps us to quantitatively reflect the time-course of the effects of drug on the body. Building and successful utilization of these models allow quantification of drug-system interactions and prediction of both therapeutic and adverse effects (Felmlee et al., 2012, Mager et al., 2003).

Diverse physiological effects of synthetic glucocorticoids has been the subject of many of these pharmacokinetic and pharmacodynamic modeling efforts. A series of models have been developed to explain the dynamics of receptor regulation and enzyme induction following MPL administration (Ramakrishnan et al., 2002, Sun et al., 1998). The models progressively enhanced to capture the effects of the drug under several doses and dosing regimens. However, these models were based on the data generated by traditional message quantification methods that only allow measurements of single end points. Together with the analysis of MPL effects on various tissues via high-throughput technologies such as gene microarrays (Almon et al., 2007a, Almon et al., 2007b), the diversity of the available models have been increased. The fifth-generation model that described the simple gene induction by MPL has been expanded to several pharmacogenomics models that may explain the response of all the hepatic genes with various dynamic patterns (Jin et al., 2003). **Error! Reference source not found.**Figure 6-5 shows the suggested mechanism for the effect of MPL on glucocorticoid receptor down-regulation in the liver, while Figure 6-6 lists various mechanistic scenarios of how MPL could drive the different expression patterns observed in the gene microarrays.

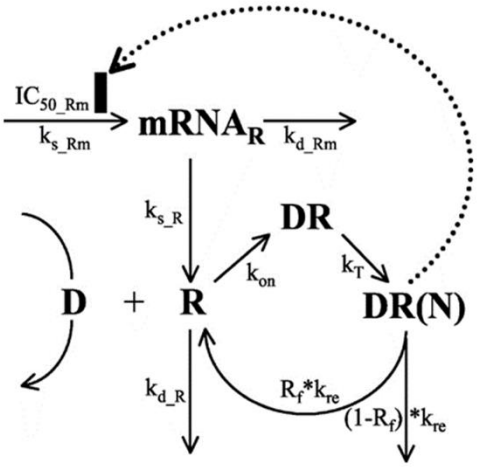

$$D = C1 \cdot e^{-\lambda_1 \times t} + C2 \cdot e^{-\lambda_2 \times t}$$

$$\frac{dR_m}{dt} = k_{syn\_Rm} \cdot \left(1 - \frac{DR(N)}{IC_{50\_Rm} + DR(N)}\right) - k_{dgr\_Rm} \cdot R_m$$

$$\frac{dR}{dt} = k_{syn\_R} \cdot R_m + R_f \cdot k_{re} \cdot DR(N) - k_{on} \cdot D \cdot R - k_{dgr\_R} \times R$$

$$\frac{dDR}{dt} = k_{on} \cdot D \cdot R - k_T \cdot DR$$

$$\frac{dDR(N)}{dt} = k_T \cdot DR - k_{re} \cdot DR(N)$$

Figure 6-5: Mechanism of receptor downregulation in liver in response to MPL administration. Starting from the kinetics of drug concentration in the plasma (D), the differential equations below the schematic define and interrelate the rates of changes in the individual elements such as the receptor mRNA (R_m), receptor protein (R), drug-receptor complex in the cytoplasm (DR) and in the nucleus (DR(N)).

Importantly, all these models concentrate on the effects observed at the gene expression level. The next quest in the development of more comprehensive models is the incorporation of information from the protein expression levels. This information made available by a novel high-throughput and reproducible method that allows the temporal profiling of tissue proteome (Nouri-Nigjeh et al., 2014a). In Chapter 5, we described multiple approaches to integrate this temporal information from the proteome level with the corresponding dynamics in the transcriptomic level through data-driven approaches. A future direction that we envision is to achieve integration of these available information from complementary studies in a model-driven approach. With this, the current PK/PD models of MPL response could be augmented to reflect the physiological response observed at the protein expression level.

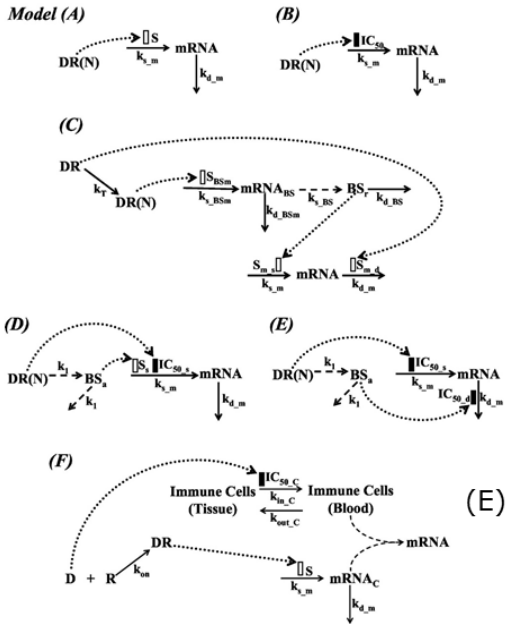

(A) $\frac{\mathrm{dmRNA}}{\mathrm{dt}} = k_{s\_m} \cdot (1 + \mathrm{S} \cdot \mathrm{DR(N)}) - k_{d\_m} \cdot \mathrm{mRNA}$

(B) $\frac{\mathrm{dmRNA}}{\mathrm{dt}} = k_{s\_m} \cdot \left(1 - \frac{\mathrm{DR(N)}}{\mathrm{IC_{50}} + \mathrm{DR(N)}}\right) - k_{d\_m} \cdot \mathrm{mRNA}$

(C)
$$\frac{\mathrm{dmRNA_{BS}}}{\mathrm{dt}} = k_{s\_BSm} \cdot (1 + \mathrm{S_{BSm}} \cdot \mathrm{DR(N)}) - k_{d\_BSm} \cdot \mathrm{mRNA_{BS}}$$
$$\frac{\mathrm{dBS_r}}{\mathrm{dt}} = k_{s\_BS} \cdot \mathrm{mRNA_{BS}} - k_{d\_BS} \cdot \mathrm{BS_r}$$
$$\frac{\mathrm{dmRNA}}{\mathrm{dt}} = k_{s\_m} \cdot (1 + \mathrm{S_{m\_s}} \cdot \mathrm{BS_r}) - k_{d\_m} \cdot (1 + \mathrm{S_{m\_d}} \cdot \mathrm{DR}) \cdot \mathrm{mRNA}$$

(D)
$$\frac{\mathrm{dBS_a}}{\mathrm{dt}} = k_1 \cdot (\mathrm{DR(N)} - \mathrm{BS_a})$$
$$\frac{\mathrm{dmRNA}}{\mathrm{dt}} = k_{s\_m} \cdot \left(1 - \frac{\mathrm{DR(N)}}{\mathrm{IC_{50\_s}} + \mathrm{DR(N)}} + \mathrm{S_s} \cdot \mathrm{BS_a}\right) - k_{d\_m} \cdot \mathrm{mRNA}$$

(E)
$$\frac{\mathrm{dBS_a}}{\mathrm{dt}} = k_1 \cdot (\mathrm{DR(N)} - \mathrm{BS_a})$$
$$\frac{\mathrm{dmRNA}}{\mathrm{dt}} = k_{s\_m} \cdot \left(1 - \frac{\mathrm{DR(N)}}{\mathrm{IC_{50\_s}} + \mathrm{DR(N)}}\right) - k_{d\_m} \cdot \left(1 - \frac{\mathrm{BS_a}}{\mathrm{IC_{50\_d}} + \mathrm{BS_a}}\right) \cdot \mathrm{mRNA}$$

(F)
$$\frac{\mathrm{dCell_B}}{\mathrm{dt}} = k_{\mathrm{in\_C}} \cdot \left(1 - \frac{\mathrm{D}}{\mathrm{IC_{50\_C}} + \mathrm{D}}\right) - k_{\mathrm{out\_C}} \cdot \mathrm{Cell_B}$$
$$\frac{\mathrm{dmRNA_C}}{\mathrm{dt}} = k_{s\_m} \cdot (1 + \mathrm{S} \cdot \mathrm{DR}) - k_{d\_m} \cdot \mathrm{mRNA_C}$$
$$\mathrm{mRNA} = \mathrm{mRNA_C} \cdot \mathrm{Cell_B}$$

Figure 6-6: Diverse pharmacogenomic models and accompanying differential equations to describe various mechanisms of MPL's effects on hepatic gene expression (adapted from (Jin et al., 2003)).

As our results demonstrated in Chapter 5, transcriptional and proteomic expression patterns roughly correlate for some of the genes, yet for others, the dynamics were more unexpected. One way to work with the existing PK/PD models would be teasing out the protein counterparts of the transcriptional clusters that are described by the dynamics shown in Figure 6-6 and examining the potential mechanisms that could explain the observed protein expression profiles corresponding to the same genes. Another approach is considering the physiologic response as a systems response composed of dynamics of individual elements.

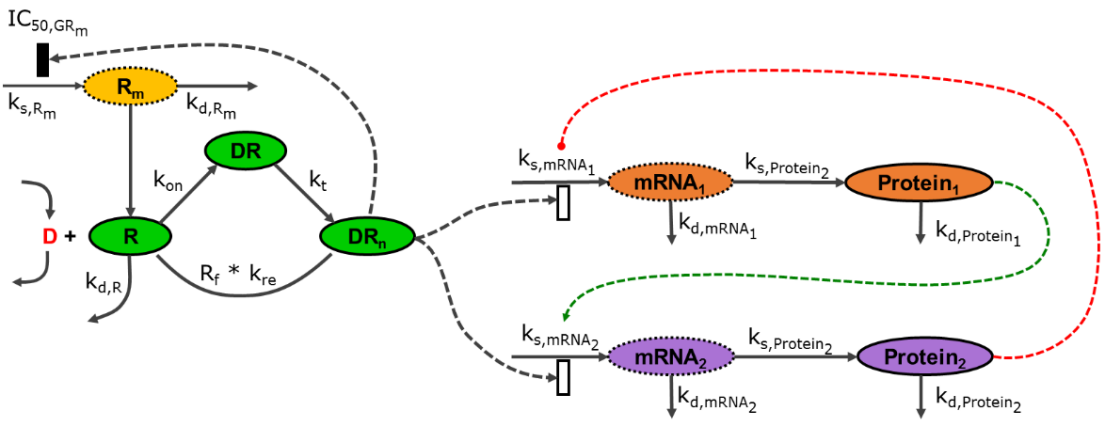

Figure 6-7: Schematic representation of the network-based indirect response model to MPL (D). Glucocorticoid receptor (R) downregulation part of the model (on the left) has already been modeled. Once the drug-receptor complex translocates into the nucleus (DR(N)), drug induces its effects on the transcription of its target genes ($mRNA_1$, $mRNA_2$) either by stimulating it (white rectangle) or by inhibiting it (black rectangle). When transcribed messages are translated to the active proteins ($Protein_1$, $Protein_2$), they can also have effects (either stimulatory (green) or inhibitory (red)) on the transcription of target genes affected by MPL. All these effects are considered as indirect as there might be additional biological processes in between.

We have done a preliminary study applying this second approach. In our study, the driver of the response is the drug-receptor complex in the nucleus; transcripts and proteins, the nodes of the network, are the individual elements with diverse dynamics. The observed phenotype reflects the systems response arising from the dynamics of these individual elements, and these elements include all of the genes affected by the MPL. Figure 6-7 illustrates this idea schematically only with two representative target genes. Number of target genes to be included in the network depends on the available biological data, literature information about the interaction of the nodes, as well as the desired complexity level. Because, as more nodes are added into the network, the

direct and indirect interactions between the elements of the network as well as the number of parameters to be estimated increases.

6.3.1 Building the response network

As described in Section 5.2.1, we had 163 genes that had both mRNA and protein expression data. An interaction database for all these 163 genes were constructed (Nguyen, T, unpublished work). This database was curated from 4 popular pathway databases (KEGG, NCI, Biocarta, Reactome) combined with text mining from Pubmed abstracts with sentences that satisfy a strict syntax to infer if A activates or inhibits B. This database for the whole common dataset included 1956 interaction links. In order to reduce the number of network elements to a more manageable size, we followed a functional approach.

We first determined the most important functions affected by MPL administration through functional enrichment analysis of both transcriptional and proteomic level data. Starting from the functions of all differential transcripts and proteins, we focused on most important common pathways. Then the genes in these pathways were

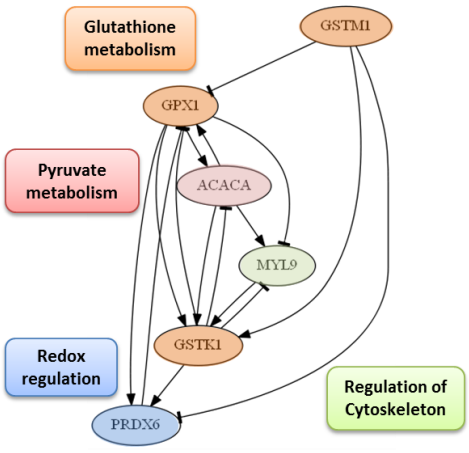

Figure 6-8: Network of MPL responsive genes determined through functional enrichment analysis of transcriptional and proteomic data, and interaction database curated from literature.

examined, and any gene with missing either the mRNA or protein expression data were removed. Then, regulatory relationships between the remaining genes were determined from the initial curated interaction database. This approach yielded a 6 node-16 edge network associated with 4 physiological functions as shown in Figure 6-8.

6.3.2 Integrating the network with existing PK/PD model for MPL

The elements of the network were determined in a data-driven way, starting from the MPL responsive genes at the transcriptional and proteomic levels. Therefore the driving force for the initial network activity was the drug bound receptor translocated in the nucleus (DR(N)). With this in mind, DR(N) was introduced as the driving force for the each element in the network, and the rest of the regulatory relationships were kept the same. Figure 6-9 illustrates the integration of gene and protein expression network with the existing receptor-downregulation model of MPL.

The system of differential equations describing the relationships are given in Eqn. 6-1 to Eqn. 6-10. The parameters for the receptor downregulation model (Eqn. 6-1 to Eqn. 6-7) was used as in the previous studies (Ramakrishnan et al., 2002, Jin et al., 2003).

The simulation results of the receptor-downregulation part of the model is shown in Figure 6-10. MPL plasma concentration (D) exhibit a biexponential decline. Following the binding of the drug to the glucocorticoid receptor (DR), this complex translocate into the nucleus (DR(N)) and act as the driving force for the MPL induced response patterns. Firstly, this effect is observed as inhibition of mRNA expression for the glucocorticoid receptor (Rm), and consecutively the receptor protein (R). DR(N) is also introduced as a stimulatory factor to all of the nodes in the network. Level of mRNA expression is modeled to be controlled by the presence of drug-receptor complex in the nucleus together with all other indirect interactions between the proteins of the

$$D = C1 \cdot e^{-\lambda_1 \cdot t} + C2 \cdot e^{-\lambda_2 \cdot t}$$ Eqn. 6-1

$$\frac{dR_m}{dt} = k_{syn\_Rm} \cdot \left(1 - \frac{DR(N)}{IC_{50\_Rm} + DR(N)}\right) - k_{dgr\_Rm} \cdot R_m$$ Eqn. 6-2

$$\frac{dR}{dt} = k_{syn\_R} \cdot R_m + R_f \cdot k_{re} \cdot DR(N) - k_{on} \cdot D \cdot R - k_{dgr\_R} \cdot R$$ Eqn. 6-3

$$k_{dgr\_Rm} = \frac{k_{syn\_Rm}}{R_{m\_o}}$$ Eqn. 6-4

$$k_{syn\_R} = \frac{R_o}{R_{m\_o}} \cdot k_{dgr\_R}$$ Eqn. 6-5

$$\frac{dDR}{dt} = k_{on} \cdot D \cdot R - k_T \cdot DR$$ Eqn. 6-6

$$\frac{dDR(N)}{dt} = k_T \cdot DR - k_{re} \cdot DR(N)$$ Eqn. 6-7

$$\frac{dmRNA}{dt} = f - k_{dgr\_m} \cdot mRNA$$ Eqn. 6-8

$$f = k_P \cdot DR(N) + \sum_{j=1}^{N} a_{ij} \cdot P_j$$ Eqn. 6-9

$$\frac{dP}{dt} = k_{syn\_P} \cdot mRNA - k_{dgr\_P} \cdot P$$ Eqn. 6-10

network. Degradation of mRNA, protein translation from mRNA and protein degradation were all modeled as linear processes.

Figure 6-11 shows the simulation results for this preliminary network. The experimental data is indicated with the dashed blue lines, and model simulations are overlaid with black solid lines. For GPX1 and MYL9 genes, the experimentally observed dynamics are very well captured. This is also true for the early dynamics of PRDX6 and GSTM1 protein levels. In general, for the most network elements early dynamics are seem to be represented well compared to later fluctuations in the response.

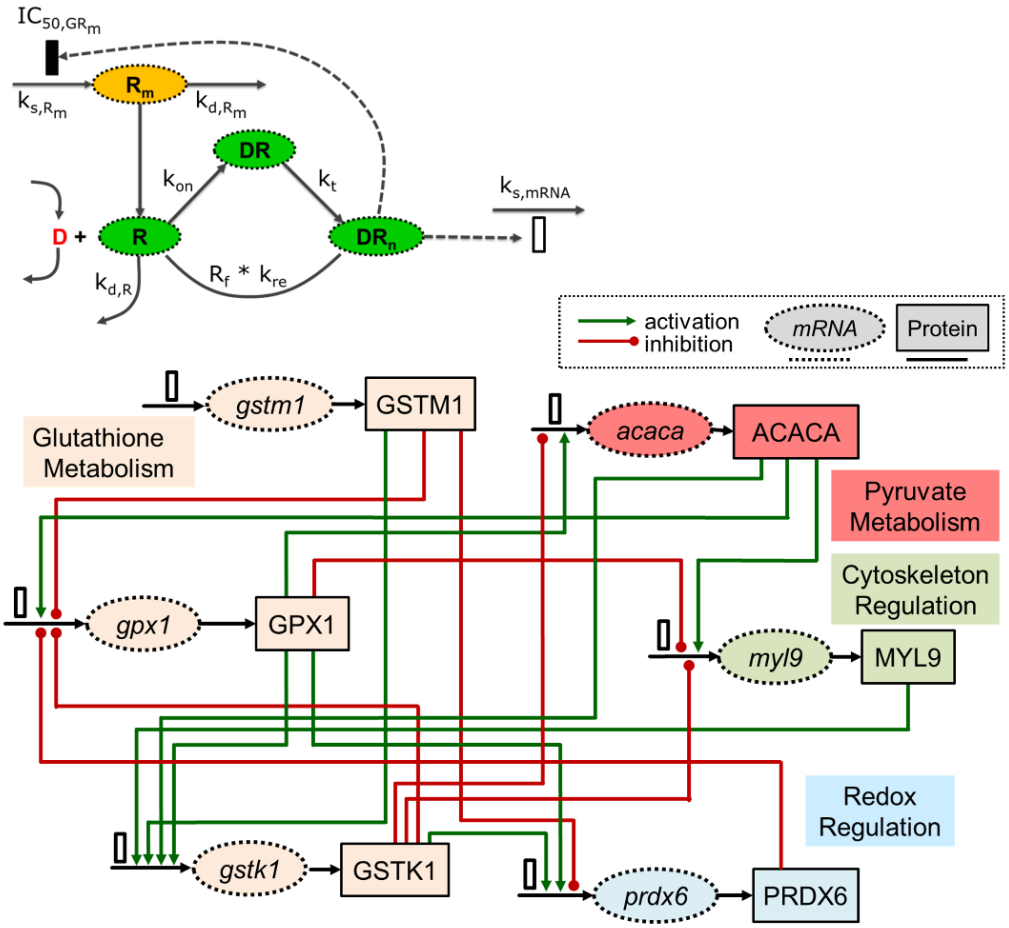

Figure 6-9: Gene and protein expression network (bottom) integrated into the receptor downregulation part (top) of the MPL PK/PD model. Black rectangle indicates an inhibition whereas white rectangles indicate stimulation by DR(N). The edges of the network are color-coded to indicate activating (green) and inhibiting (red) interactions of the nodes.

Especially for the elements which has more pronounced dynamics later in the time course, such as GSTK1 and ACACA, the model does not even come close to the experimental data. As stated before, this was the preliminary step to the bi-level model building approach and further enhancements in the model will allow better representation of the experimental data.

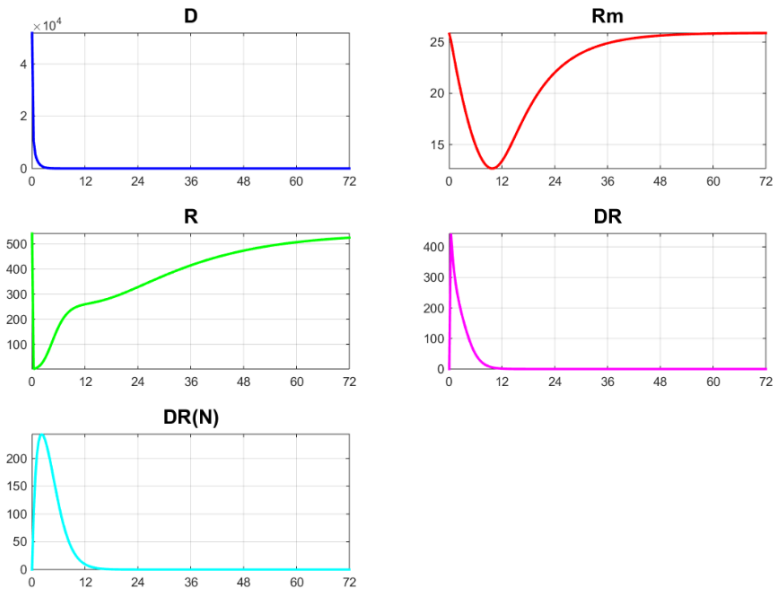

Figure 6-10: Dynamics of the response to MPL in the first part of the model that defines the regulatory effect of MPL on the glucocorticoid receptor that it binds.

Some of these efforts might include introducing time delays to the elements which demonstrate more pronounced dynamics in the later phase of the response. The synthesis of the network mRNAs currently involve linear relationships. Michaelis-Menten kinetics can be introduced to allow self-limiting responses. Finally, the network structure can also be reshaped by eliminating the nodes that are not insightful as well as introducing new nodes that carry important regulatory information about the existing parts of the network. Once the model is matured to fully capture the experimental data, then it can be utilized to make predictions about long-term effects, or different delivery kinetics.

This preliminary work introduces an approach for bridging the classic PK/PD modeling efforts with the multi-level systems response. This allows us to explore the paths of utilizing the vast amount of information made available by new *-omic* profiling tools. These tools make it possible to evaluate the response as a whole at a certain biological

level over time. The model-based integration approach discussed here ultimately aims to connect this valuable information coming from multiple layers in a useful framework which reflects the continuity of biological events in response to the pharmacological stimuli.

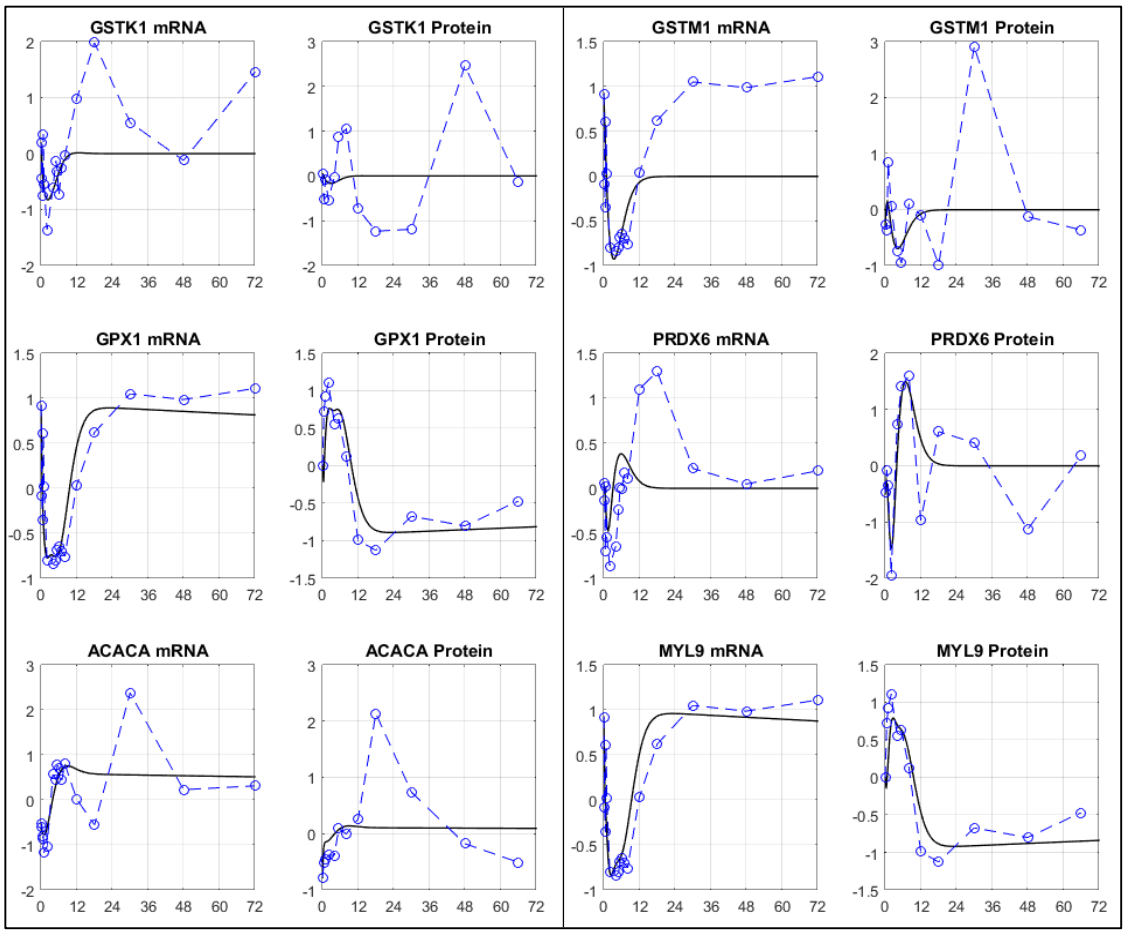

Figure 6-11: Simulation results for all mRNA and proteins taking part in the network of the MPL response model. Blue dashed lines indicate the experimental data and black solid lines show the simulation results.

Another layer of information that can be incorporated into this model in the future is the metabolome layer. As we have previously pointed out, gene expression signatures gives information about the lowest level of organization, shedding light on the origin

of a specific phenotype. Proteomics provide information about the abundance of proteins, elucidating the next level up from gene expression data. The integration of these fields provides a unified picture of cellular-level responses from transcription through translation. However, there are multiple other levels of processes that control the sequence of events from the translation of a protein until it becomes a fully functional piece of the organism that can shape processes affecting the ultimate phenotype. Metabolomics complements these more traditional -omics techniques by allowing the investigation of properties that cannot be directly assessed through gene and protein expression. Integration of metabolomics with transcriptomics and proteomics can help make the relationship between the levels of information produced by each technique more clear. Changes in gene expression levels and protein concentrations can be linked to physiological changes and interpreted in the biological context.

Future metabolomic studies in the same animal model can elicit the metabolic shifts occurring in response to MPL administration that ultimately cause the development of the adverse effects. Careful assessment of the connections of these shifts with the defined alterations in hepatic gene and protein expression levels can help identify the critical nodes that control these metabolism associated adverse effects of the drug. Importantly, the indirect effects of the drug on whole body metabolism through altering the microbiome would have to be considered here as well, since the symbiotic organisms might have tremendous influence on shaping the metabolic response to the drug. Nevertheless, integration of information from the whole-body metabolism with existing information on the hepatic response to MPL can be useful in multiple ways. Firstly, alterations in the critical nodes that are linked to long-term adverse effects can be identified and adjunct therapies that can alleviate these alterations can be devised. Secondly, patient populations which would be more susceptible for experiencing those

adverse effects or be better responders to the drug can be pre-determined based on their genomic profiles. Thirdly, more realistic models of drug response can be designed integrating information from this ultimate phenotypic level and be used to evaluate different scenarios, helping in the design and development of better therapies.

Bibliography

Agwunobi, A. O., Reid, C., Maycock, P., Little, R. A. & Carlson, G. L. 2000. Insulin Resistance and Substrate Utilization in Human Endotoxemia. *Journal of clinical endocrinology & metabolism,* 85**,** 3770-3778.

Almon, R. R., DuBois, D. C. & Jusko, W. J. 2007a. A microarray analysis of the temporal response of liver to methylprednisolone: a comparative analysis of two dosing regimens. *Endocrinology,* 148**,** 2209-25.

Almon, R. R., DuBois, D. C., Pearson, K. E., Stephan, D. A. & Jusko, W. J. 2003. Gene arrays and temporal patterns of drug response: corticosteroid effects on rat liver. *Funct Integr Genomics,* 3**,** 171-9.

Almon, R. R., DuBois, D. C., Yao, Z., Hoffman, E. P., Ghimbovschi, S. & Jusko, W. J. 2007b. Microarray analysis of the temporal response of skeletal muscle to methylprednisolone: comparative analysis of two dosing regimens. *Physiol Genomics,* 30**,** 282-99.

Almon, R. R., Lai, W., DuBois, D. C. & Jusko, W. J. 2005. Corticosteroid-regulated genes in rat kidney: mining time series array data. *Am J Physiol Endocrinol Metab,* 289**,** E870-82.

Alvarez, S. M., Katsamanis Karavidas, M., Coyle, S. M., Lu, S. E., Macor, M., Oikawa, L. O., Lehrer, P. M., Calvano, S. E. & Lowry, S. F. 2007. Low-dose steroid alters in vivo endotoxin-induced systemic inflammation but does not influence autonomic dysfunction. *J Endotoxin Res,* 13**,** 358-68.

Andreasen, A. S., Krabbe, K. S., Krogh-Madsen, R., Taudorf, S., Pedersen, B. K. & Moller, K. 2008. Human endotoxemia as a model of systemic inflammation. *Curr Med Chem,* 15**,** 1697-705.

Andrews, R. C. & Walker, B. R. 1999. Glucocorticoids and insulin resistance: old hormones, new targets. *Clin Sci (Lond),* 96**,** 513-23.

Androulakis, I. P. 2015. Systems engineering meets quantitative systems pharmacology: from low-level targets to engaging the host defenses. *Wiley Interdiscip Rev Syst Biol Med,* 7**,** 101-12.

Angus, D. C. & van der Poll, T. 2013. Severe Sepsis and Septic Shock. *New England Journal of Medicine,* 369**,** 840-851.

Barber, A. E., Coyle, S. M., Marano, M. A., Fischer, E., Calvano, S. E., Fong, Y., Moldawer, L. L. & Lowry, S. F. 1993. Glucocorticoid therapy alters hormonal and cytokine responses to endotoxin in man. *The Journal of Immunology,* 150**,** 1999-2006.

Barnes, P. J. 1998. Anti-inflammatory actions of glucocorticoids: molecular mechanisms. *Clin Sci (Lond),* 94**,** 557-72.

Benjamini, Y. & Hochberg, Y. 1995. Controlling the false discovery rate: a practical and powerful approach to multiple testing. *Journal of the Royal Statistical Society. Series B (Methodological)***,** 289-300.

Bialas, M. C. & Routledge, P. A. 1998. Adverse effects of corticosteroids. *Adverse Drug React Toxicol Rev,* 17**,** 227-35.

Bone, R. C. 1996. Immunologic dissonance: a continuing evolution in our understanding of the systemic inflammatory response syndrome (SIRS) and the multiple organ dysfunction syndrome (MODS). *Ann Intern Med,* 125**,** 680-7.

Boonen, E., Vervenne, H., Meersseman, P., Andrew, R., Mortier, L., Declercq, P. E., Vanwijngaerden, Y. M., Spriet, I., Wouters, P. J., Vander Perre, S., Langouche, L., Vanhorebeek, I., Walker, B. R. & Van den Berghe, G. 2013. Reduced cortisol metabolism during critical illness. *N Engl J Med,* 368**,** 1477-88.

Brillon, D. J., Zheng, B., Campbell, R. G. & Matthews, D. E. 1995. *Effect of cortisol on energy expenditure and amino acid metabolism in humans*.

Butte, A. 2002. The use and analysis of microarray data. *Nat Rev Drug Discov,* 1**,** 951-60.

Cain, D., del Arroyo, A. & Ackland, G. 2014. Uncontrolled sepsis: a systematic review of translational immunology studies in intensive care medicine. *Intensive Care Medicine Experimental,* 2**,** 1-25.

Calvano, S., Xiao, W., Richards, D., Felciano, R., Baker, H., Cho, R., Chen, R., Brownstein, B., Cobb, J., Tschoeke, S., Miller-Graziano, C., Moldawer, L., Mindrinos, M., Davis, R., Tompkins, R., Lowry, S., Inflamm & Host Response to Injury Large Scale Collab. Res, P. 2005. A network-based analysis of systemic inflammation in humans. *Nature,* 437**,** 1032-1039.

Calvano, S. E. & Coyle, S. M. 2012. Experimental human endotoxemia: a model of the systemic inflammatory response syndrome? *Surg Infect (Larchmt),* 13**,** 293-9.

Chandra, R., Villanueva, E., Feketova, E., Machiedo, G. W., Hasko, G., Deitch, E. A. & Spolarics, Z. 2008. Endotoxemia down-regulates bone marrow lymphopoiesis but stimulates myelopoiesis: the effect of G6PD deficiency. *J Leukoc Biol,* 83**,** 1541-50.

Chen, E. Y., Tan, C. M., Kou, Y., Duan, Q., Wang, Z., Meirelles, G. V., Clark, N. R. & Ma'ayan, A. 2013. Enrichr: interactive and collaborative HTML5 gene list enrichment analysis tool. *BMC Bioinformatics,* 14**,** 128.

Chrousos, G. P. & Kino, T. 2005. Intracellular glucocorticoid signaling: a formerly simple system turns stochastic. *Sci STKE,* 2005**,** pe48.

De Caterina, R. & Basta, G. 2001. n-3 Fatty acids and the inflammatory response — biological background. *European Heart Journal Supplements,* 3**,** D42-D49.

de Godoy, L. M., Olsen, J. V., Cox, J., Nielsen, M. L., Hubner, N. C., Frohlich, F., Walther, T. C. & Mann, M. 2008. Comprehensive mass-spectrometry-based proteome quantification of haploid versus diploid yeast. *Nature,* 455**,** 1251-4.

Deitch, E. A. 1998. Animal models of sepsis and shock: a review and lessons learned. *Shock,* 9**,** 1-11.

Deuschle, M., Schweiger, U., Weber, B., Gotthardt, U., Körner, A., Schmider, J., Standhardt, H., Lammers, C.-H. & Heuser, I. 1997. Diurnal Activity and Pulsatility of the Hypothalamus-Pituitary-Adrenal System in Male Depressed Patients and Healthy Controls. *Journal of clinical endocrinology & metabolism,* 82**,** 234-238.

Evans, A. M., DeHaven, C. D., Barrett, T., Mitchell, M. & Milgram, E. 2009. Integrated, Nontargeted Ultrahigh Performance Liquid Chromatography/Electrospray Ionization Tandem Mass Spectrometry Platform for the Identification and Relative Quantification of the Small-Molecule Complement of Biological Systems. *Analytical Chemistry,* 81**,** 6656-6667.

Felmlee, M. A., Morris, M. E. & Mager, D. E. 2012. Mechanism-Based Pharmacodynamic Modeling. *Methods in molecular biology (Clifton, N.J.),* 929**,** 583-600.

Fong, Y. M., Marano, M. A., Moldawer, L. L., Wei, H., Calvano, S. E., Kenney, J. S., Allison, A. C., Cerami, A., Shires, G. T. & Lowry, S. F. 1990. The acute splanchnic and peripheral tissue metabolic response to endotoxin in humans. *J Clin Invest,* 85**,** 1896-904.

Foteinou, P., Calvano, S., Lowry, S. & Androulakis, I. 2009. Modeling endotoxin-induced systemic inflammation using an indirect response approach. *Mathematical biosciences,* 217**,** 27-42.

Foteinou, P. T., Calvano, S. E., Lowry, S. F. & Androulakis, I. P. 2010. Multiscale model for the assessment of autonomic dysfunction in human endotoxemia. *Physiological genomics,* 42**,** 5-19.

Foteinou, P. T., Calvano, S. E., Lowry, S. F. & Androulakis, I. P. 2011. A physiological model for autonomic heart rate regulation in human endotoxemia. *Shock,* 35**,** 229.

Frank, M. G., Miguel, Z. D., Watkins, L. R. & Maier, S. F. 2010. Prior exposure to glucocorticoids sensitizes the neuroinflammatory and peripheral inflammatory responses to E. coli lipopolysaccharide. *Brain, behavior, and immunity,* 24**,** 19-30.

Frayn, K. N. 1986. Hormonal control of metabolism in trauma and sepsis. *Clin Endocrinol (Oxf),* 24**,** 577-99.

Gall, W. E., Beebe, K., Lawton, K. A., Adam, K. P., Mitchell, M. W., Nakhle, P. J., Ryals, J. A., Milburn, M. V., Nannipieri, M., Camastra, S., Natali, A. & Ferrannini, E. 2010. alpha-hydroxybutyrate is an early biomarker of insulin resistance and glucose intolerance in a nondiabetic population. *PLoS ONE,* 5**,** e10883.

Galon, J., Franchimont, D., Hiroi, N., Frey, G., Boettner, A., Ehrhart-Bornstein, M., O'SHEA, J. J., Chrousos, G. P. & Bornstein, S. R. 2002. Gene profiling reveals unknown enhancing and suppressive actions of glucocorticoids on immune cells. *The FASEB journal,* 16**,** 61-71.

Gaté, L., Paul, J., Ba, G. N., Tew, K. D. & Tapiero, H. 1999. Oxidative stress induced in pathologies: The role of antioxidants. *Biomedicine & Pharmacotherapy,* 53**,** 169-180.

Glass, C. K. & Olefsky, J. M. 2012. Inflammation and Lipid Signaling in the Etiology of Insulin Resistance. *Cell metabolism,* 15**,** 635-645.

Glickman, S. W., Cairns, C. B., Otero, R. M., Woods, C. W., Tsalik, E. L., Langley, R. J., van Velkinburgh, J. C., Park, L. P., Glickman, L. T., Fowler, V. G., Jr., Kingsmore, S. F. & Rivers, E. P. 2010. Disease progression in hemodynamically stable patients presenting to the emergency department with sepsis. *Acad Emerg Med,* 17**,** 383-90.

Greenbaum, D., Colangelo, C., Williams, K. & Gerstein, M. 2003. Comparing protein abundance and mRNA expression levels on a genomic scale. *Genome Biology,* 4**,** 117.

Gry, M., Rimini, R., Stromberg, S., Asplund, A., Ponten, F., Uhlen, M. & Nilsson, P. 2009. Correlations between RNA and protein expression profiles in 23 human cell lines. *BMC Genomics,* 10**,** 365.

Gundersen, Y., Opstad, P. K., Reistad, T., Thrane, I. & Vaagenes, P. 2006. Seven days' around the clock exhaustive physical exertion combined with energy depletion and sleep deprivation primes circulating leukocytes. *European journal of applied physiology,* 97**,** 151-157.

Haider, S. & Pal, R. 2013. Integrated Analysis of Transcriptomic and Proteomic Data. *Current Genomics,* 14**,** 91-110.

Haimovich, B., Reddell, M. T., Calvano, J. E., Calvano, S. E., Macor, M. A., Coyle, S. M. & Lowry, S. F. 2010. A novel model of common Toll-like receptor 4- and injury-induced transcriptional themes in human leukocytes. *Critical care,* 14**,** R177.

Hall, M. J., Williams, S. N., DeFrances, C. J. & Golosinskiy, A. 2011. Inpatient care for septicemia or sepsis: a challenge for patients and hospitals. *NCHS Data Brief***,** 1-8.

Hampel, F. R. 1974. The Influence Curve and its Role in Robust Estimation. *Journal of the American Statistical Association,* 69**,** 383-393.

Haslam, S. M., Julien, S., Burchell, J. M., Monk, C. R., Ceroni, A., Garden, O. A. & Dell, A. 2008. Characterizing the glycome of the mammalian immune system. *Immunol Cell Biol,* 86**,** 564-73.

Hawrylowicz, C., Guida, L. & Paleolog, E. 1994. Dexamethasone up-regulates granulocyte-macrophage colony-stimulating factor receptor expression on human monocytes. *Immunology,* 83**,** 274.

Hazra, A., DuBois, D. C., Almon, R. R., Snyder, G. H. & Jusko, W. J. 2008. Pharmacodynamic modeling of acute and chronic effects of methylprednisolone on hepatic urea cycle genes in rats. *Gene Regul Syst Bio,* 2**,** 1-19.

Hazra, A., Pyszczynski, N., DuBois, D. C., Almon, R. R. & Jusko, W. J. 2007. Pharmacokinetics of methylprednisolone after intravenous and intramuscular administration in rats. *Biopharm Drug Dispos,* 28**,** 263-73.

He, L. & Hannon, G. J. 2004. MicroRNAs: small RNAs with a big role in gene regulation. *Nat Rev Genet,* 5**,** 522-31.

Hegde, P. S., White, I. R. & Debouck, C. 2003. Interplay of transcriptomics and proteomics. *Current opinion in biotechnology,* 14**,** 647-51.

Holeček, M. 2002. Relation between glutamine, branched-chain amino acids, and protein metabolism. *Nutrition,* 18**,** 130-133.

Holmes, E., Wilson, I. D. & Nicholson, J. K. 2008. Metabolic phenotyping in health and disease. *Cell,* 134**,** 714-7.

Iyengar, R., Zhao, S., Chung, S. W., Mager, D. E. & Gallo, J. M. 2012. Merging systems biology with pharmacodynamics. *Sci Transl Med,* 4**,** 126ps7.

Jaeschke, H. 2011. Reactive oxygen and mechanisms of inflammatory liver injury: Present concepts. *Journal of Gastroenterology and Hepatology,* 26**,** 173-179.

Jan, B. U., Coyle, S. M., Macor, M. A., Reddell, M., Calvano, S. E. & Lowry, S. F. 2010. Relationship of basal heart rate variability to in vivo cytokine responses after endotoxin exposure. *Shock,* 33**,** 363-8.

Jan, B. U., Coyle, S. M., Oikawa, L. O., Lu, S. E., Calvano, S. E., Lehrer, P. M. & Lowry, S. F. 2009. Influence of acute epinephrine infusion on endotoxin-induced parameters of heart rate variability: a randomized controlled trial. *Annals of surgery,* 249**,** 750-756.

Jin, J. Y., Almon, R. R., DuBois, D. C. & Jusko, W. J. 2003. Modeling of corticosteroid pharmacogenomics in rat liver using gene microarrays. *Journal of Pharmacology and Experimental Therapeutics,* 307**,** 93-109.

Johnson, J. D., O'Connor, K. A., Deak, T., Stark, M., Watkins, L. R. & Maier, S. F. 2002. Prior stressor exposure sensitizes LPS-induced cytokine production. *Brain, behavior, and immunity,* 16**,** 461-476.

Jusko, W. J. 2013. Moving from basic toward systems pharmacodynamic models. *Journal of pharmaceutical sciences,* 102**,** 2930-2940.

Kamisoglu, K., Sleight, K., Nguyen, T. T., Calvano, S. E., Coyle, S. M., Corbett, S. A. & Androulakis, I. P. 2013a. Effects of coupled dose and rhythm manipulation of

plasma cortisol levels on leukocyte transcriptional response to endotoxin challenge in humans. *Innate Immun*.

Kamisoglu, K., Sleight, K. E., Calvano, S. E., Coyle, S. M., Corbett, S. A. & Androulakis, I. P. 2013b. Temporal Metabolic Profiling of Plasma During Endotoxemia in Humans. *Shock,* 40**,** 519-526 10.1097/SHK.0000000000000063.

Kanehisa, M. & Goto, S. 2000. KEGG: kyoto encyclopedia of genes and genomes. *Nucleic Acids Res,* 28**,** 27-30.

Khovidhunkit, W., Kim, M. S., Memon, R. A., Shigenaga, J. K., Moser, A. H., Feingold, K. R. & Grunfeld, C. 2004. Effects of infection and inflammation on lipid and lipoprotein metabolism: mechanisms and consequences to the host. *J Lipid Res,* 45**,** 1169-96.

Kosmides, A. K., Kamisoglu, K., Calvano, S. E., Corbett, S. A. & Androulakis, I. P. 2013. Metabolomic fingerprinting: challenges and opportunities. *Crit Rev Biomed Eng,* 41**,** 205-21.

Kritikou, E., Pulverer, B. & Heinrichs, A. 2006. All systems go! *Nat Rev Mol Cell Biol,* 7**,** 801-801.

Lagu, T., Rothberg, M. B., Shieh, M. S., Pekow, P. S., Steingrub, J. S. & Lindenauer, P. K. 2012. Hospitalizations, costs, and outcomes of severe sepsis in the United States 2003 to 2007. *Crit Care Med,* 40**,** 754-61.

Langley, R. J., Tsalik, E. L., van Velkinburgh, J. C., Glickman, S. W., Rice, B. J., Wang, C., Chen, B., Carin, L., Suarez, A., Mohney, R. P., Freeman, D. H., Wang, M., You, J., Wulff, J., Thompson, J. W., Moseley, M. A., Reisinger, S., Edmonds, B. T., Grinnell, B., Nelson, D. R., Dinwiddie, D. L., Miller, N. A., Saunders, C. J., Soden, S. S., Rogers, A. J., Gazourian, L., Fredenburgh, L. E., Massaro, A. F., Baron, R. M., Choi, A. M., Corey, G. R., Ginsburg, G. S., Cairns, C. B., Otero, R. M., Fowler, V. G., Jr., Rivers, E. P., Woods, C. W. & Kingsmore, S. F. 2013. An integrated clinico-metabolomic model improves prediction of death in sepsis. *Sci Transl Med,* 5**,** 195ra95.

Laroux, F. S. 2004. Mechanisms of inflammation: the good, the bad and the ugly. *Front Biosci,* 9**,** 3156-62.

Leek, J. T., Monsen, E., Dabney, A. R. & Storey, J. D. 2006. EDGE: extraction and analysis of differential gene expression. *Bioinformatics,* 22**,** 507-508.

Levy, M. M., Fink, M. P., Marshall, J. C., Abraham, E., Angus, D., Cook, D., Cohen, J., Opal, S. M., Vincent, J. L., Ramsay, G. & Sccm/Esicm/Accp/Ats/Sis 2003. 2001 SCCM/ESICM/ACCP/ATS/SIS International Sepsis Definitions Conference. *Crit Care Med,* 31**,** 1250-6.

Leys, C., Ley, C., Klein, O., Bernard, P. & Licata, L. 2013. Detecting outliers: Do not use standard deviation around the mean, use absolute deviation around the median. *Journal of Experimental Social Psychology,* 49**,** 764-766.

Lim, H. Y., Müller, N., Herold, M. J., Van Den Brandt, J. & Reichardt, H. M. 2007. Glucocorticoids exert opposing effects on macrophage function dependent on their concentration. *Immunology,* 122**,** 47-53.

Lin, E. & Lowry, S. 1998. The Human Response to Endotoxin. *Sepsis,* 2**,** 255-262.

Lissauer, M. E., Johnson, S. B., Bochicchio, G. V., Feild, C. J., Cross, A. S., Hasday, J. D., Whiteford, C. C., Nussbaumer, W. A., Towns, M. & Scalea, T. M. 2009. Differential Expression of Toll-Like Receptor Genes: Sepsis Compared With Sterile Inflammation 1 Day Before Sepsis Diagnosis. *Shock,* 31**,** 238-244 10.1097/SHK.0b013e3181834991.

Liu, T. F., Brown, C. M., El Gazzar, M., McPhail, L., Millet, P., Rao, A., Vachharajani, V. T., Yoza, B. K. & McCall, C. E. 2012a. Fueling the flame: bioenergy couples metabolism and inflammation. *J Leukoc Biol,* 92**,** 499-507.

Liu, T. F., Vachharajani, V. T., Yoza, B. K. & McCall, C. E. 2012b. NAD+-dependent sirtuin 1 and 6 proteins coordinate a switch from glucose to fatty acid oxidation during the acute inflammatory response. *J Biol Chem,* 287**,** 25758-69.

Lord, R. S. & Bralley, J. A. 2008. Clinical applications of urinary organic acids. Part I: Detoxification markers. *Altern Med Rev,* 13**,** 205-15.

Lowry, S. F. 2005. Human endotoxemia: a model for mechanistic insight and therapeutic targeting. *Shock,* 24 Suppl 1**,** 94-100.

Maciver, N. J., Jacobs, S. R., Wieman, H. L., Wofford, J. A., Coloff, J. L. & Rathmell, J. C. 2008. Glucose metabolism in lymphocytes is a regulated process with significant effects on immune cell function and survival. *J Leukoc Biol,* 84**,** 949-57.

Mager, D. E., Wyska, E. & Jusko, W. J. 2003. Diversity of mechanism-based pharmacodynamic models. *Drug Metab Dispos,* 31**,** 510-8.

Maslove, D. M. & Wong, H. R. 2014. Gene expression profiling in sepsis: timing, tissue, and translational considerations. *Trends in molecular medicine,* 20**,** 204-213.

Mattick, J. S., Kamisoglu, K., Ierapetritou, M., Androulakis, I. P. & Berthiamume, F. 2013. Branched Chain Amino Acid Supplementation: Impact on Signaling and Relevance to Critical Illness. *Wiley interdisciplinary reviews. Systems biology and medicine,* in press.

Matzinger, P. 2002. The danger model: a renewed sense of self. *Science,* 296**,** 301-5.

Mavroudis, P. D., Corbett, S. A., Calvano, S. E. & Androulakis, I. P. 2015. Circadian characteristics of permissive and suppressive effects of cortisol and their role in homeostasis and the acute inflammatory response. *Math Biosci,* 260**,** 54-64.

Mazumder, B., Li, X. & Barik, S. 2010. Translation control: a multifaceted regulator of inflammatory response. *J Immunol,* 184**,** 3311-9.

Michaeli, B., Martinez, A., Revelly, J. P., Cayeux, M. C., Chiolero, R. L., Tappy, L. & Berger, M. M. 2012. Effects of endotoxin on lactate metabolism in humans. *Critical care,* 16**,** R139.

Morand, E. F. & Leech, M. 1999. Glucocorticoid regulation of inflammation: the plot thickens. *Inflamm Res,* 48**,** 557-60.

Motley, S. T., Morrow, B. J., Liu, X., Dodge, I. L., Vitiello, A., Ward, C. K. & Shaw, K. J. 2004. Simultaneous analysis of host and pathogen interactions during an in vivo infection reveals local induction of host acute phase response proteins, a novel bacterial stress response, and evidence of a host-imposed metal ion limited environment. *Cell Microbiol,* 6**,** 849-65.

Nguyen, T. T., Almon, R. R., Dubois, D. C., Jusko, W. J. & Androulakis, I. P. 2010. Comparative analysis of acute and chronic corticosteroid pharmacogenomic effects in rat liver: transcriptional dynamics and regulatory structures. *BMC Bioinformatics,* 11**,** 515.

Nguyen, T. T., Foteinou, P. T., Calvano, S. E., Lowry, S. F. & Androulakis, I. P. 2011. Computational identification of transcriptional regulators in human endotoxemia. *PLoS ONE,* 6**,** e18889.

Nguyen, T. T., Nowakowski, R. S. & Androulakis, I. P. 2009. Unsupervised selection of highly coexpressed and noncoexpressed genes using a consensus clustering approach. *OMICS,* 13**,** 219-37.

Nicholson, J. K. 2006. Global systems biology, personalized medicine and molecular epidemiology. *Mol Syst Biol,* 2**,** 52.

Nicholson, J. K., Holmes, E., Lindon, J. C. & Wilson, I. D. 2004. The challenges of modeling mammalian biocomplexity. *Nat Biotechnol,* 22**,** 1268-74.

Nicholson, J. K. & Lindon, J. C. 2008. Systems biology: Metabonomics. *Nature,* 455**,** 1054-6.

Niculescu, M. D. & Zeisel, S. H. 2002. Diet, Methyl Donors and DNA Methylation: Interactions between Dietary Folate, Methionine and Choline. *The Journal of nutrition,* 132**,** 2333S-2335S.

Nishizuka, S., Chen, S. T., Gwadry, F. G., Alexander, J., Major, S. M., Scherf, U., Reinhold, W. C., Waltham, M., Charboneau, L., Young, L., Bussey, K. J., Kim, S., Lababidi, S., Lee, J. K., Pittaluga, S., Scudiero, D. A., Sausville, E. A., Munson, P. J., Petricoin, E. F., 3rd, Liotta, L. A., Hewitt, S. M., Raffeld, M. & Weinstein, J. N. 2003. Diagnostic markers that distinguish colon and ovarian adenocarcinomas: identification by genomic, proteomic, and tissue array profiling. *Cancer Res,* 63**,** 5243-50.

Nouri-Nigjeh, E., Sukumaran, S., Tu, C., Li, J., Shen, X., Duan, X., DuBois, D. C., Almon, R. R., Jusko, W. J. & Qu, J. 2014a. Highly Multiplexed and Reproducible Ion-Current-Based Strategy for Large-Scale Quantitative Proteomics and the Application to Protein Expression Dynamics Induced by Methylprednisolone in 60 Rats. *Analytical Chemistry,* 86**,** 8149-8157.

Nouri-Nigjeh, E., Sukumaran, S., Tu, C., Li, J., Shen, X., Duan, X., DuBois, D. C., Almon, R. R., Jusko, W. J. & Qu, J. 2014b. Highly Multiplexed and Reproducible Ion Current-Based Strategy for Large-Scale Quantitative Proteomics and the Application to Protein Expression Dynamics Induced by Methylprednisolone in 60 Rats. *Anal Chem*.

Oakley, R. H. & Cidlowski, J. A. 2011. Cellular processing of the glucocorticoid receptor gene and protein: new mechanisms for generating tissue-specific actions of glucocorticoids. *J Biol Chem,* 286**,** 3177-84.

Osuchowski, M. F., Remick, D. G., Lederer, J. A., Lang, C. H., Aasen, A. O., Aibiki, M., Azevedo, L. C., Bahrami, S., Boros, M., Cooney, R., Cuzzocrea, S., Jiang, Y., Junger, W. G., Hirasawa, H., Hotchkiss, R. S., Li, X. A., Radermacher, P., Redl, H., Salomao, R., Soebandrio, A., Thiemermann, C., Vincent, J. L., Ward, P., Yao, Y. M., Yu, H. P., Zingarelli, B. & Chaudry, I. H. 2014. Abandon the mouse research ship? Not just yet! *Shock,* 41**,** 463-75.

Pearce, E. L. & Pearce, E. J. 2013. Metabolic pathways in immune cell activation and quiescence. *Immunity,* 38**,** 633-43.

Pompeia, C., Lopes, L. R., Miyasaka, C. K., Procopio, J., Sannomiya, P. & Curi, R. 2000. Effect of fatty acids on leukocyte function. *Braz J Med Biol Res,* 33**,** 1255-68.

Qu, J., Jusko, W. J. & Straubinger, R. M. 2006. Utility of cleavable isotope-coded affinity-tagged reagents for quantification of low-copy proteins induced by methylprednisolone using liquid chromatography/tandem mass spectrometry. *Anal Chem,* 78**,** 4543-52.

Ramakrishnan, R., DuBois, D. C., Almon, R. R., Pyszczynski, N. A. & Jusko, W. J. 2002. Fifth-generation model for corticosteroid pharmacodynamics: application to steady-state receptor down-regulation and enzyme induction patterns during seven-day continuous infusion of methylprednisolone in rats. *J Pharmacokinet Pharmacodyn,* 29**,** 1-24.

Reinhart, K., Bauer, M., Riedemann, N. C. & Hartog, C. S. 2012. New approaches to sepsis: molecular diagnostics and biomarkers. *Clin Microbiol Rev,* 25**,** 609-34.

Richards, S. E., Dumas, M.-E., Fonville, J. M., Ebbels, T. M. D., Holmes, E. & Nicholson, J. K. 2010. Intra- and inter-omic fusion of metabolic profiling data in a systems biology framework. *Chemometrics and Intelligent Laboratory Systems,* 104**,** 121-131.

Rittirsch, D., Hoesel, L. M. & Ward, P. A. 2007. The disconnect between animal models of sepsis and human sepsis. *J Leukoc Biol,* 81**,** 137-43.

Rubinow, K. B., Wall, V. Z., Nelson, J., Mar, D., Bomsztyk, K., Askari, B., Lai, M. A., Smith, K. D., Han, M. S., Vivekanandan-Giri, A., Pennathur, S., Albert, C. J., Ford, D. A., Davis, R. J. & Bornfeldt, K. E. 2013. Acyl-CoA synthetase 1 is induced by Gram-negative bacteria and lipopolysaccharide and is required for phospholipid turnover in stimulated macrophages. *J Biol Chem,* 288**,** 9957-70.

Sapolsky, R. M., Romero, L. M. & Munck, A. U. 2000. How do glucocorticoids influence stress responses? Integrating permissive, suppressive, stimulatory, and preparative actions. *Endocrine reviews,* 21**,** 55-89.

Schaaf, M. J. & Cidlowski, J. A. 2002. Molecular mechanisms of glucocorticoid action and resistance. *J Steroid Biochem Mol Biol,* 83**,** 37-48.

Scheff, J. D., Calvano, S. E., Lowry, S. F. & Androulakis, I. P. 2010. Modeling the influence of circadian rhythms on the acute inflammatory response. *Journal of theoretical biology,* 264**,** 1068-76.

Scheff, J. D., Mavroudis, P. D., Calvano, S. E. & Androulakis, I. P. 2012a. Translational applications of evaluating physiologic variability in human endotoxemia. *J Clin Monit Comput*.

Scheff, J. D., Mavroudis, P. D., Calvano, S. E., Lowry, S. F. & Androulakis, I. P. 2011. Modeling autonomic regulation of cardiac function and heart rate variability in human endotoxemia. *Physiol Genomics,* 43**,** 951-64.

Scheff, J. D., Mavroudis, P. D., Foteinou, P. T., Calvano, S. E. & Androulakis, I. P. 2012b. Modeling physiologic variability in human endotoxemia. *Crit Rev Biomed Eng,* 40**,** 313-22.

Seok, J., Warren, H. S., Cuenca, A. G., Mindrinos, M. N., Baker, H. V., Xu, W., Richards, D. R., McDonald-Smith, G. P., Gao, H., Hennessy, L., Finnerty, C. C., Lopez, C. M., Honari, S., Moore, E. E., Minei, J. P., Cuschieri, J., Bankey, P. E., Johnson, J. L., Sperry, J., Nathens, A. B., Billiar, T. R., West, M. A., Jeschke, M. G., Klein, M. B., Gamelli, R. L., Gibran, N. S., Brownstein, B. H., Miller-Graziano, C., Calvano, S. E., Mason, P. H., Cobb, J. P., Rahme, L. G., Lowry, S. F., Maier, R. V., Moldawer, L. L., Herndon, D. N., Davis, R. W., Xiao, W. & Tompkins, R. G. 2013. Genomic responses in mouse models poorly mimic human inflammatory diseases. *Proc Natl Acad Sci U S A,* 110**,** 3507-12.

Serhan, C. N. & Savill, J. 2005. Resolution of inflammation: the beginning programs the end. *Nat Immunol,* 6**,** 1191-7.

Shah, O. J., Iniguez-Lluhi, J. A., Romanelli, A., Kimball, S. R. & Jefferson, L. S. 2002. The activated glucocorticoid receptor modulates presumptive autoregulation of ribosomal protein S6 protein kinase, p70 S6K. *Journal of Biological Chemistry,* 277**,** 2525-2533.

Shah, O. J., Kimball, S. R. & Jefferson, L. S. 2000. Acute attenuation of translation initiation and protein synthesis by glucocorticoids in skeletal muscle. *American Journal of Physiology - Endocrinology And Metabolism,* 278**,** E76-E82.

Shankavaram, U. T., Reinhold, W. C., Nishizuka, S., Major, S., Morita, D., Chary, K. K., Reimers, M. A., Scherf, U., Kahn, A., Dolginow, D., Cossman, J., Kaldjian, E. P., Scudiero, D. A., Petricoin, E., Liotta, L., Lee, J. K. & Weinstein, J. N. 2007. Transcript and protein expression profiles of the NCI-60 cancer cell panel: an integromic microarray study. *Mol Cancer Ther,* 6**,** 820-32.

Shieh, J. H., Peterson, R. H. & Moore, M. A. 1993. Cytokines and dexamethasone modulation of IL-1 receptors on human neutrophils in vitro. *The Journal of Immunology,* 150**,** 3515-24.

Simopoulos, A. P. 2002. Omega-3 fatty acids in inflammation and autoimmune diseases. *J Am Coll Nutr,* 21**,** 495-505.

Smyth, G. P., Stapleton, P. P., Freeman, T. A., Concannon, E. M., Mestre, J. R., Duff, M., Maddali, S. & Daly, J. M. 2004. Glucocorticoid pretreatment induces cytokine overexpression and nuclear factor-κB activation in macrophages. *Journal of Surgical Research,* 116**,** 253-261.

St-Pierre, M. V., Kullak-Ublick, G. A., Hagenbuch, B. & Meier, P. J. 2001. Transport of bile acids in hepatic and non-hepatic tissues. *J Exp Biol,* 204**,** 1673-86.

Storey, J. D., Dai, J. Y. & Leek, J. T. 2007. The optimal discovery procedure for large-scale significance testing, with applications to comparative microarray experiments. *Biostatistics,* 8**,** 414-432.

Storey, J. D., Xiao, W., Leek, J. T., Tompkins, R. G. & Davis, R. W. 2005. Significance analysis of time course microarray experiments. *Proc Natl Acad Sci U S A,* 102**,** 12837-12842.

Straub, R. H., Vogl, D., Gross, V., Lang, B., Scholmerich, J. & Andus, T. 1998. Association of humoral markers of inflammation and dehydroepiandrosterone sulfate or cortisol serum levels in patients with chronic inflammatory bowel disease. *Am J Gastroenterol,* 93**,** 2197-2202.

Sukumaran, S., Jusko, W. J., DuBois, D. C. & Almon, R. R. 2011. Mechanistic modeling of the effects of glucocorticoids and circadian rhythms on adipokine expression. *J Pharmacol Exp Ther,* 337**,** 734-46.

Sun, Y.-N., DuBois, D., Almon, R. & Jusko, W. 1998. Fourth-Generation Model for Corticosteroid Pharmacodynamics: A Model for Methylprednisolone Effects on Receptor/Gene-Mediated Glucocorticoid Receptor Down-Regulation and Tyrosine Aminotransferase Induction in Rat Liver. *Journal of Pharmacokinetics and Biopharmaceutics,* 26**,** 289-317.

Swartz, S. L. & Dluhy, R. G. 1978. Corticosteroids: clinical pharmacology and therapeutic use. *Drugs,* 16**,** 238-55.

Talwar, S., Munson, P. J., Barb, J., Fiuza, C., Cintron, A. P., Logun, C., Tropea, M., Khan, S., Reda, D., Shelhamer, J. H., Danner, R. L. & Suffredini, A. F. 2006. Gene expression profiles of peripheral blood leukocytes after endotoxin challenge in humans. *Physiol Genomics,* 25**,** 203-15.

Tu, C., Li, J., Bu, Y., Hangauer, D. & Qu, J. 2012. An ion-current-based, comprehensive and reproducible proteomic strategy for comparative characterization of the cellular responses to novel anti-cancer agents in a prostate cell model. *J Proteomics,* 77**,** 187-201.

Urbanska, A., Zolla, V., Verzani, P. & Santambrogio, L. 2014. Physiological and Pathological Role of Reactive Oxygen Species in the Immune Cells. *In:* MASSOUD, A. & REZAEI, N. (eds.) *Immunology of Aging.* Springer Berlin Heidelberg.

van der Goes, A., Hoekstra, K., van den Berg, T. K. & Dijkstra, C. D. 2000. Dexamethasone promotes phagocytosis and bacterial killing by human monocytes/macrophages in vitro. *Journal of leukocyte biology,* 67**,** 801-807.

Vaughan, G. M., Becker, R. A., Allen, J. P., Goodwin, C. W. J., Pruitt, B. A. J. & Mason, A. D. J. 1982. Cortisol and Corticotrophin in Burned Patients. *The Journal of Trauma and Acute Care Surgery,* 22**,** 263-273.

Vegiopoulos, A. & Herzig, S. 2007. Glucocorticoids, metabolism and metabolic diseases. *Mol Cell Endocrinol,* 275**,** 43-61.

Visser, T., Pillay, J., Pickkers, P., Leenen, L. P. & Koenderman, L. 2012. Homology in systemic neutrophil response induced by human experimental endotoxemia and by trauma. *Shock,* 37**,** 145-51.

Voormolen, N., Noordzij, M., Grootendorst, D. C., Beetz, I., Sijpkens, Y. W., van Manen, J. G., Boeschoten, E. W., Huisman, R. M., Krediet, R. T., Dekker, F. W. & group, t. P. s. 2007. High plasma phosphate as a risk factor for decline in renal function and mortality in pre-dialysis patients. *Nephrology Dialysis Transplantation,* 22**,** 2909-2916.

Warburg, O. 1956. On the origin of cancer cells. *Science,* 123**,** 309-14.

Warner, J. R. & McIntosh, K. B. 2009. How common are extraribosomal functions of ribosomal proteins? *Mol Cell,* 34**,** 3-11.

Waters, K. M., Pounds, J. G. & Thrall, B. D. 2006. Data merging for integrated microarray and proteomic analysis. *Brief Funct Genomic Proteomic,* 5**,** 261-72.

Wishart, D. S., Jewison, T., Guo, A. C., Wilson, M., Knox, C., Liu, Y., Djoumbou, Y., Mandal, R., Aziat, F., Dong, E., Bouatra, S., Sinelnikov, I., Arndt, D., Xia, J., Liu, P., Yallou, F., Bjorndahl, T., Perez-Pineiro, R., Eisner, R., Allen, F., Neveu, V., Greiner, R. & Scalbert, A. 2013. HMDB 3.0--The Human Metabolome Database in 2013. *Nucleic Acids Res,* 41**,** D801-7.

Wolff, S. M. 1973. Biological effects of bacterial endotoxins in man. *J Infect Dis,* 128**,** Suppl:259-64.

Yang, E. H., Almon, R. R., Dubois, D. C., Jusko, W. J. & Androulakis, I. P. 2009. Identification of global transcriptional dynamics. *PLoS ONE,* 4**,** e5992.

Yeager, M. P., Pioli, P. A. & Guyre, P. M. 2011. Cortisol exerts bi-phasic regulation of inflammation in humans. *Dose Response,* 9**,** 332-47.

Yeager, M. P., Pioli, P. A., Wardwell, K., Beach, M. L., Martel, P., Lee, H. K., Rassias, A. J. & Guyre, P. M. 2008. In Vivo Exposure to High or Low Cortisol Has Biphasic

Effects on Inflammatory Response Pathways of Human Monocytes. *Anesthesia & Analgesia,* 107**,** 1726-1734.

Yeager, M. P., Rassias, A. J., Pioli, P. A., Beach, M. L., Wardwell, K., Collins, J. E., Lee, H. K. & Guyre, P. M. 2009. Pretreatment with stress cortisol enhances the human systemic inflammatory response to bacterial endotoxin. *Critical care medicine,* 37**,** 2727.

Zhang, T. Y. & Daynes, R. A. 2007. Glucocorticoid conditioning of myeloid progenitors enhances TLR4 signaling via negative regulation of the phosphatidylinositol 3-kinase-Akt pathway. *The Journal of Immunology,* 178**,** 2517-2526.

Curriculum Vitae

Kubra Kamisoglu

EDUCATION

9/2008 – 7/2015	Ph.D., Chemical and Biochemical Engineering Rutgers, The State University of New Jersey, Piscataway, NJ USA
9/2005 – 7/2007	M.Sc., Chemical Engineering Middle East Technical University, Ankara, Turkey
9/2000 – 5/2005	B.Sc. with High Honour, Chemical Engineering Middle East Technical University, Ankara, Turkey

PROFESSIONAL EXPERIENCE

1/2012 – 7/2015	Research Assistant / Fellow Rutgers, The State University of New Jersey, Piscataway, NJ USA Supervisor: Ioannis P. Androulakis
9/2009 – 12/2011	Research Assistant Rutgers, The State University of New Jersey, Piscataway, NJ USA Supervisor: Prabhas V. Moghe
9/2008 – 8/2009	Teaching Assistant Rutgers, The State University of New Jersey, Piscataway, NJ USA
9/2005 – 8/2008	Teaching and Research Assistant Middle East Technical University, Ankara, Turkey

PUBLICATIONS

Research Articles

2015
- **Kamisoglu K**, Haimovich B, Calvano SE, Coyle SM, Corbett SA, Langley RJ, Kingsmore SF, Androulakis IP, “Human metabolic response to systemic inflammation: Concordance between experimental endotoxemia and clinical cases of sepsis/SIRS”, Critical Care, 19(1):71.
- **Kamisoglu K**, Sukumaran S, Nouri-Nigjeh E, Tu C, Li J, Shen X, Duan X, Qu J, Almon RR, Jusko WJ, Androulakis IP, “Tandem analysis of transcriptome and proteome changes after a single dose of corticosteroid: A systems approach to liver function in pharmacogenomics”, Omics: A Journal of Integrative Biology, 19(2):80-91

2014
- **Kamisoglu K**, Calvano SE, Coyle SM, Corbett SA, Androulakis IP, “Integrated transcriptional and metabolic profiling in human endotoxemia”, Shock (Augusta, GA), 42(6):499-508

2013
- **Kamisoglu K**, Sleight KE, Nguyen TT, Calvano SE, Coyle SM, Corbett SA, Androulakis IP, “Effects of coupled dose and rhythm manipulation of plasma cortisol levels on leukocyte

transcriptional response to endotoxin challenge in humans", Innate Immunity, 20(7):774-784,

- **Kamisoglu K**, Sleight KE, Calvano SE, Coyle SM, Corbett SA, Androulakis IP, "Temporal metabolic profiling of plasma during endotoxemia in humans", Shock (Augusta, Ga.), 40(6):519-26

2008

- **Kamisoglu K**, Aksoy EA, Akata B, Hasirci N, Bac N, "Preparation and characterization of antibacterial zeolite - polyurethane composites", Journal of Applied Polymer Science, 110(5):2854-2861, 2008

Review Articles

2014

- Sunderram J, Sofou S, **Kamisoglu K**, Androulakis IP, "Time-restricted feeding and the realignment of biological rhythms: Translational opportunities and challenges", Journal of Translational Medicine, 12(1):79-87
- Kosmides AK, **Kamisoglu K**, Calvano SE, Corbett SA, Androulakis IP, "Metabolomic fingerprinting: Challenges and opportunities", Critical Reviews in Biomedical Engineering, 41(3):225-221

2013

- Androulakis IP, **Kamisoglu K**, Mattick J, "Topology and dynamics of signaling networks: In search of transcriptional control of the inflammatory response", Annual Reviews of Biomedical Engineering, 15:1-28
- Mattick JSA, **Kamisoglu K**, Ierapetritou MG, Androulakis IP, Berthiaume F, "Branched-chain amino acid supplementation: impact on signaling and relevance to critical illness", Wiley Interdisciplinary Reviews: Systems Biology and Medicine, 5: 449-60

2011

- Lewis DR, **Kamisoglu K**, York AW, Moghe PV "Polymer-based therapeutics: Nanoassemblies and nanoparticles for management of atherosclerosis", Wiley Interdisciplinary Reviews: Nanomedicine and Nanobiotechnology, 3(4):400-420

Book Chapter

2015

- Scheff JD, **Kamisoglu K**, and Androulakis IP, "Mechanistic modeling of inflammation", Systems Pharmacology & Pharmacodynamics, edited by Mager D and Kimko E

Appendix

Table A. 1: Number of outliers removed from the metabolomic data in endotoxemia (LPS) and in CAPSOD studies (Sepsis and SIRS) before any statistical analysis.

	LPS		Sepsis		SIRS	
	t0	t6	t0	t24	t0	t24
Outliers	117	118	1836	1476	469	348
Data points in total	2655	2655	21417	18939	5133	4425
% removed	4.4	4.5	8.5	7.8	9.1	7.9

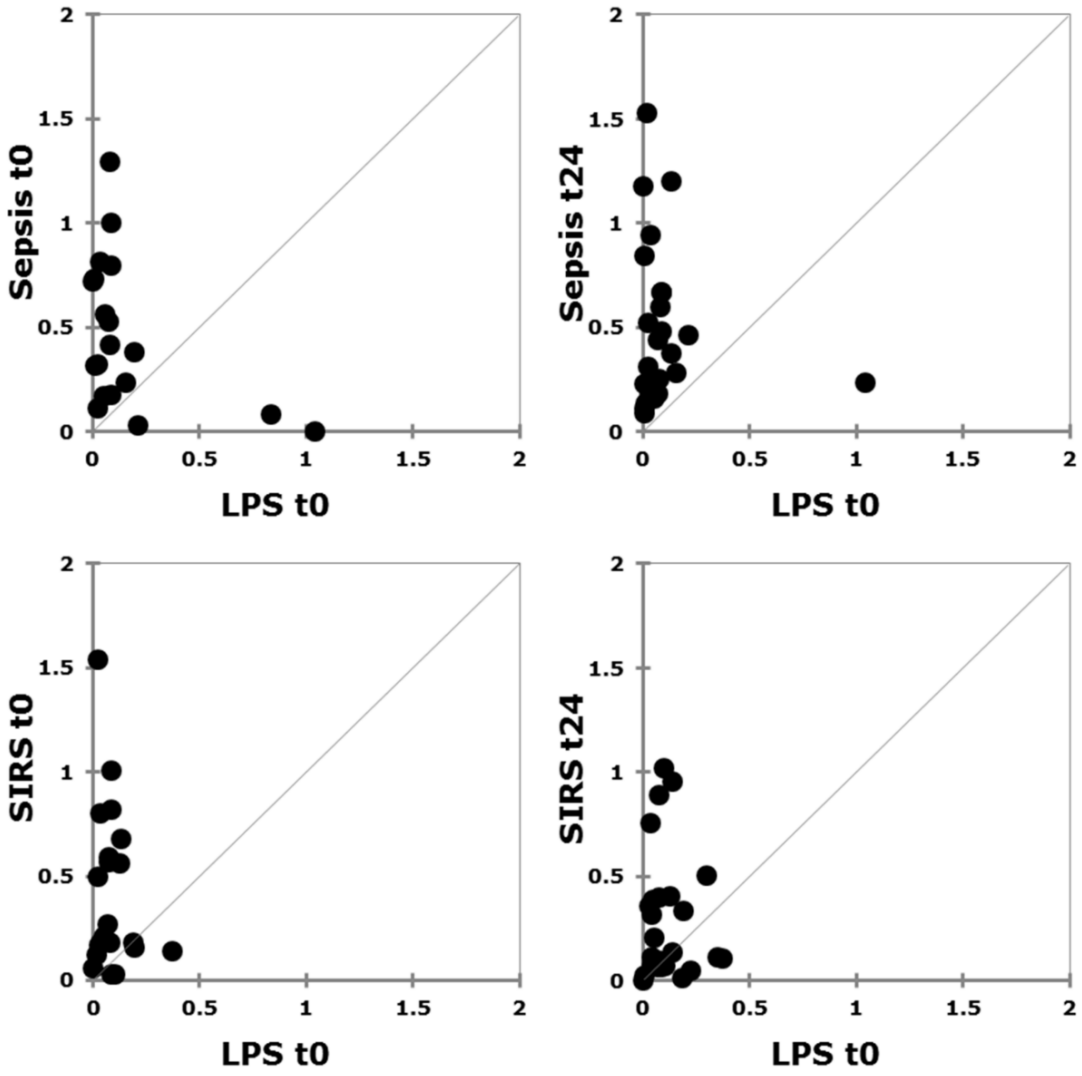

Figure A. 1: Comparison of the variances of significant metabolites in the clinical groups with respect to those in the baseline ($t_{0,LPS}$).

Table A. 2: Full list of the metabolites included in the assessment of the relevance of endotoxemia with clinical cases of systemic inflammation, together with the significance in each condition, direction and magnitude of the changes relative to the baseline ($t_{0,LPS}$).

A. Metabolites which are significantly different than the heathy basis (LPS_t0) in all conditions

		LPS	Sepsis	Sepsis	SIRS	SIRS
metabolite name	**super pathway**	**t6**	**t0**	**t24**	**t0**	**t24**
2-hydroxybutyrate (AHB)	Amino acid	▲	=	▲	=	=
alpha-ketobutyrate	Amino acid	▲	=	=	=	▼
N-acetylglycine	Amino acid	▲	=	=	=	▼
mannose	Carbohydrate	▲	=	▲	=	=
xylose	Carbohydrate	▲	=	▼	=	▼
citrate	Energy	▲	=	=	▲	▲
arachidonate (20:4n6)	Lipid	▲	=	=	▲	▲
docosahexaenoate (DHA; 22:6n3)	Lipid	▲	=	=	▲	=
eicosapentaenoate (EPA; 20:5n3)	Lipid	▲	=	=	=	▲
hexanoylcarnitine (C6)	Lipid	▲	▲	▲	=	=
octadecanedioate (C18)	Lipid	▲	=	=	=	▼
bilirubin (E,Z or Z,E)*	Cofactors and vitamins	▲▲	▲	▲▲	▲	=
3-hydroxybutyrate (BHBA)	Lipid	▲▲	=	=	=	▼▼
docosapentaenoate (DPA; 22:5n3)	Lipid	▲▲	=	▲	▲	=
hexadecanedioate (C16)	Lipid	▲▲	=	=	▼▼	▼
palmitoleate (16:1n7)	Lipid	▲▲	▲	▲	▲	▲
pregnen-diol disulfate*	Lipid	▲▲	▲	▲	=	=
5-oxoproline	Amino acid	▼	=	=	▼	=
citrulline	Amino acid	▼	▼	▼	=	=
histidine	Amino acid	▼	=	▼	=	=
proline	Amino acid	▼	=	=	=	▲
serine	Amino acid	▼	=	▼	▲	=
threonine	Amino acid	▼	▼	=	=	=
1-linoleoyl-GPC (18:2)	Lipid	▼	=	=	▲	▲
1-oleoyl-GPC (18:1)	Lipid	▼	=	=	=	▲
2-palmitoyl-GPC* (16:0)	Lipid	▼	▼	▼	=	=
uridine	Nucleotide	▼	=	▼	=	=
gamma-glutamyltyrosine	Peptide	▼	=	▼	=	=
catechol sulfate	Xenobiotics	▼▼	▼	=	=	=

B. Metabolites which are significantly different than the heathy basis (LPS_t0) in only clinical conditions

		LPS	Sepsis	Sepsis	SIRS	SIRS
metabolite name	**super pathway**	**t6**	**t0**	**t24**	**t0**	**t24**
glutamine	Amino acid	=	=	=	▲	=
3-methylhistidine	Amino acid	=	▼▼	▼▼	=	=
3-hydroxy-2-ethylpropionate	Amino acid	=	=	▼	=	▼
tiglyl carnitine (C5)	Amino acid	=	=	▼	=	=
erythrose	Carbohydrate	=	▲	▲	▲▲	▲
mannitol	Carbohydrate	=	=	=	▼▼	=
pantothenate (Vitamin B5)	Cofactors and vitamins	=	=	=	=	▼
pyridoxate	Cofactors and vitamins	=	▼	=	▼▼	=
taurocholate	Lipid	=	▲	▲▲	=	=
octanoylcarnitine (C8)	Lipid	=	▲	▲	▲	=
laurylcarnitine (C12)	Lipid	=	=	=	▲▲	▲
decanoylcarnitine (C10)	Lipid	=	=	▲	▲	=
myo-inositol	Lipid	=	=	▲	=	=
1-eicosatrienoyl-GPC* (20:3)	Lipid	=	▼▼	▼	=	=

1-palmitoleoyl-GPC* (16:1)	Lipid	=	▼▼	▼	=	=
1-oleoyl-GPE (18:1)	Lipid	=	▼	▼	=	=
1-palmitoyl-GPC (16:0)	Lipid	=	=	=	▲	▲
1-arachidoyl-GPE* (20:4)	Lipid	=	=	=	=	▲
1-stearoyl-GPC (18:0)	Lipid	=	=	=	=	▲
epiandrosterone sulfate	Lipid	=	▲	=	=	▼▼
androsterone sulfate	Lipid	=	=	=	▼▼	▼▼
dehydroisoandrosterone sulfate (DHEA-S)	Lipid	=	=	=	▼	▼
5alpha-pregnan-3beta,20alpha-diol disulfate	Lipid	=	=	=	=	▼▼
N6-carbamoylthreonyladenosine	Nucleotide	=	=	=	▼	=
p-acetamidophenylglucuronide	Xenobiotics	=	▲▲	▲▲	=	▼▼
piperine	Xenobiotics	=	▼▼	=	=	=

C. Metabolites which are significantly different than the heathy basis (LPS_t0) in only experimental condition

		LPS	Sepsis	Sepsis	SIRS	SIRS
metabolite name	**super pathway**	**t6**	**t0**	**t24**	**t0**	**t24**
3-methyl-2-oxobutyrate	Amino acid	▲	=	=	=	=
pyruvate	Carbohydrate	▲	=	=	=	=
alpha-ketoglutarate	Energy	▲	=	=	=	=
malate	Energy	▲	=	=	=	=
10-nonadecenoate (19:1n9)	Lipid	▲	=	=	=	=
2-hydroxypalmitate	Lipid	▲	=	=	=	=
2-hydroxystearate	Lipid	▲	=	=	=	=
5-dodecenoate (12:1n7)	Lipid	▲	=	=	=	=
dihomolinolenate (20:3n3 or 3n6)	Lipid	▲	=	=	=	=
laurate (12:0)	Lipid	▲	=	=	=	=
linoleate (18:2n6)	Lipid	▲	=	=	=	=
margarate (17:0)	Lipid	▲	=	=	=	=
myristate (14:0)	Lipid	▲	=	=	=	=
myristoleate (14:1n5)	Lipid	▲	=	=	=	=
oleate (18:1n9)	Lipid	▲	=	=	=	=
pregn steroid monosulfate*	Lipid	▲	=	=	=	=
stearate (18:0)	Lipid	▲	=	=	=	=
hypoxanthine	Nucleotide	▲	=	=	=	=
biliverdin	Cofactors and vitamins	▲▲	=	=	=	=
10-heptadecenoate (17:1n7)	Lipid	▲▲	=	=	=	=
dihomolinoleate (20:2n6)	Lipid	▲▲	=	=	=	=
eicosenoate (20:1n9 or 1n11)	Lipid	▲▲	=	=	=	=
linolenate (18:3n3 or 3n6)	Lipid	▲▲	=	=	=	=
palmitate (16:0)	Lipid	▲▲	=	=	=	=
stearidonate (18:4n3)	Lipid	▲▲	=	=	=	=
2-methylbutyroylcarnitine (C5)	Amino acid	▼	=	=	=	=
3-indoxyl sulfate	Amino acid	▼	=	=	=	=
alanine	Amino acid	▼	=	=	=	=
arginine	Amino acid	▼	=	=	=	=
asparagine	Amino acid	▼	=	=	=	=
cysteine	Amino acid	▼	=	=	=	=
isobutyrylcarnitine (C4)	Amino acid	▼	=	=	=	=
isoleucine	Amino acid	▼	=	=	=	=
kynurenine	Amino acid	▼	=	=	=	=
leucine	Amino acid	▼	=	=	=	=
lysine	Amino acid	▼	=	=	=	=
methionine	Amino acid	▼	=	=	=	=
N-acetylornithine	Amino acid	▼	=	=	=	=
ornithine	Amino acid	▼	=	=	=	=
pipecolate	Amino acid	▼	=	=	=	=
tryptophan	Amino acid	▼	=	=	=	=

tyrosine	Amino acid	▼	=	=	=	=
valine	Amino acid	▼	=	=	=	=
threitol	Carbohydrate	▼	=	=	=	=
threonate	Cofactors and vitamins	▼	=	=	=	=
phosphate	Energy	▼	=	=	=	=
choline	Lipid	▼	=	=	=	=
glycerol 3-phosphate (G3P)	Lipid	▼	=	=	=	=
propionylcarnitine (C3)	Lipid	▼	=	=	=	=
allantoin	Nucleotide	▼	=	=	=	=
gamma-glutamylleucine	Peptide	▼	=	=	=	=
gamma-glutamylphenylalanine	Peptide	▼	=	=	=	=
glycochenodeoxycholate	Lipid	▼▼	=	=	=	=
hippurate	Xenobiotics	▼▼	=	=	=	=

D. Metabolites which are NOT significantly different than the heathy basis (LPS_t0) in any condition

		LPS	Sepsis	Sepsis	SIRS	SIRS
metabolite name	**super pathway**	**t6**	**t0**	**t24**	**t0**	**t24**
N-acetylalanine	Amino acid	=	=	=	=	=
2-aminobutyrate	Amino acid	=	=	=	=	=
creatine	Amino acid	=	=	=	=	=
creatinine	Amino acid	=	=	=	=	=
glutamate	Amino acid	=	=	=	=	=
pyroglutamine*	Amino acid	=	=	=	=	=
betaine	Amino acid	=	=	=	=	=
glycine	Amino acid	=	=	=	=	=
N-acetylthreonine	Amino acid	=	=	=	=	=
3-(4-hydroxyphenyl)lactate (HPLA)	Amino acid	=	=	=	=	=
3-methoxytyrosine	Amino acid	=	=	=	=	=
p-cresol sulfate	Amino acid	=	=	=	=	=
phenol sulfate	Amino acid	=	=	=	=	=
phenylacetylglutamine	Amino acid	=	=	=	=	=
phenylalanine	Amino acid	=	=	=	=	=
indolelactate	Amino acid	=	=	=	=	=
stachydrine	Amino acid	=	=	=	=	=
urea	Amino acid	=	=	=	=	=
3-methyl-2-oxovalerate	Amino acid	=	=	=	=	=
4-methyl-2-oxopentanoate	Amino acid	=	=	=	=	=
alpha-hydroxyisovalerate	Amino acid	=	=	=	=	=
beta-hydroxyisovalerate	Amino acid	=	=	=	=	=
isovalerylcarnitine (C5)	Amino acid	=	=	=	=	=
erythronate*	Carbohydrate	=	=	=	=	=
fructose	Carbohydrate	=	=	=	=	=
1,5-anhydroglucitol (1,5-AG)	Carbohydrate	=	=	=	=	=
glucose	Carbohydrate	=	=	=	=	=
glycerate	Carbohydrate	=	=	=	=	=
lactate	Carbohydrate	=	=	=	=	=
arabinose	Carbohydrate	=	=	=	=	=
arabitol	Carbohydrate	=	=	=	=	=
gluconate	Carbohydrate	=	=	=	=	=
xylonate	Carbohydrate	=	=	=	=	=
heme*	Cofactors and vitamins	=	=	=	=	=
alpha-tocopherol	Cofactors and vitamins	=	=	=	=	=
glycocholate	Lipid	=	=	=	=	=
taurochenodeoxycholate	Lipid	=	=	=	=	=
taurolithocholate 3-sulfate	Lipid	=	=	=	=	=
3-dehydrocarnitine*	Lipid	=	=	=	=	=
acetylcarnitine (C2)	Lipid	=	=	=	=	=
carnitine	Lipid	=	=	=	=	=

cis-4-decenoyl carnitine	Lipid	=	=	=	=	=
deoxycarnitine	Lipid	=	=	=	=	=
butyrylcarnitine (C4)	Lipid	=	=	=	=	=
3-carboxy-4-methyl-5-propyl-2-furanpropanoate (CMPF)	Lipid	=	=	=	=	=
glycerol	Lipid	=	=	=	=	=
adrenate (22:4n6)	Lipid	=	=	=	=	=
1-arachidoyl-GPC* (20:4)	Lipid	=	=	=	=	=
1-arachidoyl-GPI* (20:4)	Lipid	=	=	=	=	=
caprate (10:0)	Lipid	=	=	=	=	=
caproate (6:0)	Lipid	=	=	=	=	=
caprylate (8:0)	Lipid	=	=	=	=	=
heptanoate (7:0)	Lipid	=	=	=	=	=
pelargonate (9:0)	Lipid	=	=	=	=	=
1-palmitoylglycerol (16:0)	Lipid	=	=	=	=	=
1-stearoylglycerol (18:0)	Lipid	=	=	=	=	=
7-alpha-hydroxy-3-oxo-4-cholestenoate (7-HOCA)	Lipid	=	=	=	=	=
cholesterol	Lipid	=	=	=	=	=
cortisol	Lipid	=	=	=	=	=
xanthine	Nucleotide	=	=	=	=	=
adenosine 5'-monophosphate (AMP)	Nucleotide	=	=	=	=	=
urate	Nucleotide	=	=	=	=	=
pseudouridine	Nucleotide	=	=	=	=	=
4-vinylphenol sulfate	Xenobiotics	=	=	=	=	=
iminodiacetate (IDA)	Xenobiotics	=	=	=	=	=
quinate	Xenobiotics	=	=	=	=	=
erythritol	Xenobiotics	=	=	=	=	=
caffeine	Xenobiotics	=	=	=	=	=

Table A. 3: Results of t-test for acyl-GPCs and acyl-carnitines, between SS and SNS groups at each time point, and between $t_{0,LPS}$ and $t_{6,LPS}$ in endotoxemia group, together with their direction of change from the common baseline t0,LPS. (Changes from the healthy baseline, $t_{0,LPS}$: ▲/▼: less than 2 fold change; ▲▲/▼▼: more than 2 fold change).

	Significance of metabolites			Direction of change from common baseline				
	Metabolites significantly differ between SS and SNS at		LPS at	SS		SNS		LPS
	t0	t24	t6	t0	t24	t0	t24	t6
1-arachidonyl-GPC (20:4)	No	Yes	No	-	▼	-	▼▼	-
1-eicosatrienoyl-GPC (20:3)	Yes	Yes	No	▼▼	▼	▼▼	▼▼	-
1-linoleoyl-GPC (18:2)	No	Yes	Yes	-	▼	-	▼	▼
1-oleoyl-GPC (18:1)	No	Yes	Yes	-	▼	-	▼	▼
1-palmitoleoyl-GPC (16:1)	Yes	Yes	No	▼	▼	▼▼	▼▼	-
1-palmitoyl-GPC (16:0)	No	Yes	No	-	▲	-	▼	-
1-stearoyl-GPC (18:0)	No	Yes	No	-	▼	-	▼▼	-
2-palmitoyl-GPC (16:0)	Yes	Yes	Yes	▼	▼	▼▼	▼▼	▼
2-methylbutyroylcarnitine (C5)	Yes	Yes	Yes	▼	▼	▲	▲	▼
isobutyrylcarnitine (C4)	No	Yes	Yes	-	▼	-	▲	▼
isovalerylcarnitine (C5)	No	No	No	-	-	-	-	-
tiglyl carnitine (C5)	Yes	Yes	No	▼	▼▼	▲	▲	-
deoxycarnitine	No	Yes	No	-	▼	-	▲	-
hexanoylcarnitine (C6)	Yes	Yes	Yes	▲	▲	▲▲	▲▲	▲
octanoylcarnitine (C8)	Yes	Yes	No	▲	▲	▲▲	▲▲	-
propionylcarnitine (C3)	Yes	Yes	Yes	▲	▼	▲	▲	▼
acetylcarnitine (C2)	Yes	Yes	No	▼	▼	▲	▲	-
butyrylcarnitine (C4)	Yes	Yes	No	▼	▼	▲	▲	-
decanoylcarnitine (C10)	Yes	Yes	No	▲	▲	▲▲	▲▲	-
cis-4-decenoyl carnitine	Yes	Yes	No	▲	▲	▲	▲▲	-

Table A. 4: Functional annotation of groups of proteins with distinct expression patterns in response to MPL as identified in clustering analysis (cluster profiles are shown in Figure 5.6).

	Canonical Pathway	**Genes**
Cluster 1	L-cysteine Degradation II	CTH
	Citrulline Degradation	OTC
	Formaldehyde Oxidation II (Glutathione-dependent)	ADH5
	Fatty Acid β-oxidation I	ACAA1, ACAA2
	LPS/IL-1 Mediated Inhibition of RXR Function	GSTM2, Cyp2a2, SULT1E1, FABP1
	Methylglyoxal Degradation I	HAGH
	Cysteine Biosynthesis/Homocysteine Degradation	CTH
	Estrogen Biosynthesis	CYP2C18, HSD17B2
	Proline Biosynthesis II (from Arginine)	OTC
	Phenylalanine Degradation I (Aerobic)	QDPR
	CMP-N-acetylneuraminate Biosynthesis I (Eukaryotes)	GNE
	PPARα/RXRα Activation	ACAA1, CYP2C18, Cyp2c44
	Arginine Biosynthesis IV	OTC
	Urea Cycle	OTC
	Citrulline Biosynthesis	OTC
	Acyl-CoA Hydrolysis	Ces1e
	Glutathione Redox Reactions I	GPX1
Cluster 2	Ketogenesis	HADHB, BDH1, HMGCL
	Ketolysis	HADHB, BDH1
	Serotonin Degradation	UGT2B17, ADH1C, UGT2B15
	Xenobiotic Metabolism Signaling	ALDH1L2, UGT2B17, UGT2B15, Gsta3, HSP90AA1
	Isoleucine Degradation I	HADHB, ACADSB
	Valine Degradation I	HADHB, ACADSB
	Thyroid Hormone Metabolism II (via Conjugation and/or Degradation)	UGT2B17, UGT2B15
	Sulfate Activation for Sulfonation	PAPSS2
	Thiosulfate Disproportionation III (Rhodanese)	TST
	Sorbitol Degradation I	SORD
	Aryl Hydrocarbon Receptor Signaling	ALDH1L2, Gsta3, HSP90AA1
	Nicotine Degradation	UGT2B17, UGT2B15
	Glutamate Degradation II	GOT2
	Aspartate Biosynthesis	GOT2
	Superpathway of Melatonin Degradation	UGT2B17, UGT2B15
	Glycogen Biosynthesis II (from UDP-D-Glucose)	UGP2
	L-cysteine Degradation I	GOT2
	Aspartate Degradation II	GOT2
	LPS/IL-1 Mediated Inhibition of RXR Function	ALDH1L2, Gsta3, PAPSS2
	Sucrose Degradation V	KHK
	Leucine Degradation I	HMGCL
	Colanic Acid Building Blocks Biosynthesis	UGP2
	Mevalonate Pathway I	HADHB
	Phenylalanine Degradation IV (Mammalian, via Side Chain)	GOT2
	Superpathway of Geranylgeranyldiphosphate Biosynthesis I (via Mevalonate)	HADHB
	Glutaryl-CoA Degradation	HADHB
Cluster 3	Mitochondrial Dysfunction	HSD17B10, SDHA, NDUFA9, XDH, CYB5R3, COX5A, NDUFS3, MAOA, AIFM1
	TCA Cycle II	SDHA, SUCLA2, ACO2, ACO1
	Serotonin Degradation	HSD17B10, ALDH3A2, PECR, SULT1C3, MAOA
	Ethanol Degradation II	HSD17B10, ALDH3A2, PECR, ACSL1
	Noradrenaline and Adrenaline Degradation	HSD17B10, ALDH3A2, PECR, MAOA
	Tryptophan Degradation X (Mammalian, via Tryptamine)	ALDH3A2, DDC, MAOA
	Dopamine Degradation	ALDH3A2, SULT1C3, MAOA
	LPS/IL-1 Mediated Inhibition of RXR Function	ALDH3A2, ACOX1, ALDH8A1, Cyp2a12/Cyp2a22, SULT1C3, ACSL1, MAOA

	Adenosine Nucleotides Degradation II	XDH, AOX1
	Urate Biosynthesis/Inosine 5'-phosphate Degradation	XDH, AOX1
	Guanosine Nucleotides Degradation III	XDH, AOX1
	Purine Nucleotides Degradation II (Aerobic)	XDH, AOX1
	Oxidative Ethanol Degradation III	ALDH3A2, ACSL1
	Phenylalanine Degradation IV (Mammalian, via Side Chain)	ALDH3A2, MAOA
	Serotonin Receptor Signaling	DDC, MAOA
	Putrescine Degradation III	ALDH3A2, MAOA
	Ethanol Degradation IV	ALDH3A2, ACSL1
	γ-linolenate Biosynthesis II (Animals)	CYB5R3, ACSL1
	tRNA Charging	DARS, TARS
	Glutamine Biosynthesis I	Glul
	Thyroid Hormone Biosynthesis	CTSD
	GDP-glucose Biosynthesis	PGM1
	4-aminobutyrate Degradation I	SUCLG2
	Acetate Conversion to Acetyl-CoA	ACSL1
	Fatty Acid β-oxidation I	HSD17B10, ACSL1
	Glucose and Glucose-1-phosphate Degradation	PGM1
	Pentose Phosphate Pathway (Oxidative Branch)	PGLS
	Heme Degradation	BLVRB
	Serotonin and Melatonin Biosynthesis	DDC
	Catecholamine Biosynthesis	DDC
	Phenylethylamine Degradation I	ALDH3A2
	Melatonin Degradation II	MAOA
	Glutamate Degradation III (via 4-aminobutyrate)	SUCLG2
	Glycogen Degradation II	PGM1
	NAD Phosphorylation and Dephosphorylation	NADK2
	Pentose Phosphate Pathway	PGLS
	Glycogen Degradation III	PGM1
	Leucine Degradation I	MCCC2
	Purine Nucleotides De Novo Biosynthesis II	ADSS
Cluster 4	EIF2 Signaling	RPL3, EIF4A2, EIF4G1, RPLP0
	Acetyl-CoA Biosynthesis III (from Citrate)	ACLY
	4-hydroxybenzoate Biosynthesis	TAT
	4-hydroxyphenylpyruvate Biosynthesis	TAT
	Remodeling of Epithelial Adherens Junctions	TUBB3, ARF6
	Methylmalonyl Pathway	MUT
	Histidine Degradation III	FTCD
	2-oxobutanoate Degradation I	MUT
	Tyrosine Degradation I	TAT
	Aspartate Degradation II	MDH1
	Tryptophan Degradation to 2-amino-3-carboxymuconate Semialdehyde	TDO2
	NAD biosynthesis II (from tryptophan)	TDO2
	Regulation of eIF4 and p70S6K Signaling	EIF4A2, EIF4G1
	Lipid Antigen Presentation by CD1	ARF6
	Bile Acid Biosynthesis, Neutral Pathway	CYP27A1
	Gluconeogenesis I	MDH1
Cluster 5	Superpathway of Methionine Degradation	CBS, MAT1A, GOT1, MAT2A, BHMT2
	Cysteine Biosynthesis III (mammalia)	CBS, MAT1A, MAT2A
	S-adenosyl-L-methionine Biosynthesis	MAT1A, MAT2A
	Acute Phase Response Signaling	HPX, HP, C3, TF, FGB
	LXR/RXR Activation	HPX, C3, TF, ACACA
	Methionine Degradation I (to Homocysteine)	MAT1A, MAT2A
	L-cysteine Degradation III	GOT1
	Cysteine Biosynthesis/Homocysteine Degradation	CBS
	Tyrosine Biosynthesis IV	PAH
	Melatonin Degradation I	POR, Sult1a1
	1, 25-dihydroxyvitamin D3 Biosynthesis	POR
	Methionine Salvage II (Mammalian)	BHMT2
	Phenylalanine Degradation I (Aerobic)	PAH
	Glutamate Degradation II	GOT1

	Aspartate Biosynthesis	GOT1
	Superpathway of Melatonin Degradation	POR, Sult1a1
	Biotin-carboxyl Carrier Protein Assembly	ACACA
	L-cysteine Degradation I	GOT1
	Aspartate Degradation II	GOT1
	TR/RXR Activation	HP, ACACA
	Glycine Betaine Degradation	BHMT2
	Lipid Antigen Presentation by CD1	CANX
	Phenylalanine Degradation IV (Mammalian, via Side Chain)	GOT1

Table A. 5: Functional annotation and representative probesets associated with up- and down-regulated clusters in response to continuous cortisol infusion in -24h to 0h time period.

	Classification	***Molecules***
Up (a)	Cytokine and pattern recognition receptors	CSF2RA, IL10RB, IL13RA1, IL1R2, IL4R, TNFRSF10C, TNFRSF1A, TNFRSF9, TLR1, TLR8
	Receptor regulatory elements	IL18RAP, GRB10, IRS2
	Signal transduction proteins	NFKBIA, CAMK1D, LIMK2, MAP2K4, MAP2K6, PPP2R5A
	Transcription factors	ATF6, FOS, STAT5B
	Negative regulators of complement system	CD55, CD59, SERPINB1
	Cytoskeletal proteins	IQGAP1, GIT2, TUBA1A
	Protein degradation enzymes	UB2B, UBE2D1
	ECM degradation enzymes and their inhibitor	MMP25, MMP9, TIMP2
	Amino acid degradation	ARG1
Down (b)	Protein translation regulatory elements and translation machinery	EEF2, EIF3H, CCNC, RPSs – 5 probesets–, RPLs – 8 probesets–
	Mitochondrial proteins	NDUFs–3 probesets–, UQCRFS1
	Free radical scavenging	SOD1
	Transcription factors	LEF1, STAT4
	Antigen presentation	HLA-DPB1

Table A. 6: Functional annotation and representative probesets associated with up- and down-regulated clusters in response to continuous cortisol infusion within the full time period of the study (-24h to 24h).

	Classification	***Molecules***
LPS dominated (a)	Cell-cell and cell-ECM interaction	ICAM1, THBS1
	Cytokines, chemokine, receptor antagonist	IL1B, CCL20, CCL3, IL1RN
	Signal transduction elements	NFKBIA, TNFAIP3
	Transcription regulator	EGR1
Cortisol enhanced (b)	Cytokine, complement, scavenger receptors	CXCR1, IFNGR2, IL13RA1, IL18R1, IL1R2, CD163
	Receptor regulatory proteins	GAB2, IL1RAP, IRAK3, IRS2
	Signal transduction elements	DUSP1, GRB10
	Transcription factors	ATF6, BCL6, CEBPD, FOS
	Nucleotide metabolism	ENTPD1, ENTPD7, MAK, UPP1
	Chaperone and stress response proteins	FKBP5, GADD45A
	Amino acid degradation	ARG1
	Anti-apoptotic proteins	BCL2A1, NAIP
	Pro-apoptotic protein	CASP5
	Acute phase protein	HP
	Complement regulatory protein	CD59
Cortisol suppressed (c)	Transcription and protein translation	POLR1C, RPSs (5 probesets), RPLs (9 probesets), EEF2, EIF3H
	Protein degradation	PSMC5
	Mitochondrial proteins	UQCRH, COX4I1, NDUFs (3 probesets)
	Antigen presentation	HLA-DA1, HLA-DRA
	Antigen recognition	LAT
	Free radical scavenging	SOD1
	Receptors	CD48, FPR3
	Nucleotide metabolism	ADSL, NME1
	TCA cycle enzyme	IDH3B

Acknowledgement of Previous Publications

This dissertation contains significant amount of text, figures and tables from the following publications:

1. **Kamisoglu K**, Haimovich B, Calvano SE, Coyle SM, Corbett SA, Langley RJ, Kingsmore SF, Androulakis IP, "Human metabolic response to systemic inflammation: Concordance between experimental endotoxemia and clinical cases of sepsis/SIRS", Critical Care, 19(1):71, 2015.
2. **Kamisoglu K**, Sukumaran S, Nouri-Nigjeh E, Tu C, Li J, Shen X, Duan X, Qu J, Almon RR, Jusko WJ, Androulakis IP, "Tandem analysis of transcriptome and proteome changes after a single dose of corticosteroid: A systems approach to liver function in pharmacogenomics", Omics: A Journal of Integrative Biology, in press.
3. **Kamisoglu K**, Calvano SE, Coyle SM, Corbett SA, Androulakis IP, "Integrated transcriptional and metabolic profiling in human endotoxemia", Shock (Augusta, GA), 42(6):499-508, 2014.
4. **Kamisoglu K**, Sleight KE, Nguyen TT, Calvano SE, Coyle SM, Corbett SA, Androulakis IP, "Effects of coupled dose and rhythm manipulation of plasma cortisol levels on leukocyte transcriptional response to endotoxin challenge in humans", Innate Immunity, 20(7):774-784, 2013.
5. **Kamisoglu K**, Sleight KE, Calvano SE, Coyle SM, Corbett SA, Androulakis IP, "Temporal metabolic profiling of plasma during endotoxemia in humans", Shock (Augusta, Ga.), 40(6):519-26, 2013.
6. Kosmides AK, **Kamisoglu K**, Calvano SE, Corbett SA, Androulakis IP, "Metabolomic fingerprinting: Challenges and opportunities", Critical Reviews in Biomedical Engineering, 41(3):225-221, 2014.
7. Androulakis IP, **Kamisoglu K**, Mattick J, "Topology and dynamics of signaling networks: In search of transcriptional control of the inflammatory response", Annual Reviews of Biomedical Engineering, 15:1-28, 2013.